ornl

OAK RIDGE NATIONAL LABORATORY

LOCKHEED MARTIN

ORNL/Sub/92-SL922/1

Development of NZP Ceramic Based "Cast-in Place" Diesel Engine Port Liners

R. Nagaswaran
S. Y. Limaye

CERAMIC TECHNOLOGY PROJECT

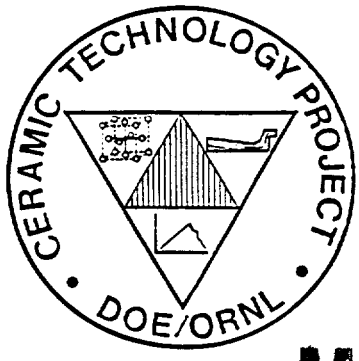

MANAGED AND OPERATED BY
LOCKHEED MARTIN ENERGY RESEARCH CORPORATION
FOR THE UNITED STATES
DEPARTMENT OF ENERGY

ORNL-27 (3-96)

ORNL/Sub/92-SL922/1

DEVELOPMENT OF NZP CERAMIC BASED "CAST-IN-PLACE" DIESEL ENGINE PORT LINERS

R. Nagaswaran
S. Y. Limaye

Date Published: February 1996

Prepared by
LoTEC, Inc.
1840 West Parkway Boulevard
West Valley City, Utah 84119

Funded by
U.S. Department of Energy
Assistant Secretary for Energy Efficiency and Renewable Energy
Office of Transportation Technologies
Propulsion System Materials Program
EE 51 05 00 0

for
OAK RIDGE NATIONAL LABORATORY
Oak Ridge, Tennessee 37831-6285
managed by
LOCKHEED MARTIN ENERGY RESEARCH CORPORATION
for the
U.S. DEPARTMENT OF ENERGY
under Contract DE-AC05-96OR22464

DISCLAIMER

TABLE OF CONTENTS

LIST OF FIGURES

LIST OF TABLES

ABSTRACT

BSX ($Ba_{1+x}Zr_4P_{6-2x}Si_{2x}O_{24}$) and CSX ($Ca_{1-x}Sr_xZr_4P_6O_{24}$) type NZP ceramics were fabricated and characterized for: (i) thermal properties viz., thermal conductivity, thermal expansion, thermal stability and thermal shock resistance; (ii) mechanical properties viz., flexure strength and elastic modulus; and (iii) microstructures. Results of these tests and analysis indicated that the BS-25 (x=0.25 in BSX) and CS-50 (x=0.50 in CSX) ceramics had the most desirable properties for casting metal with ceramic in place. Finite element analysis (FEA) of metal casting (with ceramic in place) was conducted to analyze thermomechanical stresses generated and determine material property requirements. Actual metal casting trials were also conducted to verify the results of finite element analysis. In initial trials, the ceramic cracked because of the large thermal expansion mismatch (hoop) stresses (predicted by FEA also). A process for introduction of a compliant layer between the metal and ceramic to alleviate such destructive stresses was developed. The compliant layer was successful in preventing cracking of either the ceramic or the metal. In addition to these achievements, pressure slip casting and gel-casting processes for fabrication of NZP components; and acoustic emission and ultrasonics-based NDE techniques for detection of microcracks and internal flaws, respectively, were successfully developed.

INTRODUCTION

Low thermal expansion, good thermal shock resistance, high melting temperature and thermal stability are attractive properties for numerous applications (such as in diesel-engine port liners) involving ceramics. In general, NZP ceramics have low thermal expansion coefficients but their thermal shock properties and melting temperatures are highly composition dependent. Also, it has been recognized that low thermal expansion, per se, is not so beneficial if it is accompanied by anisotropy[1-4]. However, because of their unique crystal structure specific NZP ceramic compositions could be tailored to have all of the requisite properties including very low anisotropy. This potential gives NZP ceramics a significant edge over conventional low expansion materials such as cordierite, mullite, aluminum titanate, LAS and fused silica.

Of the numerous NZP materials investigated thus far, the BSX ($Ba_{1+x}Zr_4P_{6-2x}Si_{2x}O_{24}$) and CSX ($Ca_{1-x}Sr_xZr_4P_6O_{24}$) type of materials have both ultra-low thermal expansions[4-5] and high melting temperature. Even so, evaluation of their thermal expansion anisotropy, thermal shock resistance and mechanical properties as a function of composition is important from an applications standpoint. For instance, in the diesel engine port-liner application mechanical vibrations are an important issue in addition to thermal loads associated with the high temperature environment. The need to integrate or bond two widely different materials such as ceramic and metal in the port further complicates material requirements.

The above discussed were the motivating factors for Phase I research; the broad purpose of which was to identify NZP materials with optimum properties such as would permit fabrication of "cast-in-place" diesel engine port liners. As an extension of this, exploration of alternate NZP type materials and fabrication and characterization processes will also be conducted. The overall objective of this Phase I research program was to develop sodium-zirconium-phosphate (NZP) ceramic based "cast-in-place" diesel engine port liners. Specific objectives were: (1) Materials requirement analysis, (2) Successful demonstration of metal casting around the ceramic, (3) Cost-effective process development, and (4) Development of high temperature database (stability, thermal cycling, thermal shock etc.).

TECHNICAL APPROACH AND RESULTS

Following the initial group meeting held at Chicago in October 1992 the work plan for Phase I research, in the form of a series of tasks, was formalized. The technical approach used to fulfill these tasks and results obtained have been discussed in the following.

MATERIALS REQUIREMENT ANALYSIS

A preliminary finite element analysis (FEA) was carried out to evaluate the stresses involved in the metal casting process. A set of properties based on prior information was chosen for the NZP ceramic, metal and the sand used in metal casting process. Table 1

summarizes the properties that were chosen for this finite element stress analysis. Two different casting configurations were considered for this finite element analysis; a straight tube and an L-shaped tube as shown in Figure 1. Instead of using commercially available FEA software packages such as ANSYS, a set of public domain software packages called INGRID (for grid generation), TOPAZ2D (for thermal analysis) and NIKE2D (for stress analysis) were used. These software packages are less expensive and provide similar results. In order to verify the functionality of these software packages, a standard "high confidence" problem was analyzed using these software packages and the solutions were found to be satisfactory. The results of the preliminary FEA are shown in Figure 2 and Table II. These results show that the NZP ceramic is subjected to large compressive hoop stresses along the radial directions.

In this work, metal casting trials were used to verify the finite element (FEA) results and further refine the FEA model. Initial trials were designed to measure actual temperatures during casting for comparison with the theoretical temperature profiles generated using the finite element modeling (FEA). Figures 3 and 4 depict the details of the set-up used for metal casting trials. Molten metal was cast around the ceramic tubes (BS-25) in a sand mold. Four tubes (2" dia, 6" long) were used for these trials. A series of four thermocouples were buried at various locations to obtain temperature profiles during the actual casting trial. The temperature was recorded using a standard A/D data-acquisition board. This data was then compared with the thermal gradient patterns generated by FEA (as shown in Figure 2).

The results of the temperature measurement trials show that the initial finite element model approximates the actual casting trials. This is evident from Figures 5 and 6. Based on the results of the first metal casting trials, further modifications to the FEA model were made to initiate iterative refinement of the FEA model. Eventually, this model would be so refined as to perform a parametric study of the effects of various materials' properties on thermal stresses. Later in this Phase I program, NZP ceramic tubes were fabricated for further metal casting trials to verify the results of the analytical model. Prior to this, a detailed characterization of the material properties of the various NZP ceramics had to be conducted to enable selection of a few ceramics with suitable properties. The fabrication and characterization methods used to produce baseline NZP ceramic materials and assess their properties, respectively, are described in the following sections.

Table 1. Preliminary data used for developing the thermal analysis model.

Material Properties and Model Inputs (Presented in the MKS, cgs units system)	**NZP**	**Gray Cast Iron**	**Sand**
General Properties			
Length (cm)	15	15	15
Thickness (cm)	0.3	1	30
Density (kg/m^^3)	3200-3650	7000	1450
Mechanical Properties			
Flexural Strength (MOR) (MPa)	***	***	***
25 C	70	***	***
1000 C	70	***	***
1500 C	65	***	***
Young's Modulus 25 C to 1000 C (GPa)	70	***	***
Fracture Toughness (MPa)	1.5-2.0	***	***
Ultimate Strength (MPa)	***	***	***
Tension	30-90	370	***
Compression	90-300	830	***
Shear	***	330	***
Yield Strength (MPa)	***	***	***
Tension	30-90	250	***
Shear	***	165	***
Allowable Stresses (kPa)	***	***	***
Tension or Compression	***	165475	***
Shear	***	99975	***
Elastic Modulii (GPa)	***	***	***
Tension or Compression	35-100	172	***
Shear	***	83	***
Poisson Ratio	0.24	0.28	
Thermal Properties			
Thermal Conductivity (W/m K)	1	41.9	1.26
Thermal Conductivity as a f(Temp) (W/m K) (Sand) 0.6606-2.084E-4 T+7.741E-7 T^^2			
Specific Heat (J/kg K)	***	***	***
Ambient	460	628	838
473 K	***	***	975.7
673 K	***	***	1092.9
873 K	***	***	1151.5
1073 K	***	***	1159.9
1273 K	***	***	1176.7
Thermal Diffusivity (m^^2/sec)	6.00E-07	9.50E-06	9.10E-07
Coeff. of Thermal Expansion (1/C) (NZP 5 - 6 ppm)	1.00E-06	1.21E-05	***
Heat Transfer Coefficient at Interface (W/m^^2 K) mold/outside air = 83.8	***	***	***
Ambient Temperature K	293	293	293
Liquidus Temperature K	2173	1573	***
Solidus Temperature K	2073	1275	***
Initial Temperature K	293	1273	293

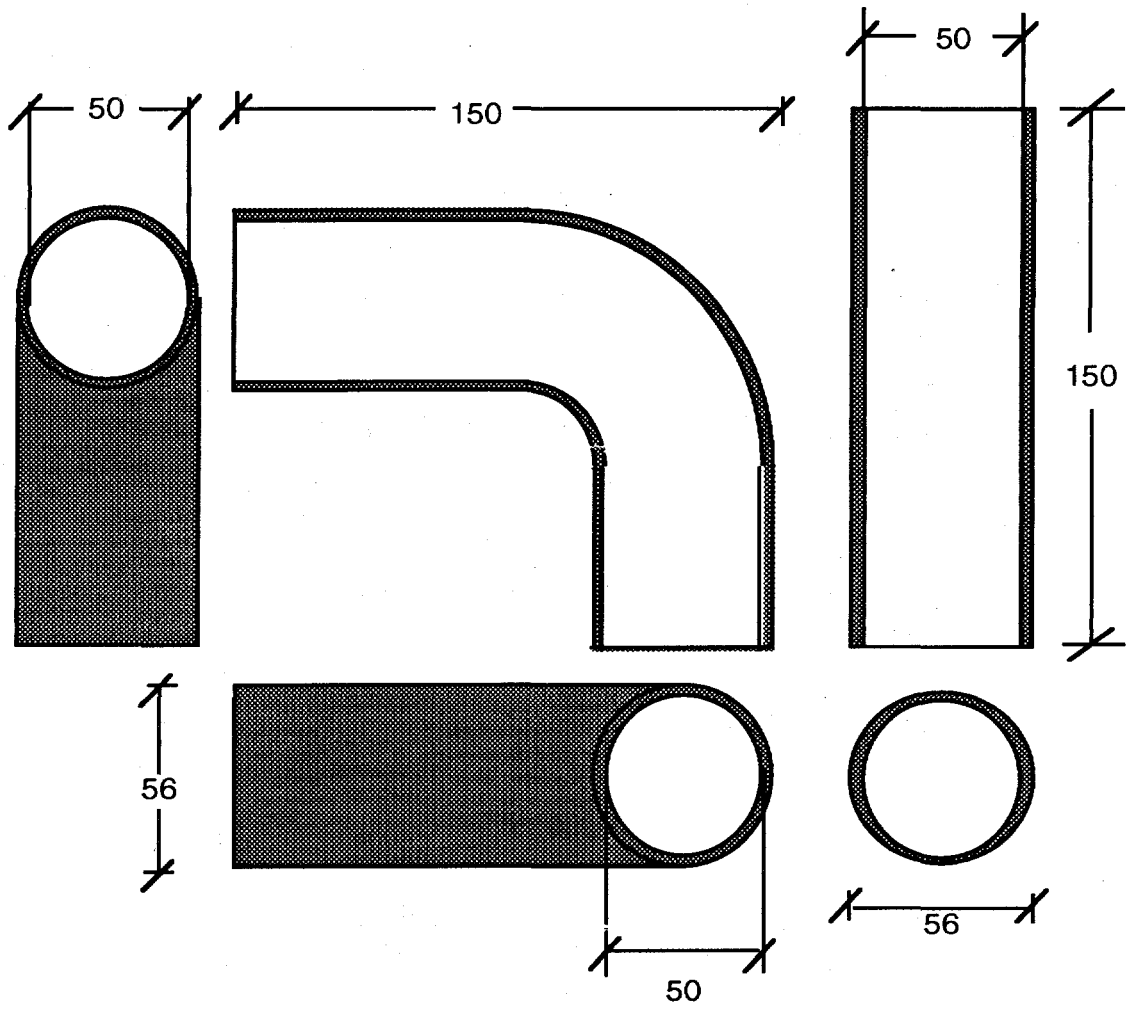

Figure 1. Dimensions of ceramic tubes for molten metal casting trials.

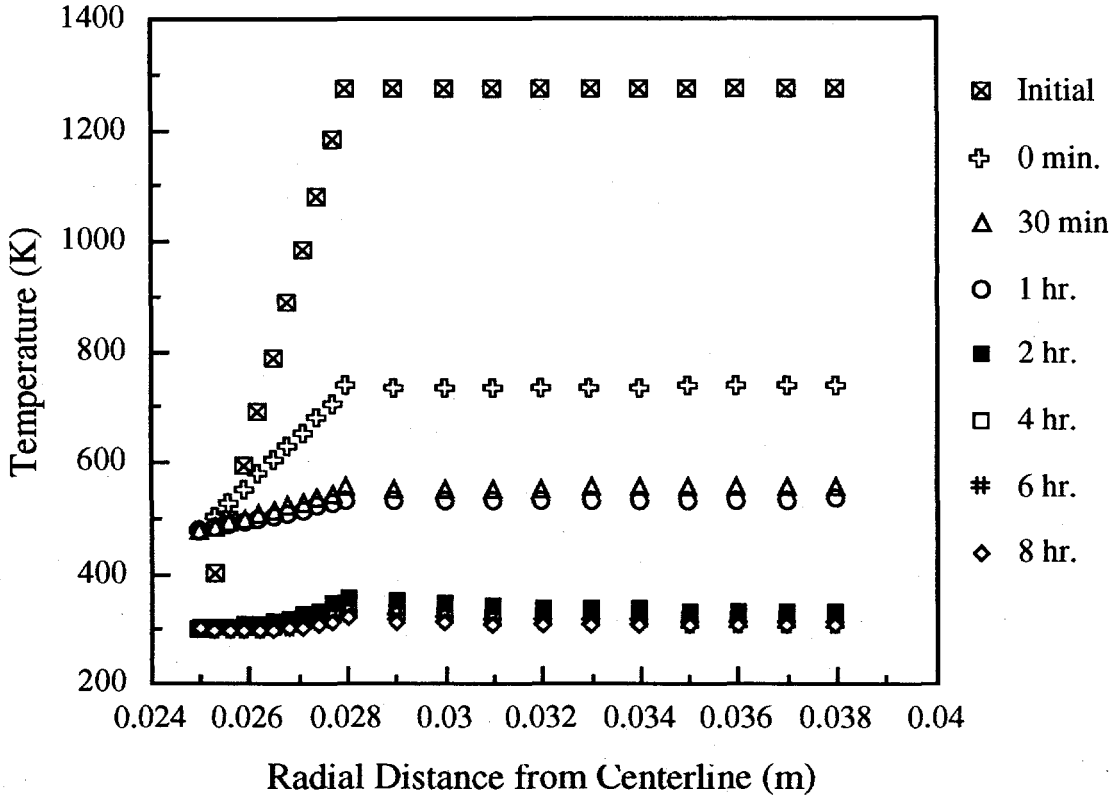

Figure 2. Temperature distribution as a function of time during molten metal casting process. (These results were obtained using TOPAZ2D software package.)

Table 2. Mechanical stresses as a function of time and radial distance during metal casting with NZP ceramic in place.

Material	Radial Dist. (m)	Tangential Stresses (MPa)			Type of Stress
		30 min.	2 hr.	4 hr.	
NZP	0.025	-718.9	-578.3	-344.1	Compressive
NZP	0.028	-646.0	-519.6	-309.2	Compressive
Cast Iron	0.028	246.1	198.0	117.8	Tensile
Cast Iron	0.038	173.2	139.3	82.9	Tensile

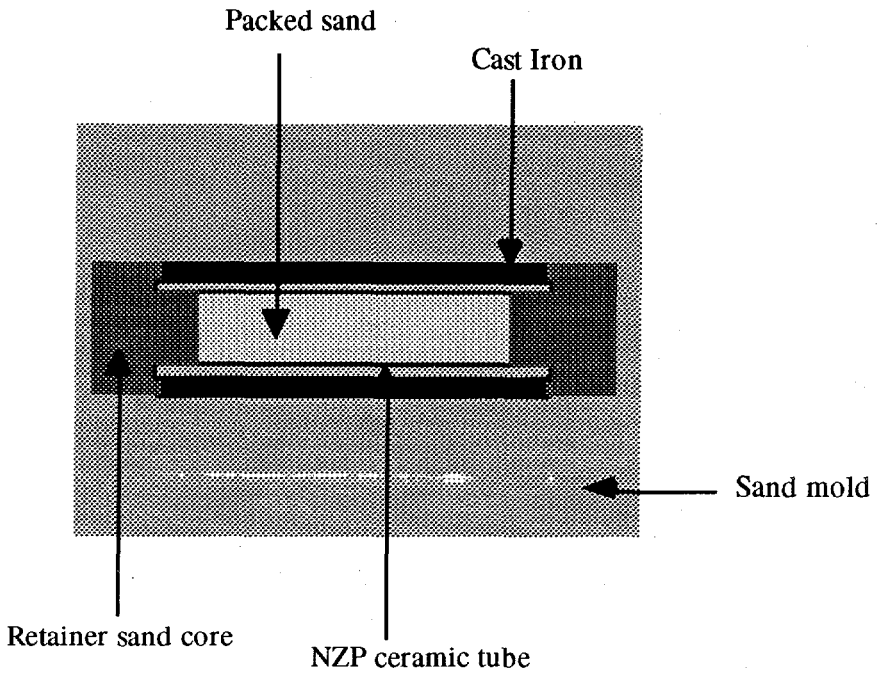

Figure 3. Schematic of set-up for molten metal casting trials.

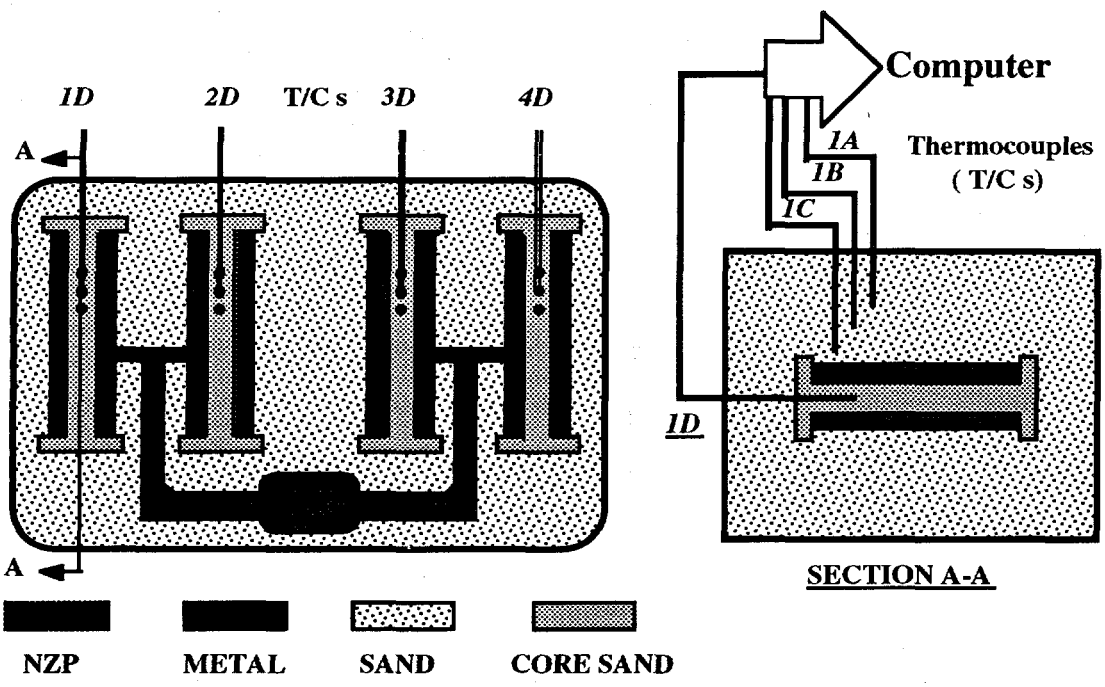

Figure 4. Detailed sectional view of the set-up for Metal Casting trials.

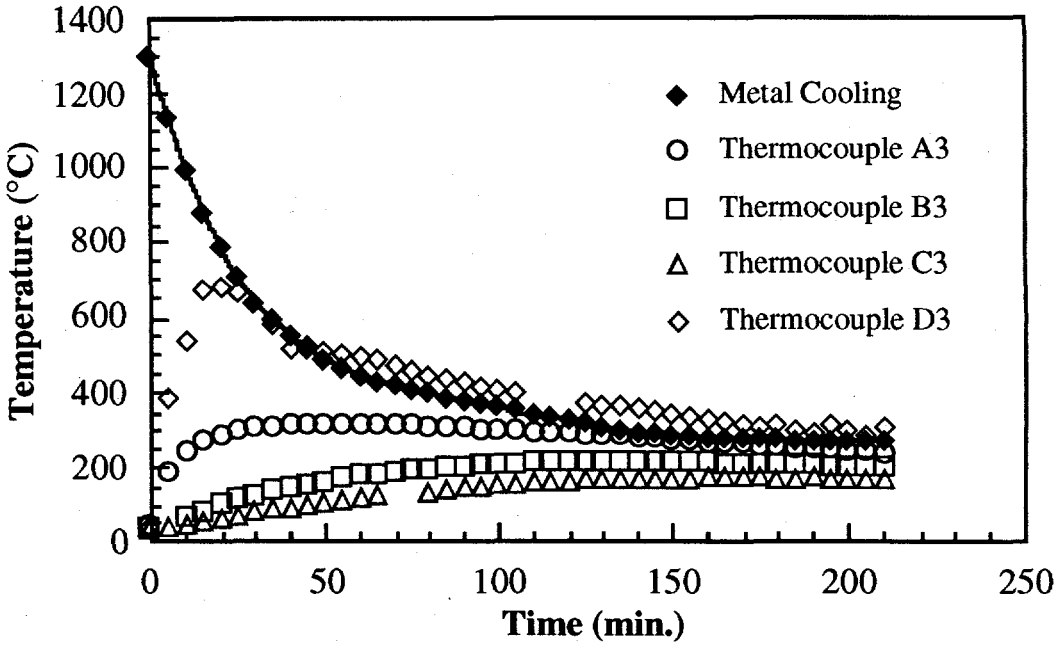

Figure 5. Metal cooling curves generated by finite element analysis (FEA).

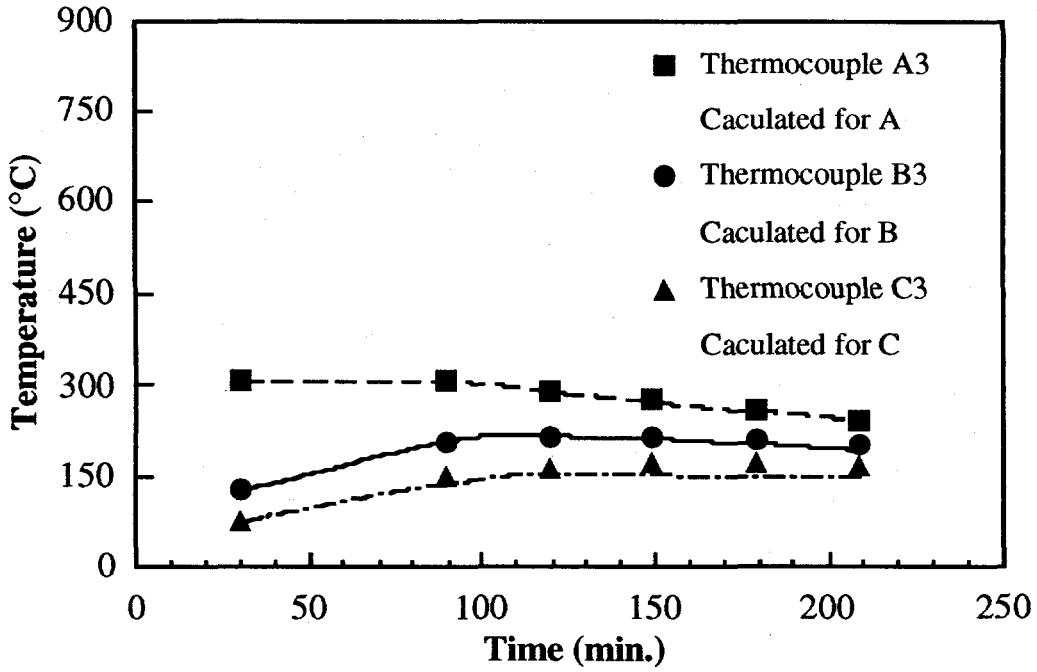

Figure 6. FEM calculated (curves) vs. actual temperatures as a function of time for various thermocouple locations.

MATERIALS PROCESSING AND PROCESS OPTIMIZATION

Based on past experience, BSX ($Ba_{1+x}Zr_4P_{6-2x}Si_{2x}O_{24}$) and CSX ($Ca_{1-x}Sr_xZr_4P_6O_{24}$) series low thermal expansion NZP compositions with 'x' varying as 0, 0.17, 0.25, 0.375 and 0.50, and 0, 0.25 and 0.50, respectively, were designated for processing and detailed evaluation of properties. Routine steps involved in the processing of these materials are shown in the schematic of Figure 7 here.

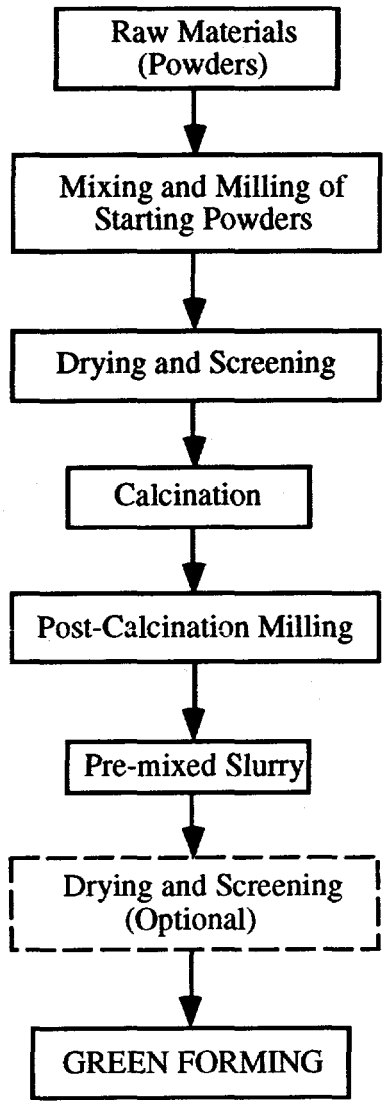

Figure 7. Flow chart detailing steps involved in the fabrication of NZP green bodies.

Large (20 kg) batches of the powders were synthesized using the routine oxide batch mixing process. The size of the batches was chosen so as to insure availability of enough material to perform all the required testing and evaluation on each individual batch. Batching consisted of mixing and milling the raw materials together, drying and screening the milled powder, calcining each composition at its required calcination temperature to produce the single phase NZP structure, and post calcination screening. Routine characterization such as powder X-ray diffraction, particle size measurement and surface area analysis was carried out to ensure that the powders had appropriate set of properties.

In order to obtain strong and dense components of the BSX and CSX series NZP materials, considerable effort was devoted to optimizing the existing process of fabricating slip cast components. This optimization procedure identified specific challenges that needed to be addressed such as milling process, use of appropriate binder and dispersant system and pH of the slurry. A systematic parametric study of these variables was then undertaken. Table 3 shows a typical experimental test matrix used to evaluate the effects of important variables involved in the fabrication process. Two important sub-processes, namely, calcination process and milling process were first evaluated.

The raw materials for a typical NZP ceramic viz., $Ba_{1.25}Zr_4P_{5.5}Si_{0.5}O_{24}$ (BS-25), were blended in stoichiometric proportions and calcined at 1150 and 1200°C for 4 and 12 hours. These calcined samples were examined for their particle size, surface area and phase purity. Table 3 shows the results of particle size and surface area analysis as a function of calcination temperature and time. As is evident from this table, there is little correlation between calcination time and particle size or surface area. However, as the calcination temperature increases, the surface area is reduced significantly. The X-ray diffraction patterns of Figure 8 of powders calcined at 1150°C vs. 1250°C show that the higher calcination temperature reduces the appearance of the second phase zirconium phosphate. Based on these results, it was determined that 1150°C is too low a temperature to calcine BS-25. Another independent calcination experiment showed that BS-25 could be calcined at 1200°C without the formation of the second phase (Figure 9). The effect of time on the composition is negligible, hence, calcination at 1200°C for 4 hours was chosen as a standard calcination temperature.

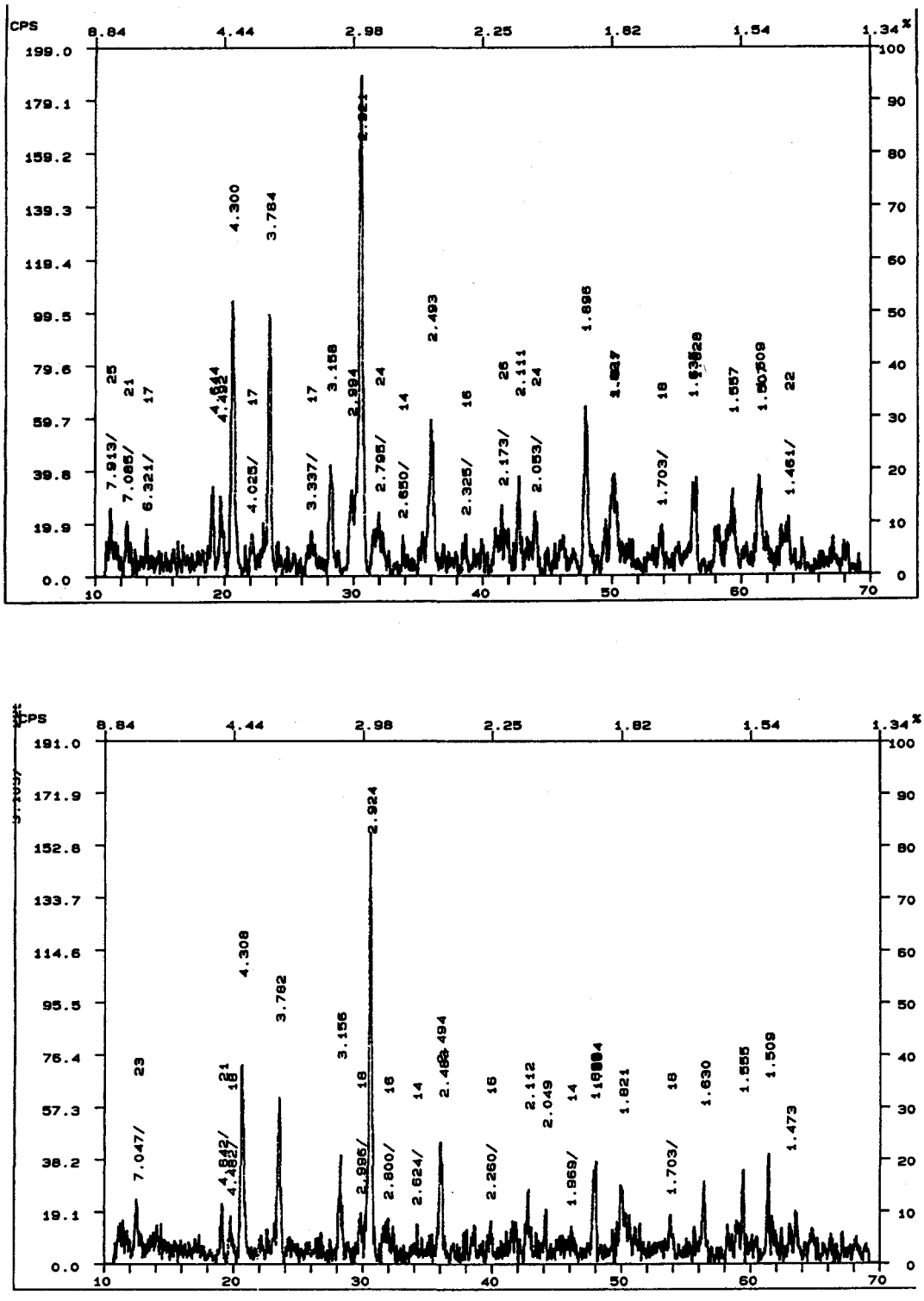

Figure 8 (a)&(b). XRD traces of BS-25 powders calcined at (a) 1150°C and (b) 1250°C.

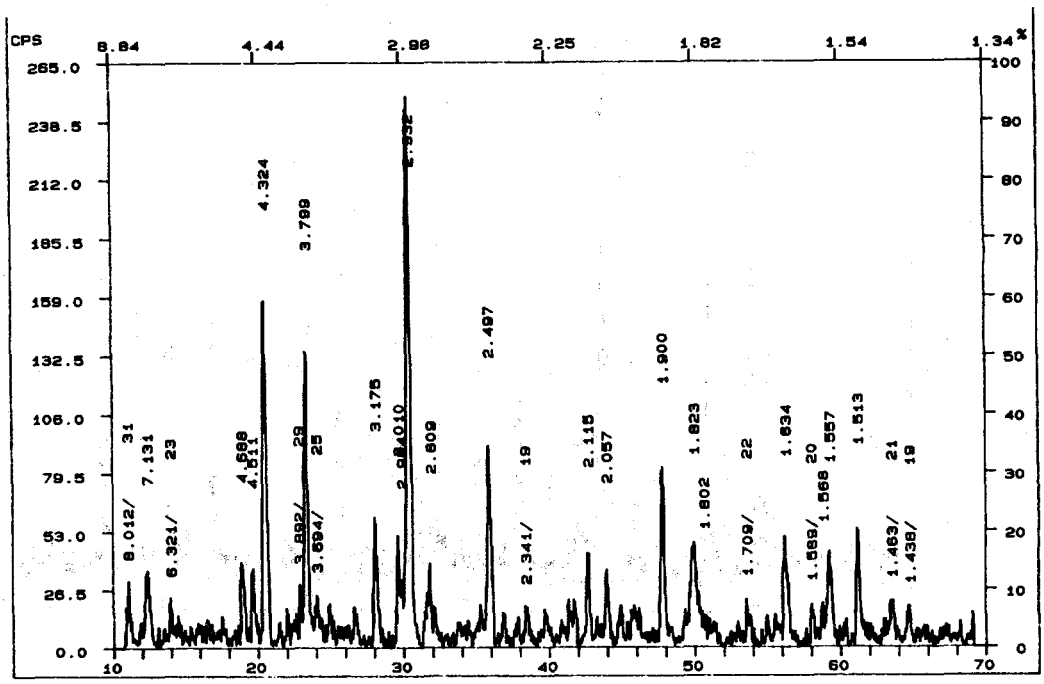

Figure 9. XRD pattern of BS-25 powder calcined at 1200°C showing only NZP phase.

Table 3. Results of Test Matrix for Evaluating and Improving Calcination Process.

Temperature ⇒ **Time ⇓**	1150°C	1250°C
4 Hours	Mean Particle Size: 5.5 µm Surface Area: 1.27 m^2/g	Mean Particle Size: 5.5 µm Surface Area: 1.13 m^2/g
12 Hours	Mean Particle Size: 6.8 µm Surface Area: 1.65 m^2/g	Mean Particle Size: 5.5 µm Surface Area: 1.18 m^2/g

In order to determine the optimum milling conditions, a series of calcined samples (calcined at 1200°C for 4 hours) were milled by vibratory milling and ball milling. In the case of ball milling, two variables, the weight ratio of milling media to ceramic powder, and milling time were varied. In the case of vibratory milling, time was used as the only variable and media to powder weight ratio was held constant (at 6:1) due to the difficulties associated with changing this ratio in the vibratory mill. Particle size and surface area of these samples were measured after milling. Figure 10 illustrates the effect of milling media content and milling time on milling efficiency. This study indicates that vibratory milling is more efficient than ball milling with media to powder weight ratio of 5:1. When the media to powder ratio for ball milling is increased to 8:1, the efficiency of ball milling matches that of vibratory milling. However, such a high media to powder ratio during ball milling leads to contamination of the powders due to wear of the milling media. Thus, vibratory milling was considered a preferred milling technique. A typical batch size for the vibratory mill is approximately 25 lb. When smaller batches are needed ball milling with intermediate media-to-powder (6:1) ratio should be preferred, since the jar size is adjustable.

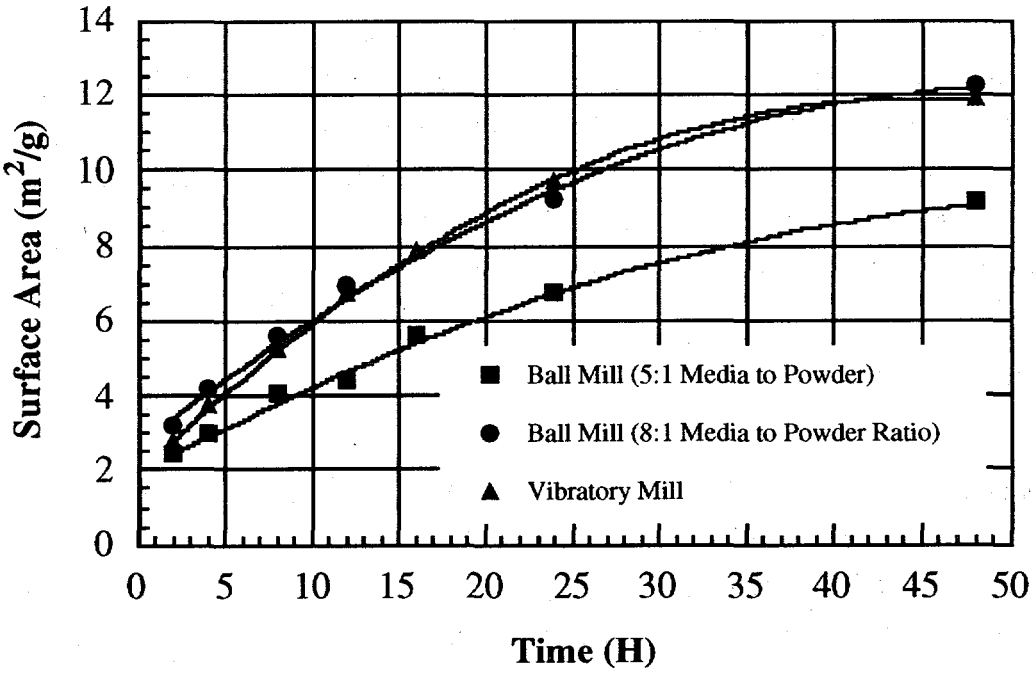

Figure 10. Effect of milling time and conditions on surface area of BS-25 powders calcined at 1200°C for 4 hours.

The binder/dispersant system is a crucial factor in determining the success of the slip-casting process. Accordingly, several combinations of binders and dispersants were investigated for preparing slips of the various compositions. Some of the binders assessed were PEGs (Polyethylene Glycol)[¶] and Goodrite K-type[§], and one of the evaluated dispersants was Darvan C™. Preliminary results showed that certain proprietary binders and dispersants performed better than others in providing satisfactory flow properties for the BS-25 system, although, even these binders and dispersants had a tendency to migrate to the surface during the drying stage of the slip casting process. New binders and dispersants are being evaluated to better optimize the rheological properties of the slip. Another important parameter that governs the flow characteristics of the slip and, thereby, the properties of the formed body is the pH of the slip. Studies to optimize the pH for slips of each composition are underway. A suitable binder-dispersant system and pH of the slip would lead to slip-cast bodies (such as port liners) with good properties and consistent quality.

Using the thusfar optimized process variables i.e., vibratory milling (media to powder ratio 5:1) and calcination of the milled and dried powders at 1200°C for 4 hours, ceramic slurry was prepared for slip casting by using the standard method of wet-milling the calcined powders with an appropriate dispersant, binder, and weight percent distilled water using grinding media. A series of tiles of size 2" x 2" x 0.25" were slip cast in molds with only small amounts of moisture (typically 5% by volume). Cast tiles were sintered at 1550°C for 4 hours - conditions determined to be optimum based on previous work on NZP ceramics. These tiles were then machined (sliced and ground) to appropriate shapes and sizes for further characterization.

MATERIALS CHARACTERIZATION

As-sintered BSX and CSX series specimens of appropriate sizes and shapes were used for preliminary characterization of mechanical properties (flexural strength, Weibull modulus, and elastic modulus), thermal properties (thermal conductivity, thermal expansion, thermal stability, and heat capacity), and microstructures. Because it was

¶ Union Carbide, Cleveland, OH.
§ BF Goodrich, Cleveland OH.
™ RT Vanderbilt Co., Norwalk CT.

intended to study the effect of high temperature thermal cycling on important material properties, some of the specimens were subjected to 1, 25, and 250 heat-cool cycles between room temperature and 1250°C prior to a second stage of characterization. Compositions of the BSX ($Ba_{1+x}Zr_4P_{6-2x}Si_{2x}O_{24}$) series corresponding to x=0.0, 0.17, 0.25, 0.375 and 0.5, and CSX ($Ca_{1-x}Sr_xZr_4P_6O_{24}$) series corresponding to x=0.25, 0.375 and 0.5 were evaluated. Characterization efforts at LoTEC and Penn State University were supplemented by work performed by Mr. T. Barrett Jackson at the High Temperature Materials Laboratory (HTML) of ORNL as LoTEC's Industrial Fellow.

Flexural Strength

Both as-sintered and thermally cycled bar specimens of nominal dimensions 5.5 mm x 6.5 mm x 50 mm were first prepared. The tension face of the each bar was then polished to a fine finish and its edges chamfered. Fracture loads (P_f in Newtons) of the bar samples subjected to four-point bending were first determined using loading fixtures and procedures recommended in Ref. 6. The cross head speed was 0.5 mm/min. and the load at failure was recorded. From the load at failure and the cross-sectional dimensions of the test specimens the flexural strength was calculated. The fracture strengths (σ_f in MPa) were then calculated using the elastic bending formula given below:

$$\sigma_f = \frac{1.5\ P_f\ (S - l)}{b\ t^2} \qquad \text{.....(1)}$$

where, b and t represent the width and thickness, respectively, of the bar samples.

Table 4 provides the room temperature flexure strength data of both as-sintered and thermally cycled (1250°C) specimens along with the standard deviation (m) of each set of data. Three important observations can be made from Table 4: (i) flexure strengths of BS-25 and CS-50 are the highest among the BSX and CSX compositions, respectively, irrespective of the extent of thermal cycling (0 to 250 cycles), (ii) there is no noticeable degradation in strengths of the BS-25 and CS-50 materials even after 250 cycles at 1250°C (see Figs. 11(a) & (b)), and (iii) standard deviations and, hence, Weibull modulii of strengths of the BS-25 and CS-50 materials are reasonably high. This is indicative of the superior low and high temperature mechanical properties of the BS-25 and CS-50 compositions in the BSX and CSX system, respectively. However, between the two, the BS-25 material possesses better mechanical properties.

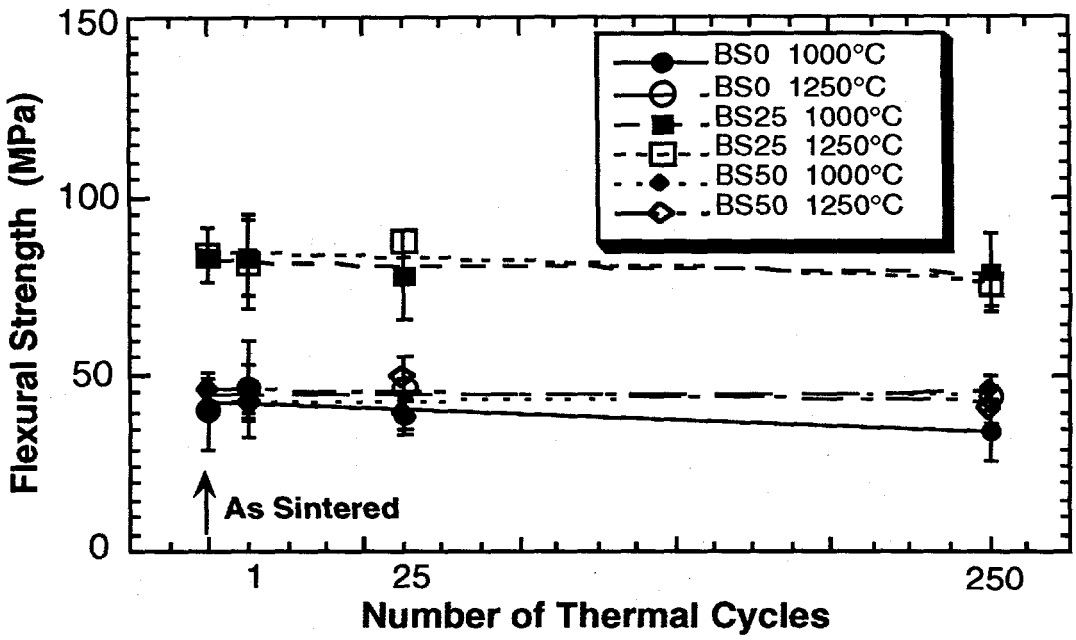

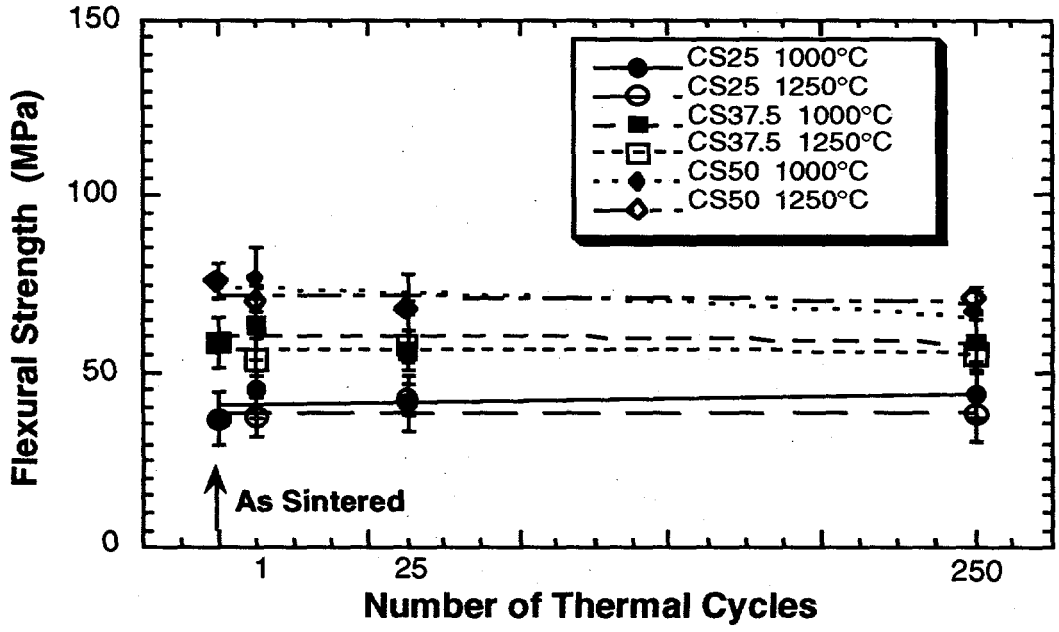

Figure 11 (a)&(b). Flexure strength 'vs.' number of thermal cycles to 1250°C for (a) BSX and (b) CSX compositions.

Table 4. Summary of the room temperature flexural strengths of as-sintered and thermally-cycled (1250°C) BSX and CSX materials.

Thermal Cycling between R.T and 1250°C				
Composition	Flexure strength (MPa)			
(BSX and CSX)	As Sintered	1 Cycle	25 Cycles	250 Cycles
BS-0	40.13 ± 10.85	46.52 ± 6.34	46.90 ± 2.24	44.25 ± 3.29
BS-17	49.76 ± 5.61	46.53 ± 4.90	-	46.49 ± 4.95
BS-25	84.20 ± 7.61	81.43 ± 12.51	88.19 ± 3.03	75.92 ± 5.95
BS-37.5	46.13 ± 4.13	46.82 ± 6.59	48.99 ± 6.17	45.14 ± 6.16
BS-50	45.55 ± 3.48	42.50 ± 3.61	49.19 ± 6.70	41.21 ± 4.76
CS-25	36.87 ± 7.55	37.47 ± 5.36	42.02 ± 4.73	37.95 ± 7.26
CS-37.5	58.41 ± 6.82	53.88 ± 5.57	57.60 ± 4.73	54.90 ± 5.17
CS-50	75.52 ± 4.83	69.81 ± 4.91	67.88 ± 1.62	70.16 ± 3.86

Thermal Diffusivity

Thermal diffusivity measurements were made using a xenon flash system. Eight different compositions viz., BS-0, BS-17, BS-25, BS-37.5, BS-50, CS-25, CS-37.5, and CS-50 were characterized at room temperature; and the thermal diffusivity of only the BS-25 composition was evaluated as a function of temperature. Five test specimens of each composition were prepared and thermal diffusivity measured. Test specimens consisted of disks 12.5 mm in diameter and approximately 1.5 mm thick. The test specimens were first coated with a layer of Au/Pd followed by a layer of colloidal graphite. The metal layer prevents light penetration into the sample and the graphite layer enhances the absorption of the xenon light pulse at the face of the sample. The heat rise as a function of time was measured at the rear face of the sample.

Results of thermal diffusivity measurements are given in Table 5. The thermal diffusivity value for each test specimen is the average of 10 acceptable measurements.

Table 5. Thermal Diffusivity of various BSX and CSX Compositions.

Composition	Thermal Diffusivity ($cm^2/sec.$)
BS-0	0.0071
BS-17	0.0064
BS-25	0.0061
BS-37.5	0.0052
BS-50	0.0051
CS-25	0.0058
CS-37.5	0.0063
CS-50	0.0070

There was less than 1% difference between the acceptable measurements. In addition, there was excellent agreement between the 5 test specimens of each composition. The density of the test specimens ranged from 85% to 90% of theoretical. Therefore, a correction for differences in porosity would have to be made when thermal conductivity is calculated.

Heat Capacity

Measurement of specific heat capacity of all compositions was important to calculate the thermal conductivity from thermal diffusivity and the density data. However, only the BS-25 material has been evaluated in this Phase I program. (The characterization of the CS-50 and other materials has been scheduled for the ongoing Phase II work.) Specimens for heat capacity measurement were made by core drilling 1.5mm plates to produce a 4 mm disk. Three specimens of the BS-25 composition were made. After drilling, the specimens were clean fired to 1000°C and held at temperature for 2 hours. The heat capacity measurements were conducted in a differential scanning calorimeter (DSC). These values have been tabulated in Table 6 below.

Thermal Conductivity

Using the measured thermal diffusivity and specific heat data, and the density of the test specimen, the thermal conductivity of BS-25 was calculated from Equation 2, which relates thermal conductivity, κ, to thermal diffusivity, α, specific heat capacity, c_p, and density, ρ;

$$\alpha = \frac{\kappa}{\rho\, c_p} \quad \text{.....(2)}$$

Table 6 and Figure 12 provide the values of thermal conductivity of BS-25 as a function of temperature up to 1100°C. Similar data are being compiled for the other compositions as part of the ongoing Phase II research.

Thermal Expansion

Thermal expansion measurements were made on as-sintered and thermally cycled (1 to 250 cycles from R.T. to 1250°C) BSX and CSX compositions. Two as-sintered specimens of each composition were tested to confirm the consistency of data from sample to sample. The results of these runs have been presented for three compositions of the BSX series and two of the CSX series in Figures 13-17. From these figures, it is clear that sample to sample difference of thermal expansion data is very small.

Table 6. Thermal Conductivity (κ) of BS-25 material as a function of temperature.

Temperature °K (°C)	c_p (cal/gm)	α (cm^2/sec)	ρ (gm/cc)	κ (W/m°K)
298.15 (25)	0.4898	0.0061	3.09	0.9232
373.15 (100)	0.5548	0.0056	3.09	0.9600
573.15 (300)	0.6449	0.0051	3.09	1.0163
773.15 (500)	0.6884	0.0049	3.09	1.0424
973.15 (700)	0.7141	0.0046	3.09	1.0150
1173.15 (900)	0.7310	0.0048	3.09	1.0841
1373.15 (1100)	0.7429	0.0050	3.09	1.1478

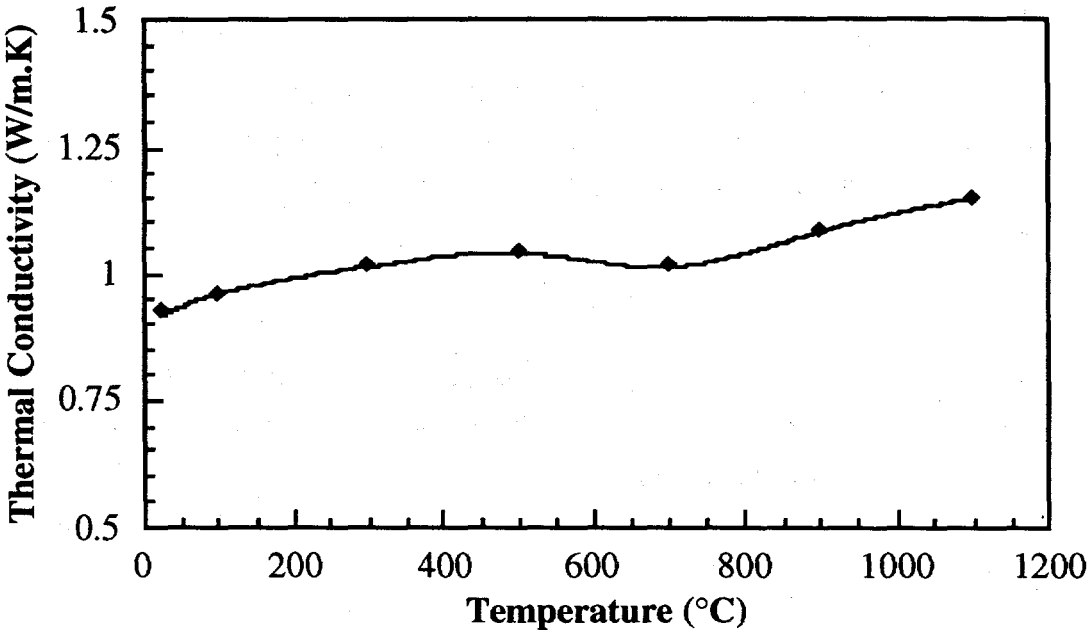

Figure 12. Thermal Conductivity of BS-25 composition as a function of temperature.

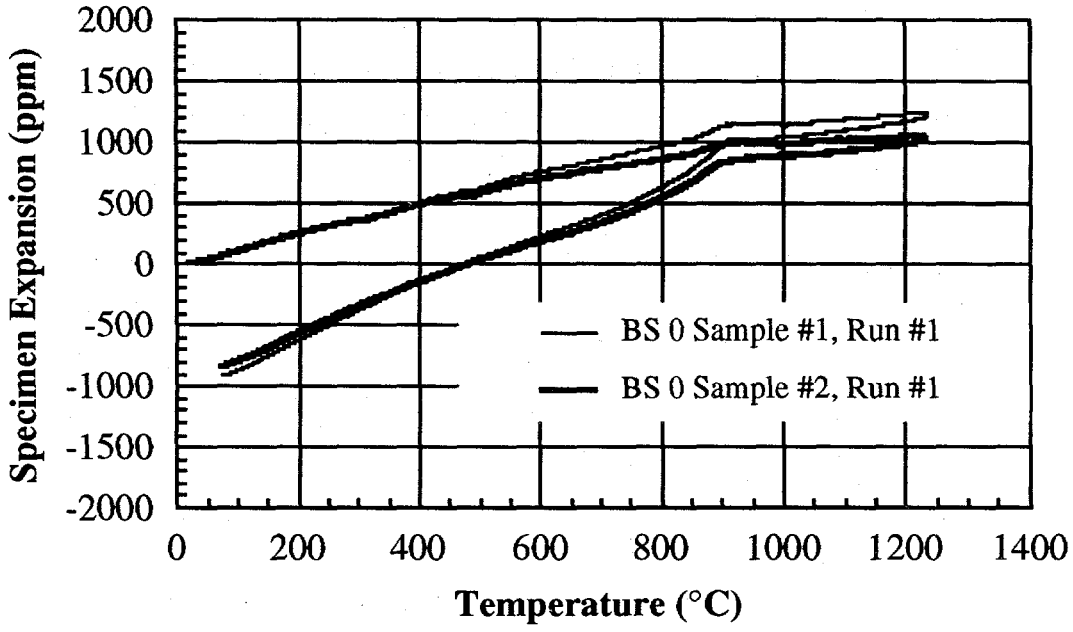

Figure 13. Thermal expansion measurements of two different samples of BS-0 composition.

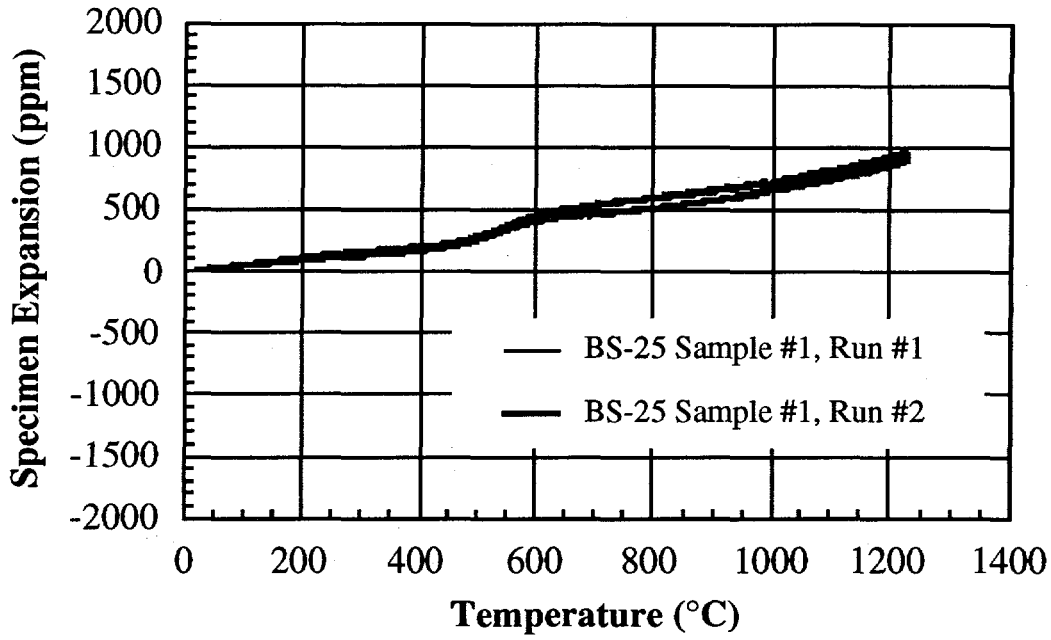

Figure 14. Thermal expansion measurements of two different samples of BS-25 composition.

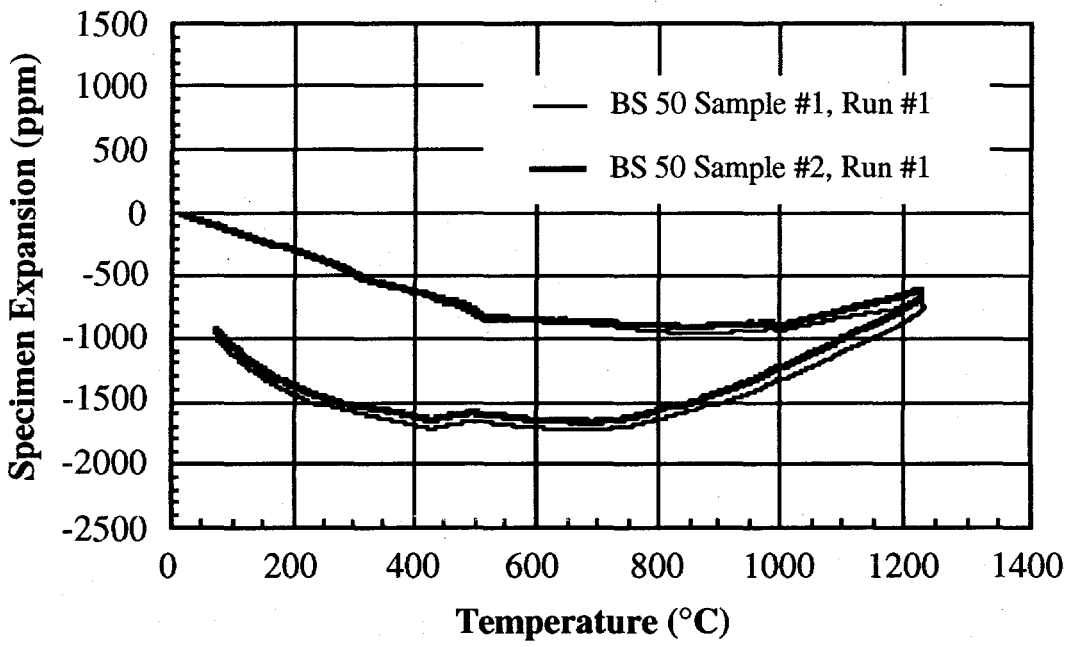

Figure 15. Thermal expansion measurements of two different samples of BS-50 composition.

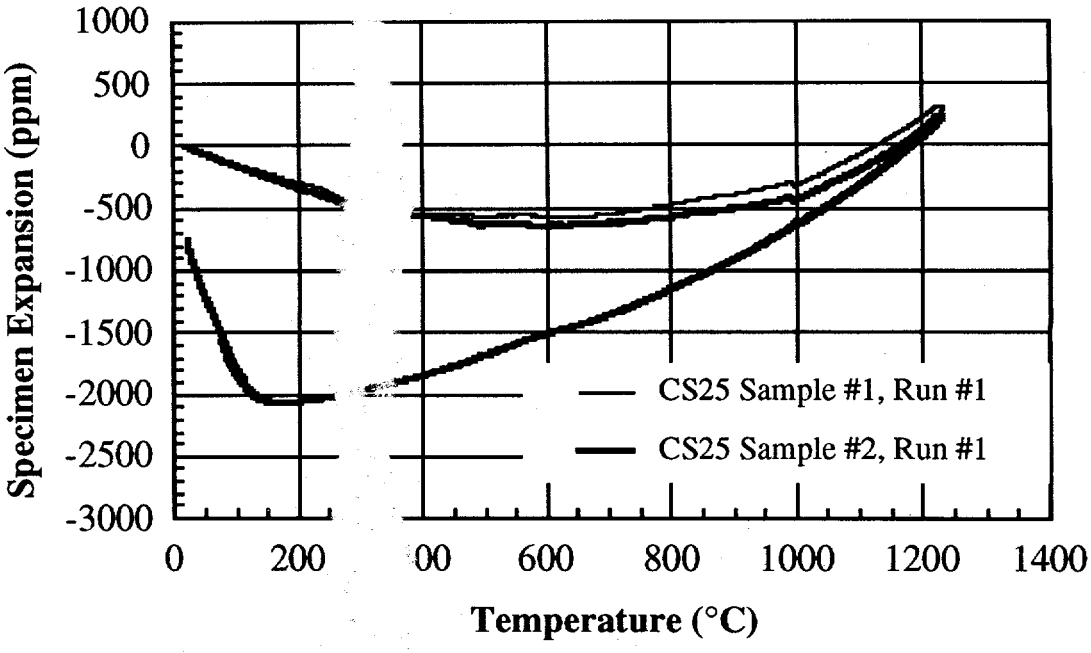

Figure 16. Thermal ex n measurements of two different samples of CS-25 composition.

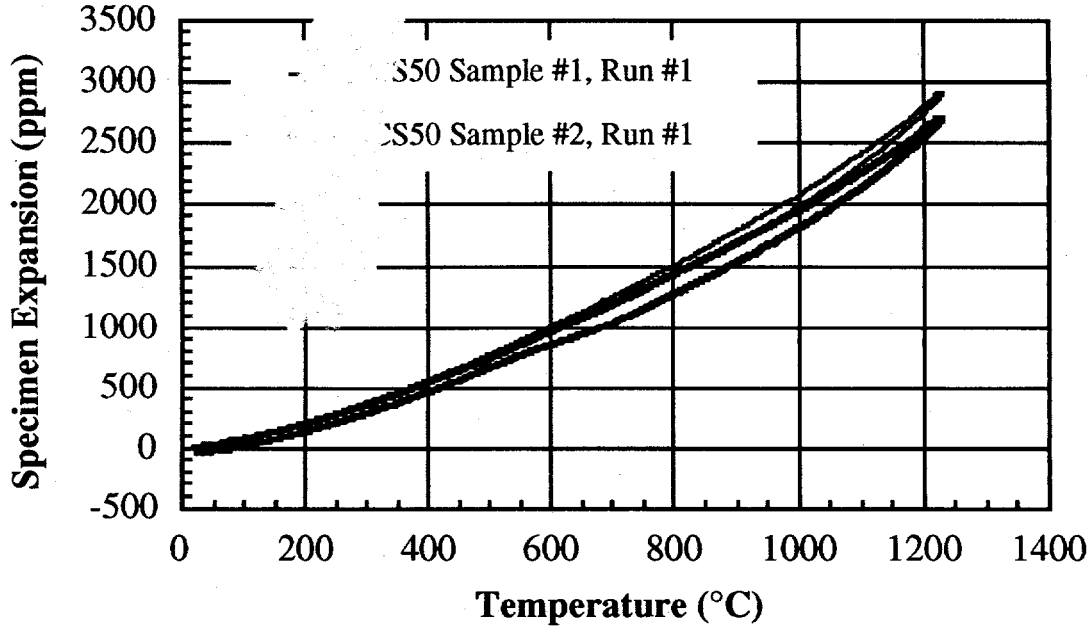

Figure 17. Thermal expansion measurements of two different samples of CS-50 composition.

Figures 18-22 show the bulk thermal expansion curves for the various as-sintered and thermally cycled BSX compositions. Several interesting observations could be made with respect to these thermal expansion curves. Samples of different compositions from the BSX series exhibit varying degrees of anisotropy as a function of concentration of silicon upon thermal cycling. BSX materials that exhibit high degree of thermal expansion anisotropy - BS-0, BS-37.5 and BS-50 - tend to have large thermal hysteresis which decreases with increasing amount of cycling and those with small anisotropy - BS-17 and BS-25 - have relatively negligible hysteresis. In the range of x=0.00 to x=0.50, one particular composition -x ≈ 0.22- showed no (zero) anisotropy. The anisotropic compositions from the BSX series show a permanent shrinkage associated with cooling of the specimen during thermal expansion measurements. These trends have been depicted in Figure 23 which is a plot of the effect of composition on thermal expansion anisotropy for the BSX series of materials.

Similarly, in the CSX compositional series, $Ca_{0.5}Sr_{0.5}Zr_4P_6O_{24}$ (CS-50) shows minimal thermal expansion anisotropy and hence it has the least amount of thermal expansion hysteresis associated with it. Figures 24 through 26 show the thermal expansion curves for the as-sintered and thermally cycled CSX materials. From these curves it can be noted that the highly anisotropic CS-25 and CS-37.5 materials show extensive shrinkage up to 150°C and anomalous expansion as they cool below 150°C. As with the BS compositions, the hysteresis associated with the CS materials decreases with the extent of cycling.

To understand better the difference in thermal hysteresis behaviors between the isotropic and anisotropic compositions, one specimen each of the isotropic type - BS-25 - and anisotropic type - CS-25 - was cycled 3 times to 1250°C in a He atmosphere. The results of these runs revealed that the BS-25 material has an average expansion of 0.5 ppm/°C over this temperature range, with very little difference from run to run. The hysteresis was small and the specimen returned to its original length after each run. On the other hand, the CS-25 test bars subjected to thermal cycling between 20°C and 1250°C in He atmosphere showed the expected anomalous expansion behavior below 150°C. This behavior was believed to be possibly due to room temperature micro-cracking. The phenomenon that furthered this belief was the continued expansion of the test specimen after it had cooled to room temperature (see Figure 27). This room temperature expansion was enhanced in the presence of room air (70% to 80% relative humidity) suggesting a possible reaction with either oxygen or water vapor. The

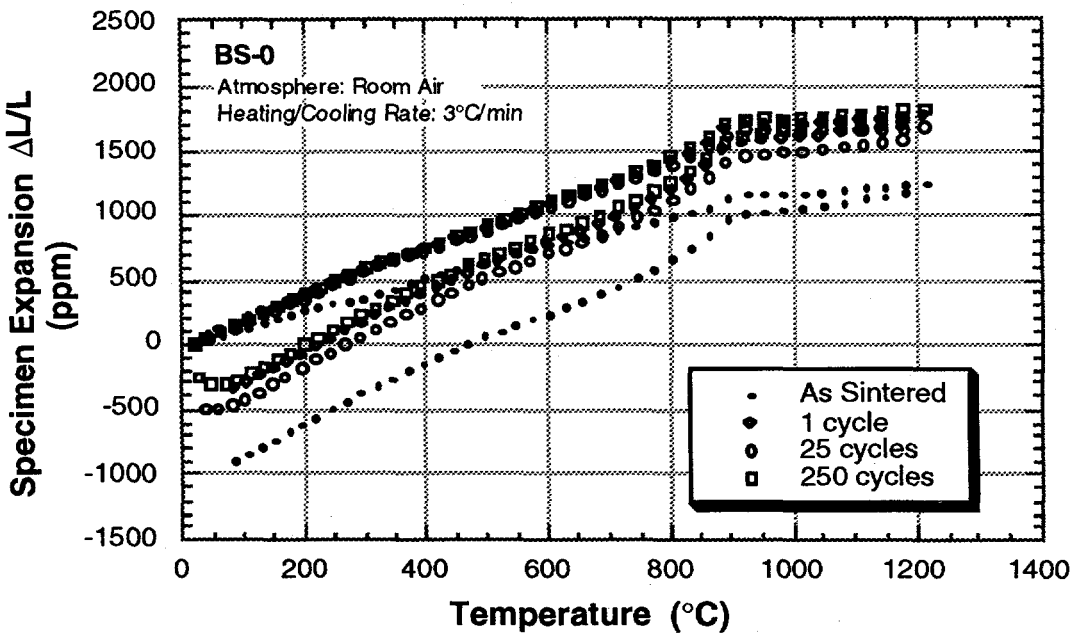

Figure 18. Effect of thermal cycling on the bulk linear thermal expansion of BS-0 material.

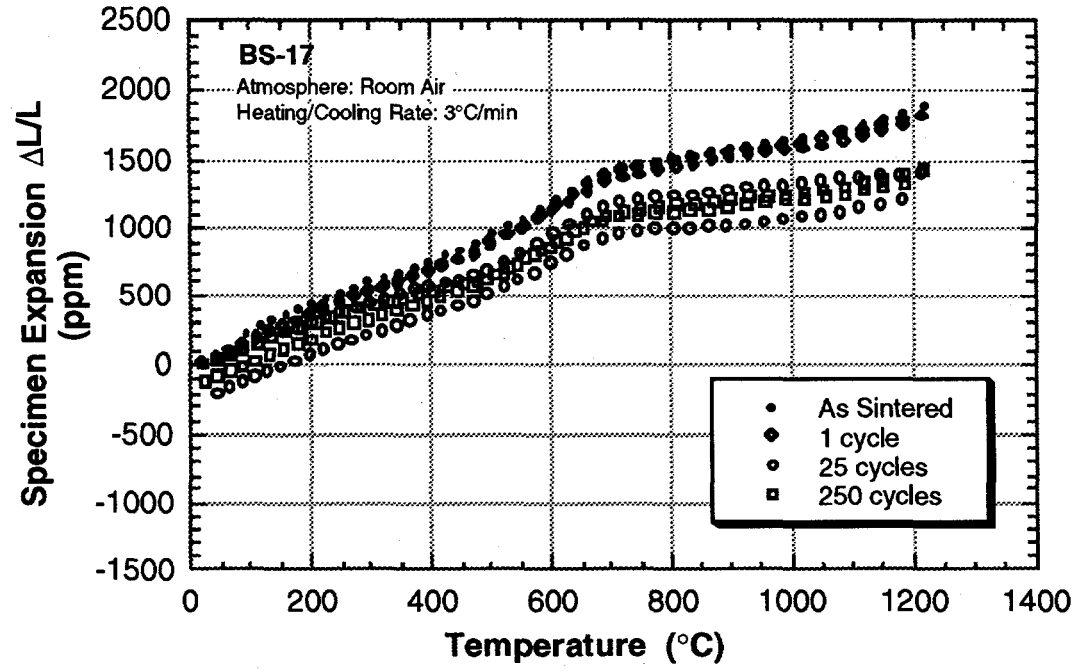

Figure 19. Effect of thermal cycling on the bulk linear thermal expansion of BS-17 material.

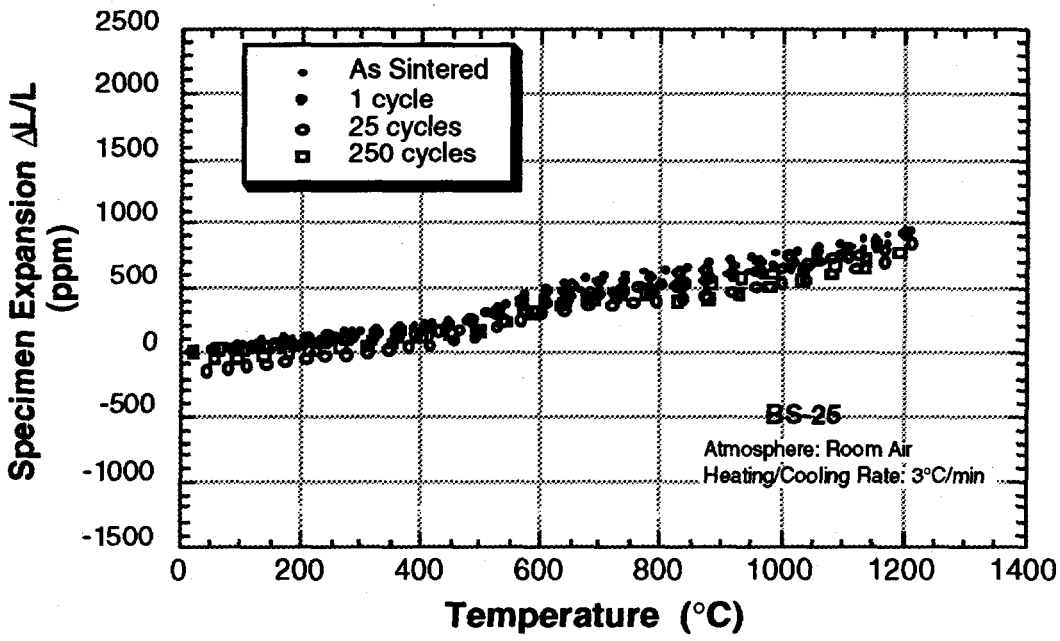

Figure 20. Effect of thermal cycling on the bulk linear thermal expansion of BS-25 material.

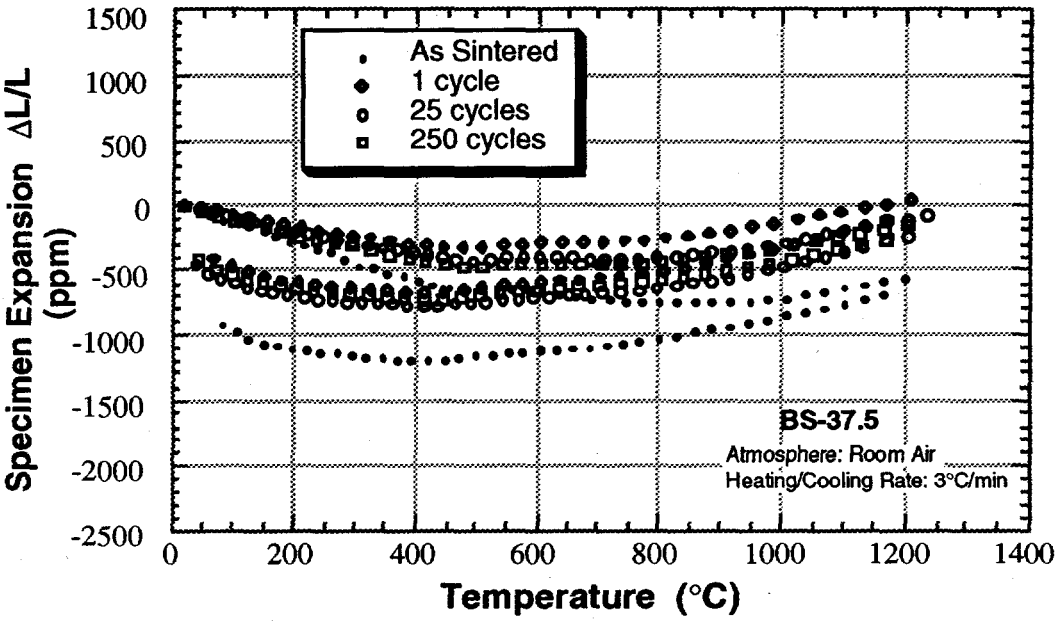

Figure 21. Effect of thermal cycling on the bulk linear thermal expansion of BS-37.5 material.

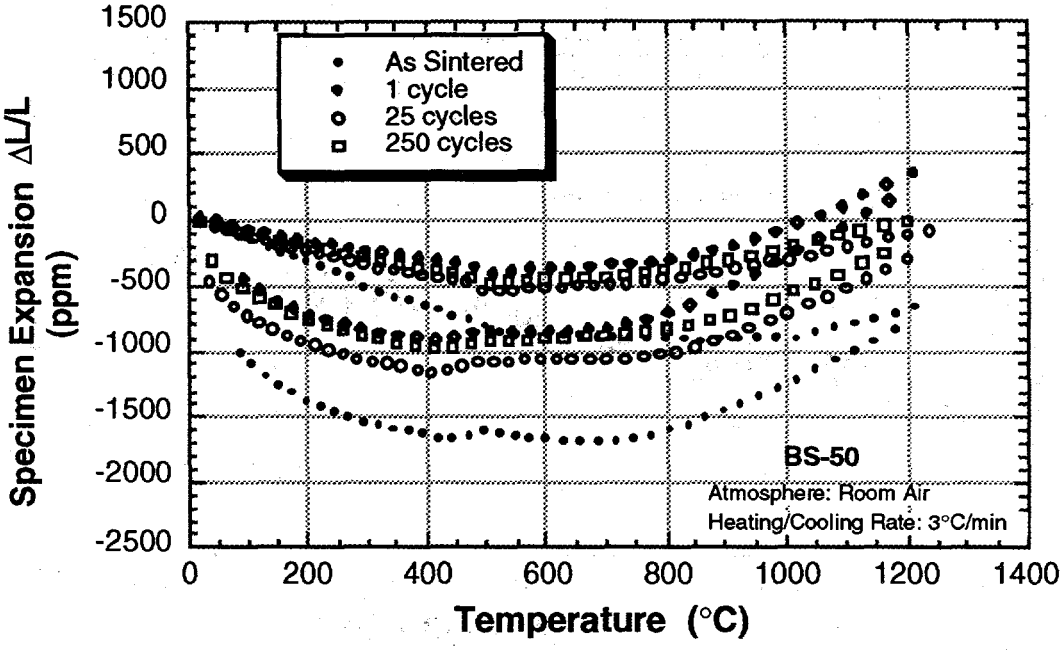

Figure 22. Effect of thermal cycling on the bulk linear thermal expansion of BS-50 material.

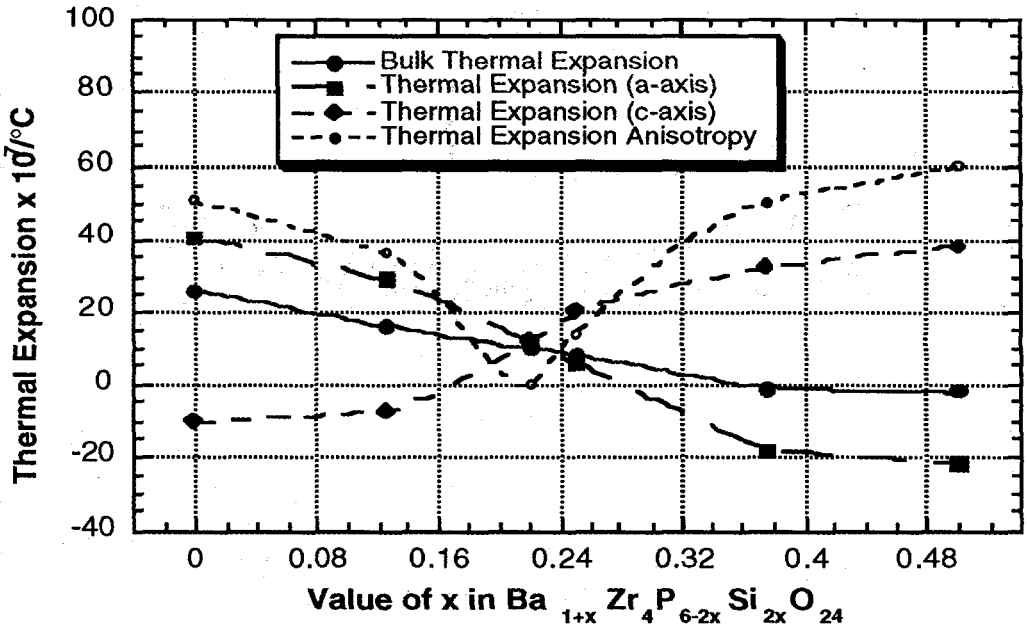

Figure 23. Thermal expansion anisotropy and the axial expansion of BSX as a function of composition (silicon content).

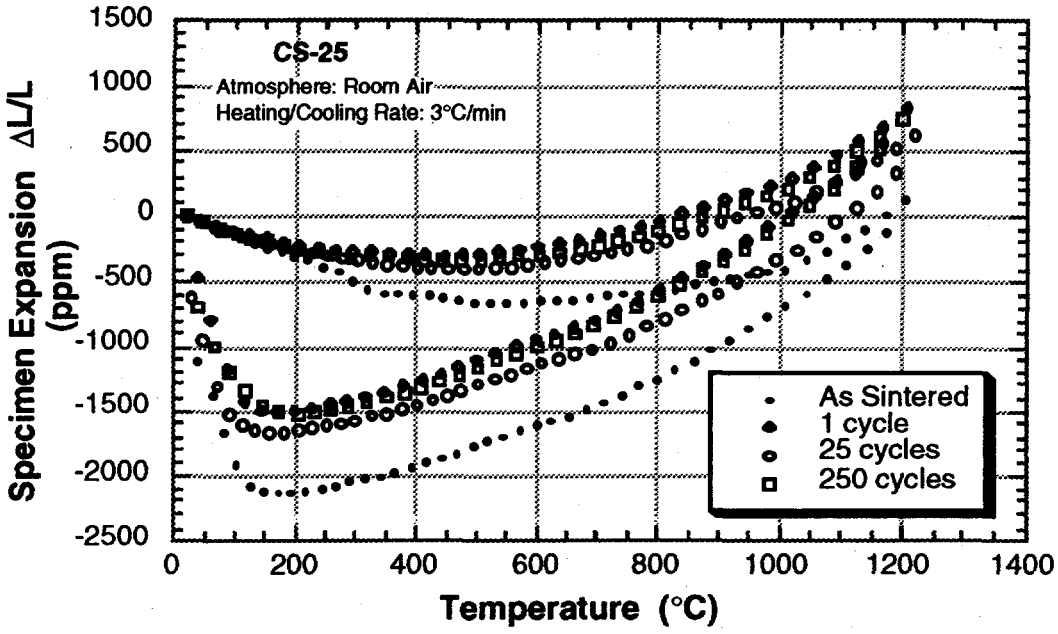

Figure 24. Effect of thermal cycling on the bulk linear thermal expansion of CS-25 material.

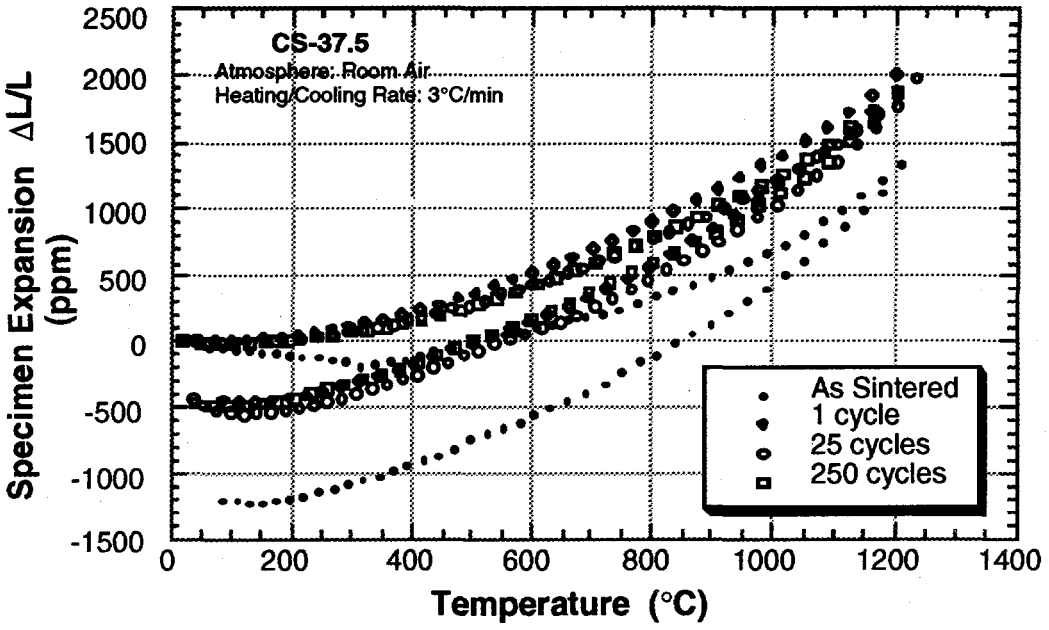

Figure 25. Effect of thermal cycling on the bulk linear thermal expansion of CS-37.5 material.

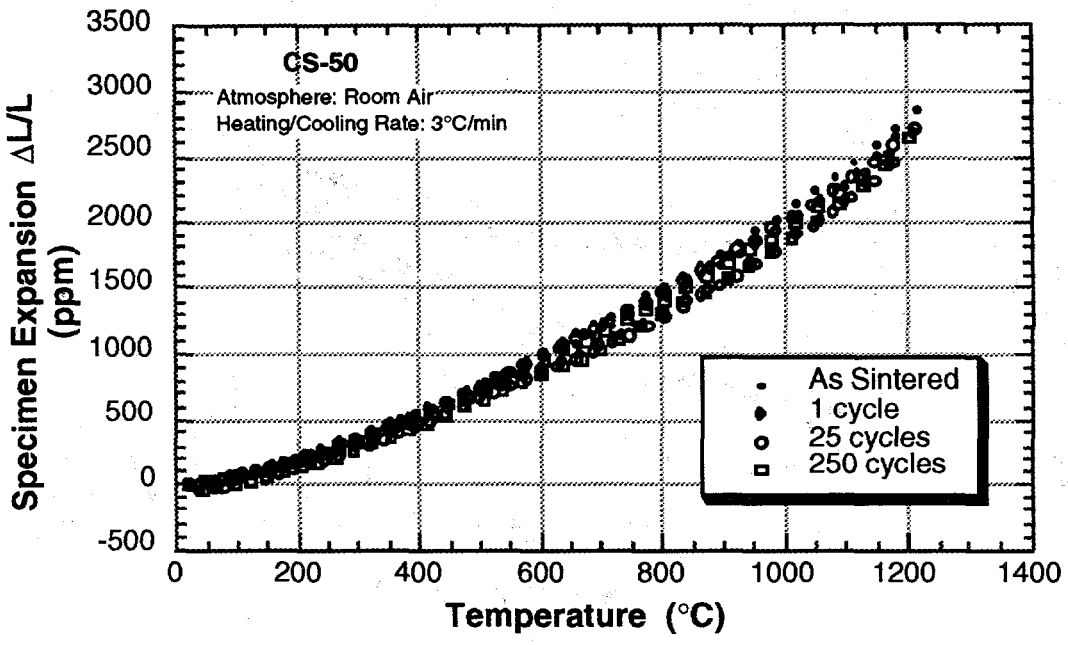

Figure 26. Effect of thermal cycling on the bulk linear thermal expansion of CS-50 material.

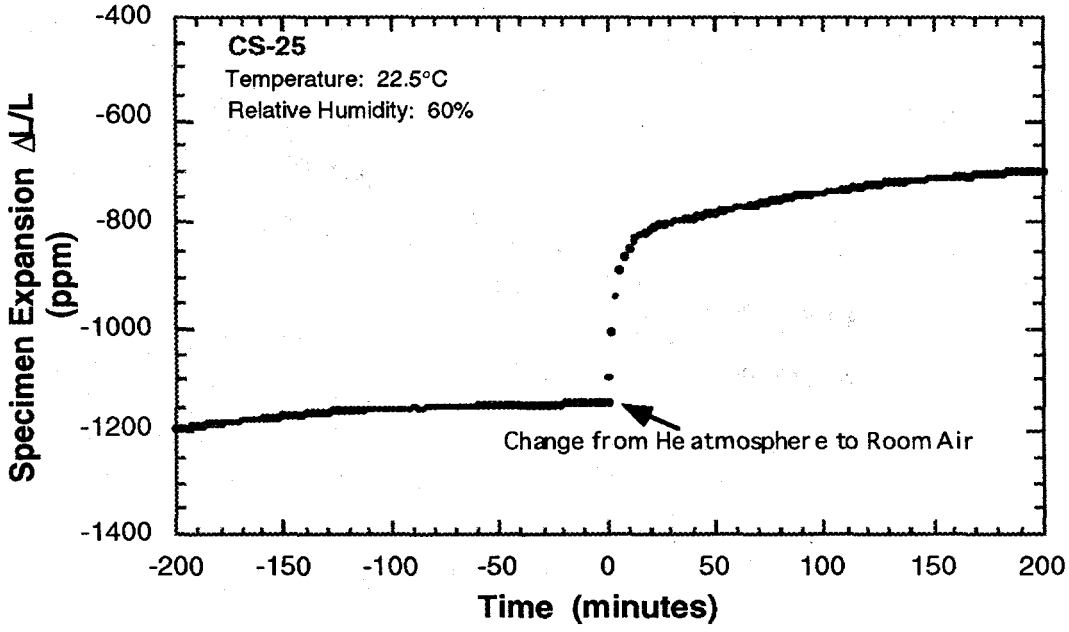

Figure 27. Room temperature expansion of CS-25 material in the presence of air.

specimen also exhibited considerable hysteresis and some permanent change in length. After 3 cycles between 20°C and 1250°C, measurement of the length of the test specimen after removal from the dilatometer revealed a decrease in length of 0.03 mm (corresponding to 0.12 percent).

With these results, it was conceived that the isotropic compositions (BS-25 and CS-50) have little or no microcracking associated with cooling from either the sintering temperature or the heat treatment temperature. Without the presence of microcracking there is very little thermal hysteresis and thus very reproducible thermal expansion curves. Whereas, the anisotropic compositions (BS-0, BS-37.5, BS-50, CS-25, and CS-37.5) microcrack upon cooling from the sintering temperature and thus have thermal expansion curves with varying amounts of hysteresis.

In the BSX compositions, it was speculated that many of the microcracks close above 1200°C and the intergranular stresses due to thermal expansion anisotropy are not strong enough to open the microcracks at room temperature. As a result there is net shrinkage associated with thermal cycling. During subsequent cycles, the number of microcracks closing would be less and hence there is less shrinkage associated with the second cycle and so on during the cooling process.

In the case of CSX compositions, the intergranular stresses during cooling may be strong enough that some of the microcracks tend to open up and lead to expansion during cooling. The difference in these shrinkages is very pronounced when CS-25 and CS-37.5 are compared. CS-25 has the larger anisotropy compared to CS-37.5, hence, the hysteresis as well as intergranular stresses are very large for CS-25. Accordingly, the "knee" at 150°C is also very pronounced for CS-25 as compared to CS-37.5 (see Figs. 24 and 25). Further investigation of the variation in the measured bulk linear thermal expansion when comparing measurements made on as sintered specimens to measurements made on thermally cycled specimens will be discussed in the next two sections.

In addition to the above discussed, a systematic literature search was carried out and all the thermal expansion data (bulk as well as axial thermal expansion for various compositions) have been compiled. This data is being maintained at LoTEC as a Microsoft Word file formatted for Macintosh and is available upon request.

Microstructural Considerations. Preliminary SEM examinations were carried out on fracture surfaces of flexure tested specimens of three CSX compositions viz. CS-25,

CS-37.5, and CS-50 and one BSX composition - BS-25. The fracture mode in each of these compositions was generally transgranular. The fracture surface of the BS-25 specimen revealed very little micro-cracking which is consistent with the low thermal expansion anisotropy of this material. On the other hand, from the CSX samples the following was observed; more internal cracking (micro-cracks) in the CS-25 material with lesser amounts in CS-37.5 and very little in the CS-50. These observations confirm that the anisotropic compositions CS-25 and CS-37.5 are associated with microcracking behavior. Such microcracks likely formed during cooling of the sintered specimens to room temperature. Microcracking in the anisotropic materials (CS-25, CS-37.5 etc.) also explains their much lower fracture strengths as compared to the isotropic ones (CS-50, BS-25 etc.).

To examine further the microcracking behavior during thermal cycling, fracture surfaces of selected isotropic - BS-25 and CS-50 - and anisotropic - BS-0, BS-50 and CS-25 - flexure specimens that were either as-sintered or thermally-cycled (up to 250 cycles at 1250°C) were observed using scanning electron microscopy (SEM). SEM was used to evaluate structural changes in the various compositions due to thermal cycling to 1250°C in a room air environment. The thermal cycling process consisted of placing the fractured bars in crucibles made from that [NZP] composition and placing the crucibles in a furnace, and heating and cooling according to the following schedule:

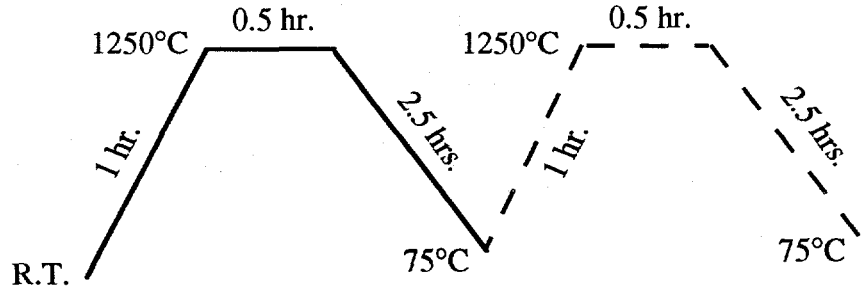

Figures 28 to 32 compare the microstructure (morphology) of the as-sintered specimens with the specimens cycled 250 times for the studied compositions. In the BSX series, there are two anisotropic compositions - BS-0 and BS-50 (Figs. 28, 30) - with either positive or negative bulk thermal expansion, respectively, and one isotropic composition - BS-25 (Fig. 29) - with a very low positive bulk thermal expansion. Evidence of microcracking is seen in the anisotropic compositions, both in the as-sintered and thermally cycled condition. This microcracking accounts for the low mechanical

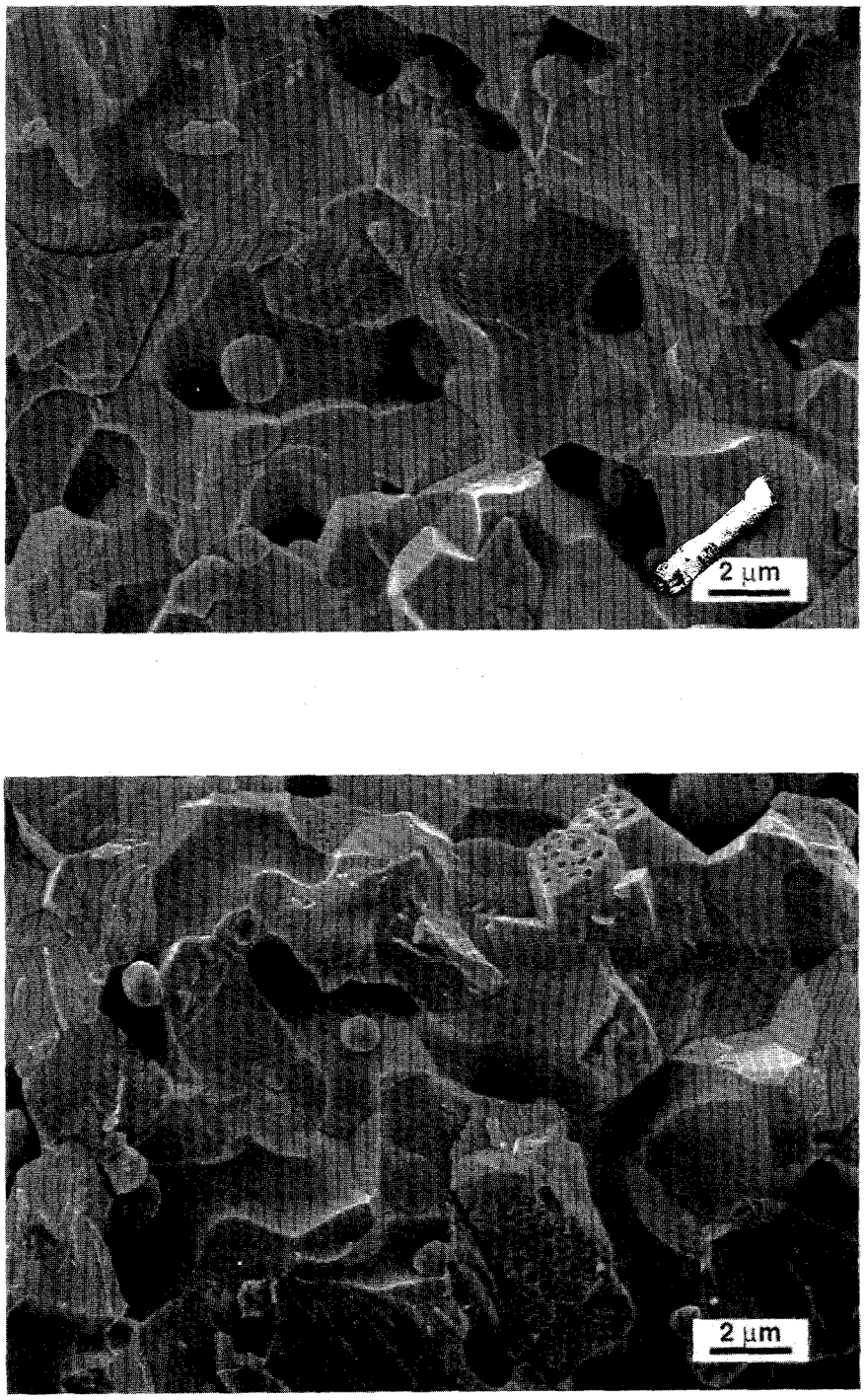

Figure 28. SEM fracture surface microstructures of (a) as-sintered and (b) thermally cycled (250 cycles to 1250°C) BS-0 specimens.

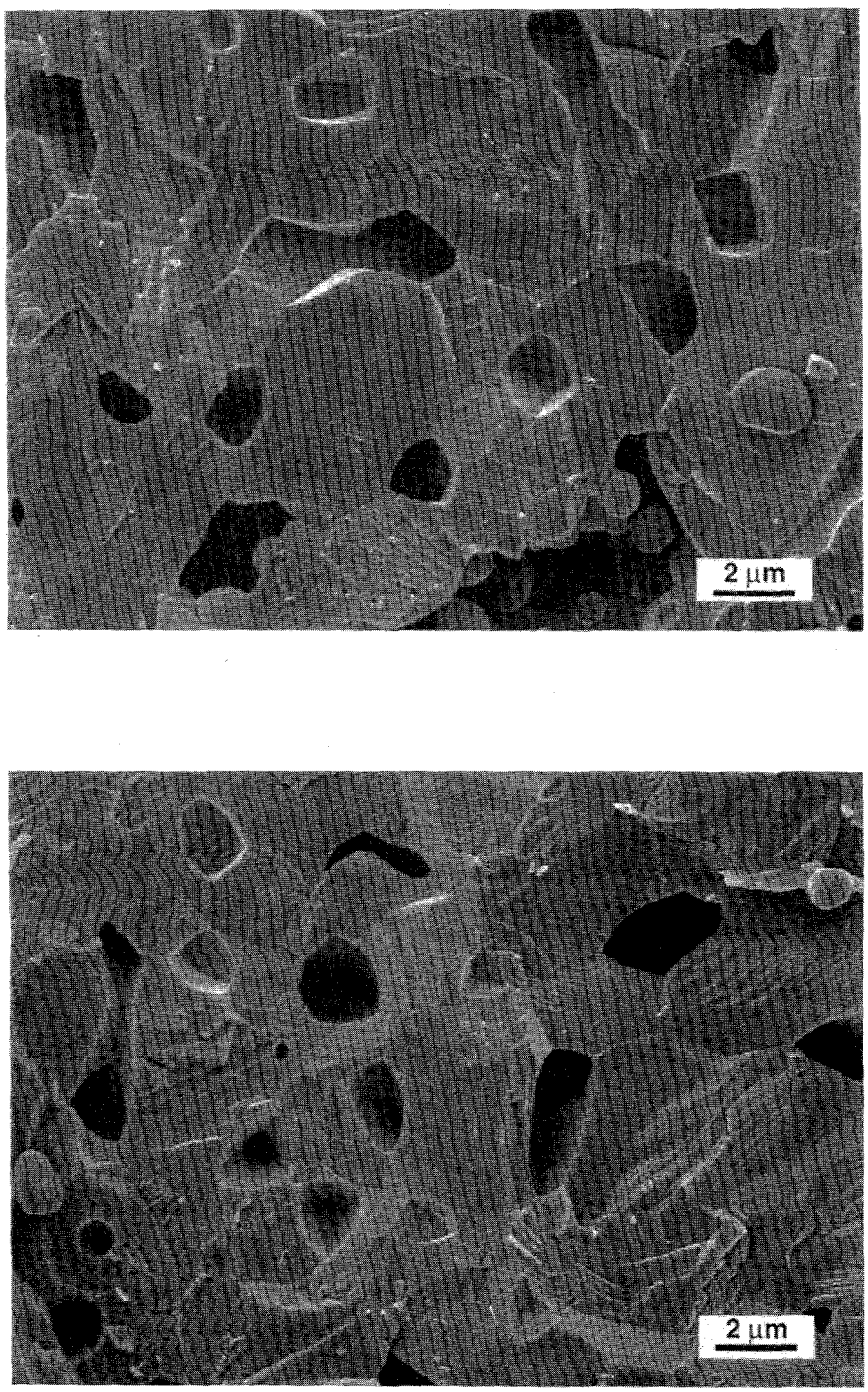

Figure 29. SEM fracture surface microstructures of (a) as-sintered and (b) thermally cycled (250 cycles to 1250°C) BS-25 specimens.

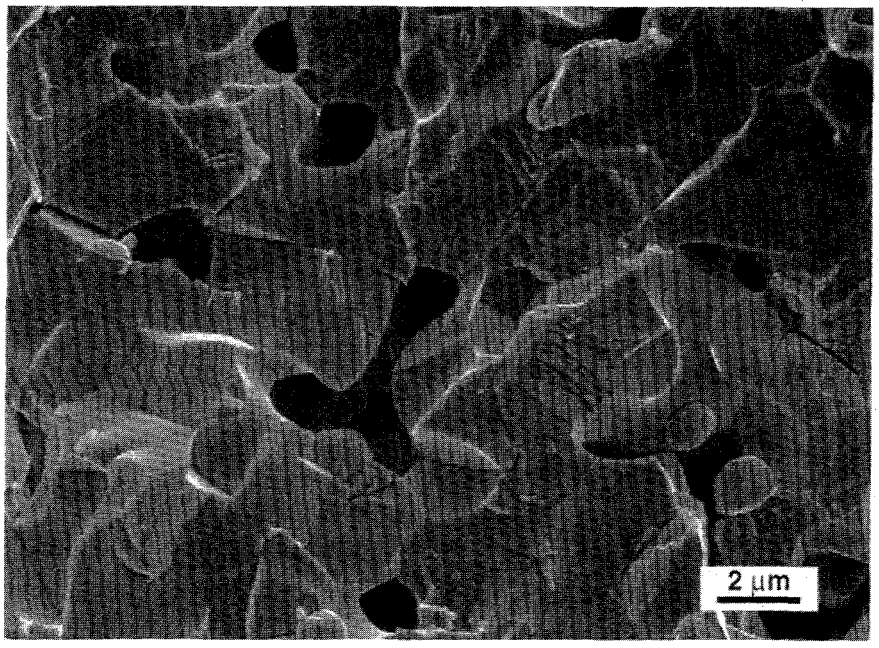

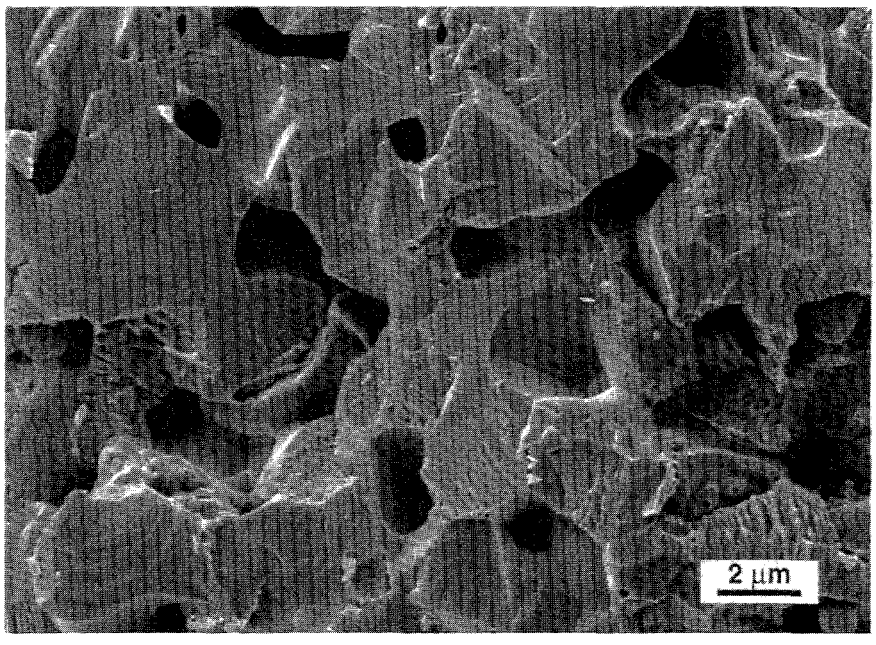

Figure 30. SEM fracture surface microstructures of (a) as-sintered and (b) thermally cycled (250 cycles to 1250°C) BS-50 specimens.

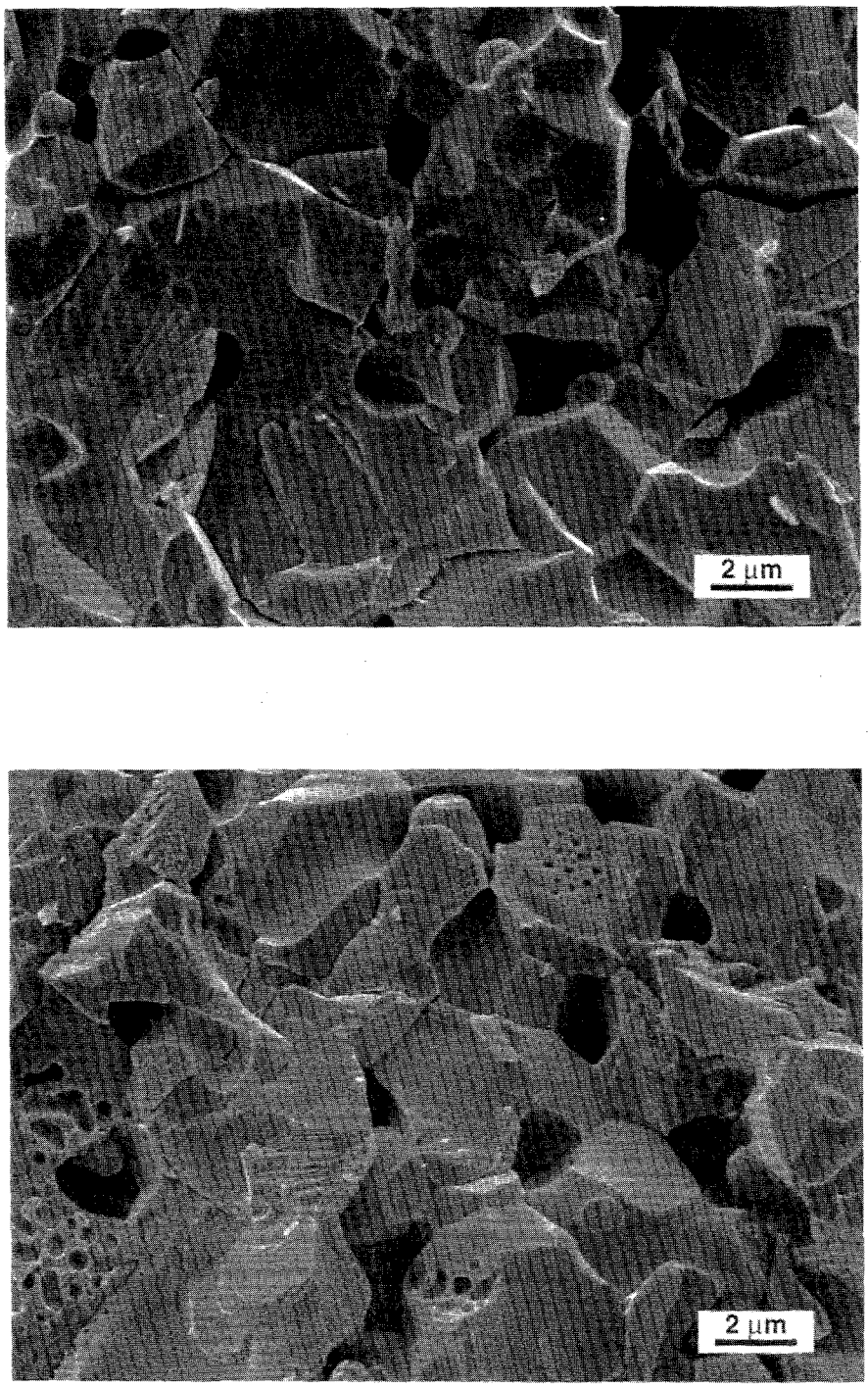

Figure 31. SEM fracture surface microstructures of (a) as-sintered and (b) thermally cycled (250 cycles to 1250°C) CS-25 specimens.

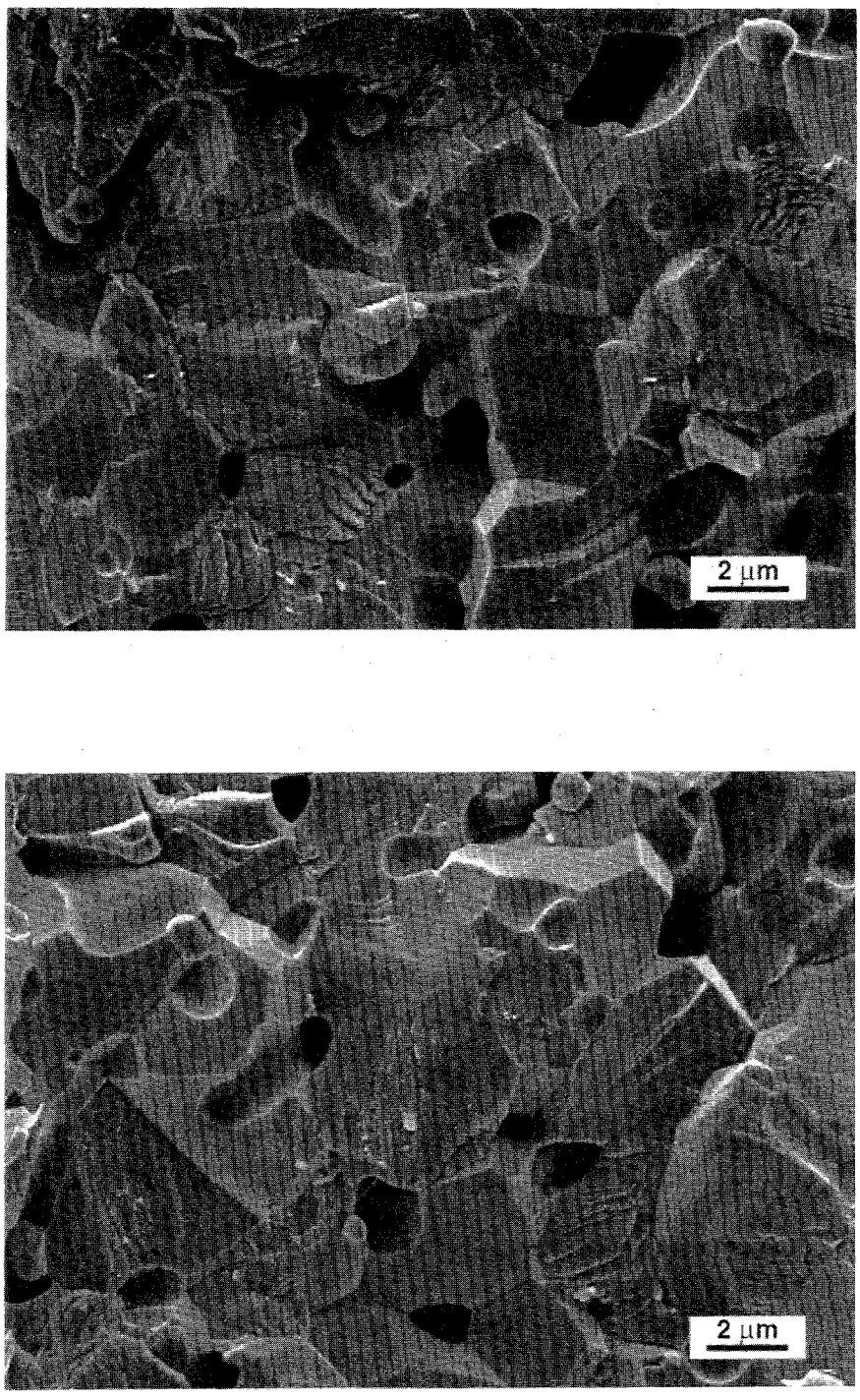

Figure 32. SEM fracture surface microstructures of (a) as-sintered and (b) thermally cycled (250 cycles to 1250°C) CS-50 specimens.

strengths of the anisotropic compositions, discussed earlier in this report. There is little evidence of microcracking in the BS-25 specimen even after 250 cycles to 1250°C. The observed porosity is consistent with the 85-90% theoretically dense specimens. An unexpected but significant feature of the microstructures is the fine porosity (cavitation) developed in the anisotropic compositions, BS-0 and BS-50, when subjected to thermal cycling. It is believed that this porosity, which has a similar appearance to that found in tensile creep specimens, is due to the anisotropic axial thermal expansion and the internal stresses developed between individual grains during thermal cycling. However, cavitation is not evident in the BS-25 specimen.

The microstructures of the CSX series specimens yielded results similar to those of the BSX compositions (see Figs. 31 and 32). Again, microcracking and cavity formation were found in the anisotropic CS-25 material while there was no evidence of microcracking or cavity formation in the isotropic CS-50 composition.

Environmental Effects (Moisture, Temperature) As stated before there was substantial variation in bulk thermal expansion of anisotropic, microcracked compositions. Upon cooling from the sintering temperature, the ceramic microcracks due to the stresses associated with the anisotropic axial thermal expansion of the individual ceramic grains. The microcracks are further opened by the absorption of moisture from either the air or when the ceramic is ground into test specimens in a manner similar to stress corrosion cracking observed in other ceramic materials. When the test specimen is reheated during the thermal expansion measurement the absorbed moisture is driven off and the microcracks close. Further heating promotes microcrack healing. Taken together this explains the apparent lower bulk thermal expansion obtained for the as sintered and ground specimens. If the subsequent thermal expansion measurements are made shortly after the heat treatment, before any substantial amount of moisture is reabsorbed, consistent results should be obtained. This view finds corroboration in the almost identical expansion curves of Figure 24 for an anisotropic material, such as CS-25, subjected to 1 and 250 thermal cycles between room temperature and 1250°C.

To test the hypothesis that it is moisture that promotes crack opening, the following experiments were performed. An anisotropic (CS-25) specimen was heated and cooled in a dilatometer surrounded by an inert (helium) atmosphere. When the specimen reached an equilibrium length during cooling (close to room temperature), the helium atmosphere

was displaced by dry air. Next, air with controlled relative humidity was allowed to surround the specimen. With each increase in relative humidity there was a corresponding increase in specimen length. Finally, the dilatometer was carefully opened and water was dripped on to the specimen; this resulted in a sharp increase in the specimen length. The results of this experiment are shown in Fig. 33.

The above said experiment was performed using an isotropic behavior (CS-50) specimen. Since the isotropic material returns to its original length by the time it cools down to room temperature and there are not any microcracks present to open up, moisture had virtually no effect on the CS-50 specimen. To determine if the other anisotropic compositions like BS-0 and BS-50 exhibited similar behavior as that of the CS-25 specimen, they were heated and cooled in the dilatometer, which was then followed by controlled application of drops of water. The results obtained for all the anisotropic materials - BS-0, BS-50 and CS-25 - are shown in Fig. 34 and contrasted with that for isotropic BS-25. Figures 35(a) and (b) (results derived from verisimilar experiments) provide a closer look into the moisture-assisted microcracking behavior of the BS-0 material.

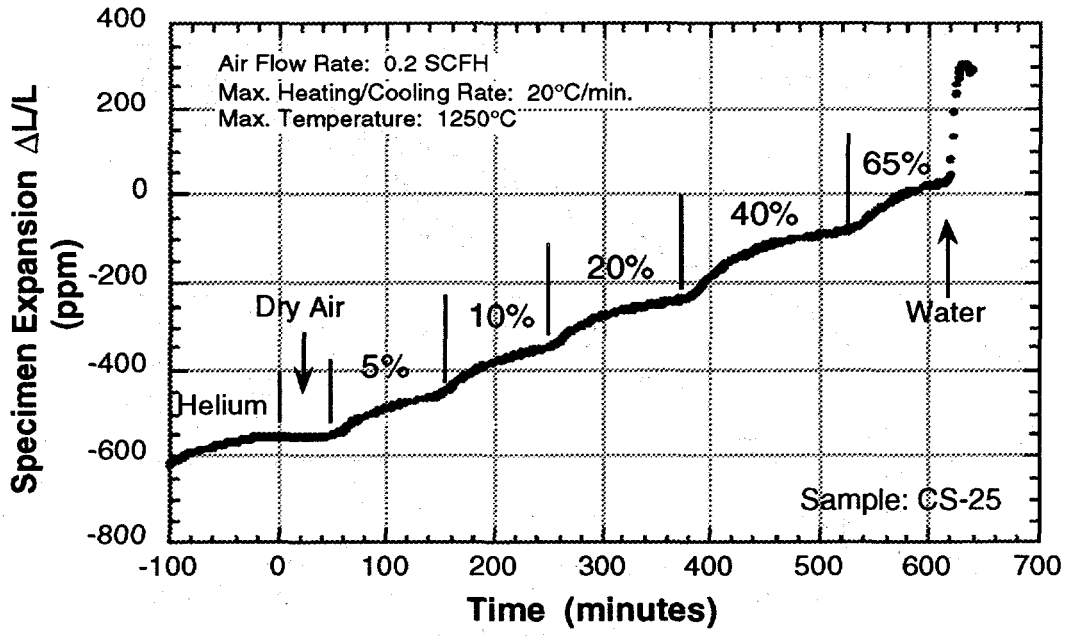

Figure 33. Moisture-assisted microcracking of anisotropic composition CS-25.

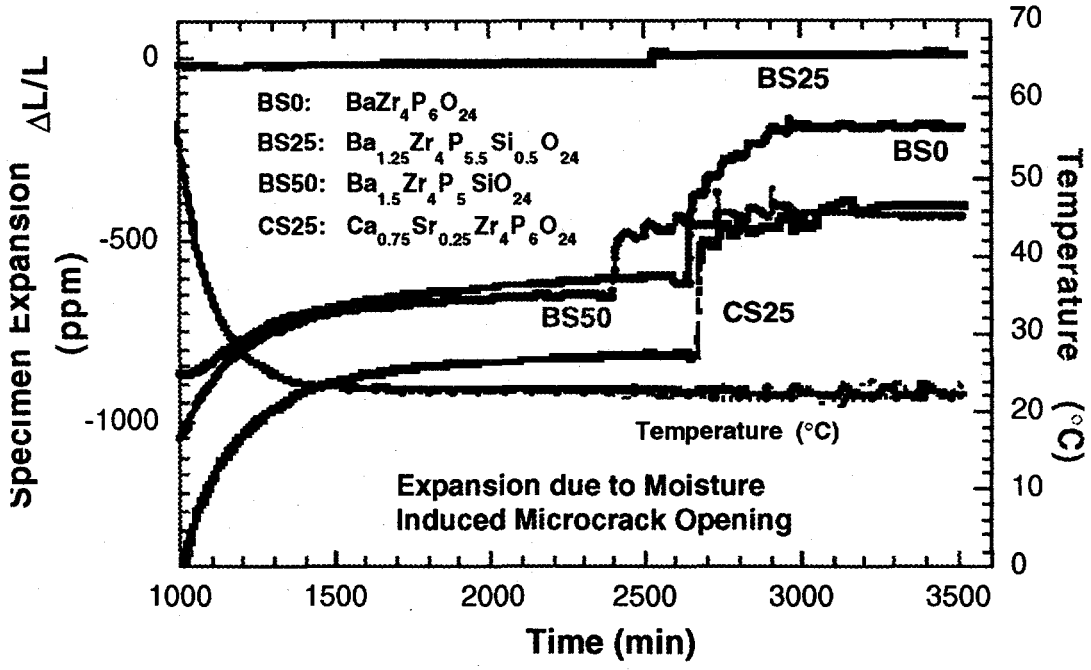

Figure 34. Environmental Effect on Room Temperature Expansion of various NZP compositions.

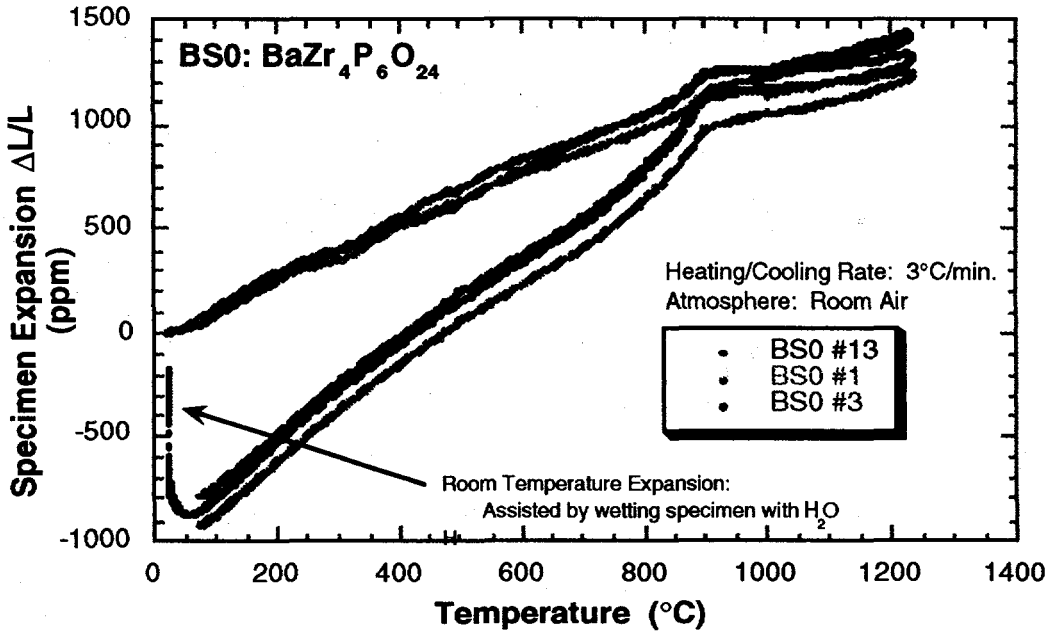

Figure 35(a). Environmental Effect on Room Temperature Expansion of BS-0.

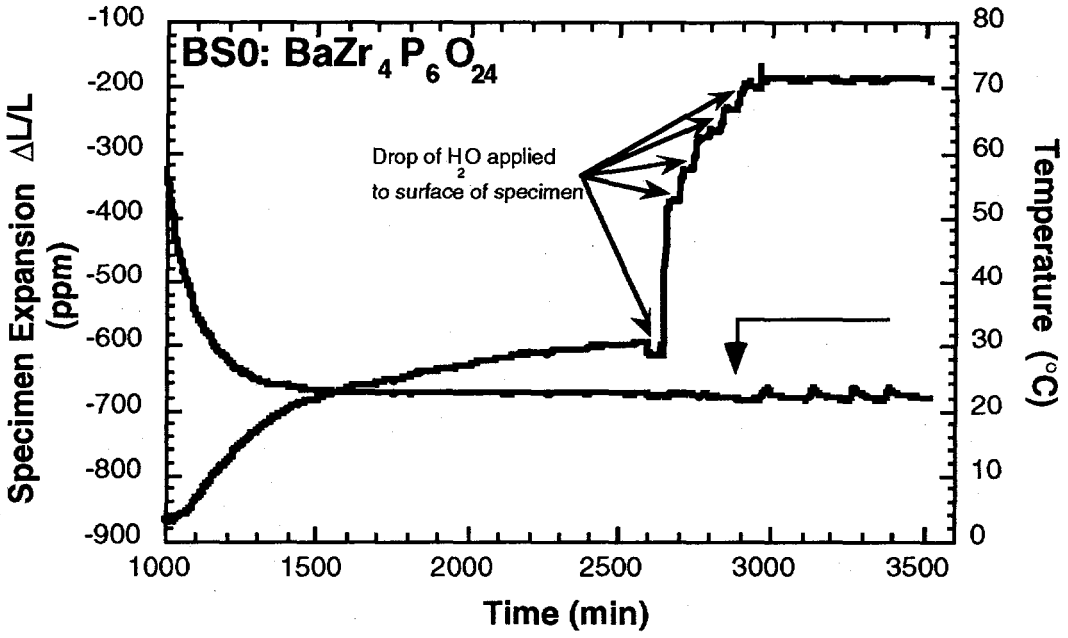

Figure 35(b). Environmental Effect on Room Temperature Expansion of BS-0.

To determine if there was any chemical change (hydration) associated with the absorption of water, powder X-Ray diffraction analysis was performed. A sintered test specimen was crushed to form a fine powder. A portion of this powder was heated to 1000°C to drive of any moisture present and then x-rayed. A similar amount of powder was mixed with water, allowed to dry and then x-rayed. The powder diffraction patterns for the two samples are shown in Fig. 36. It was not possible to detect any secondary phases by this analytical method.

Thermal Stability

Long-term thermal stability of the BSX and CSX compositions were assessed by cycling samples between room temperature and 1250°C for up to 250 times and measuring weight changes, especially weight loss due to reduction. All compositions tested showed very little weight loss indicating good thermal stability. However, the anisotropic materials revealed slightly greater losses than the isotropic ones (BS-25 and CS-50) after the first thermal cycle. Further cycling (up to 250 cycles) resulted in less than 0.05 percent weight loss in all compositions. The greater weight loss of the anisotropic samples after the first cycle could be attributed to the loss of moisture,

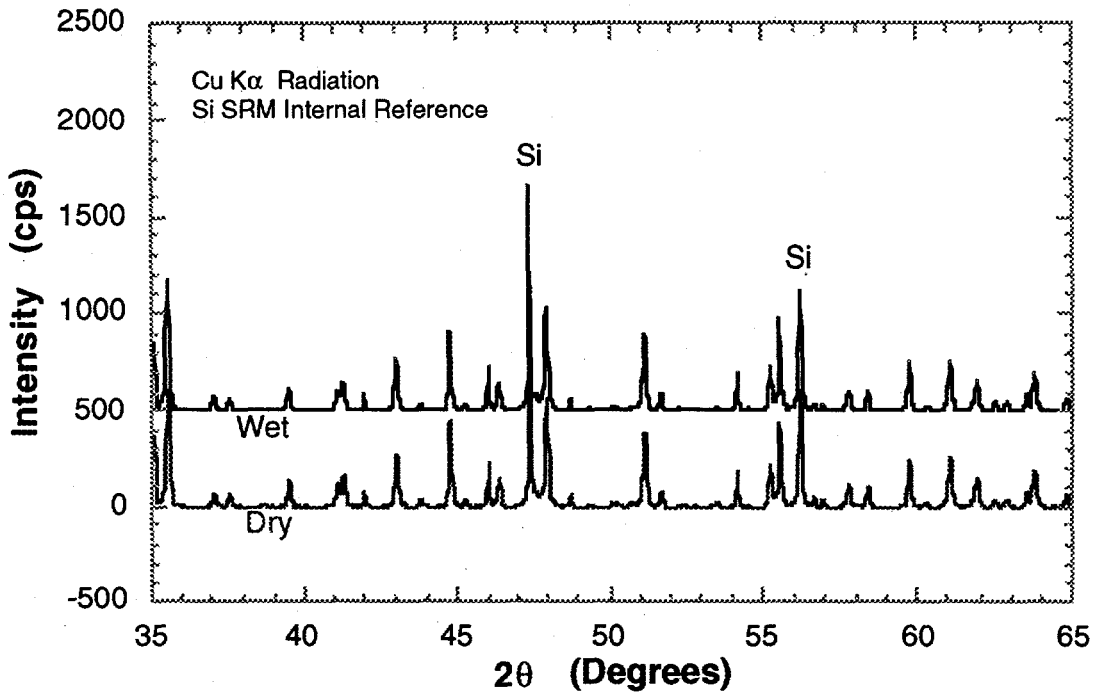

Figure 36. Powder X-ray diffraction patterns of "As-Sintered" and "Moisture-treated" CS-25 material.

organic solvents (absorbed during specimen grinding process) present in the microcracks, and any low volatile phosphates etc. Figure 37 depicts normalized weight loss as a function of the number of cycles. The weight loss has been normalized to the weight of the specimens after 1 cycle to 1250°C. In future work, X-ray analysis will be conducted to ensure presence of the original NZP phases after thermal cycling.

Thermal Shock Resistance

Thermal shock tests were conducted on the BSX compositions in two ways: first, by quenching the samples from progressively higher temperatures into a bath of liquid nitrogen until the samples (macro) cracked; and second, by cyclically quenching BS-25 bar samples previously heated to 1250°C into water at 2°C for up to 50 cycles and measuring the residual strengths of the bars in four-point flexure.

The results of the first test are summarized in the bar plot of Figures 38 (ΔT in Fig. 38 represents the maximum temperature drop that could be survived). As expected,

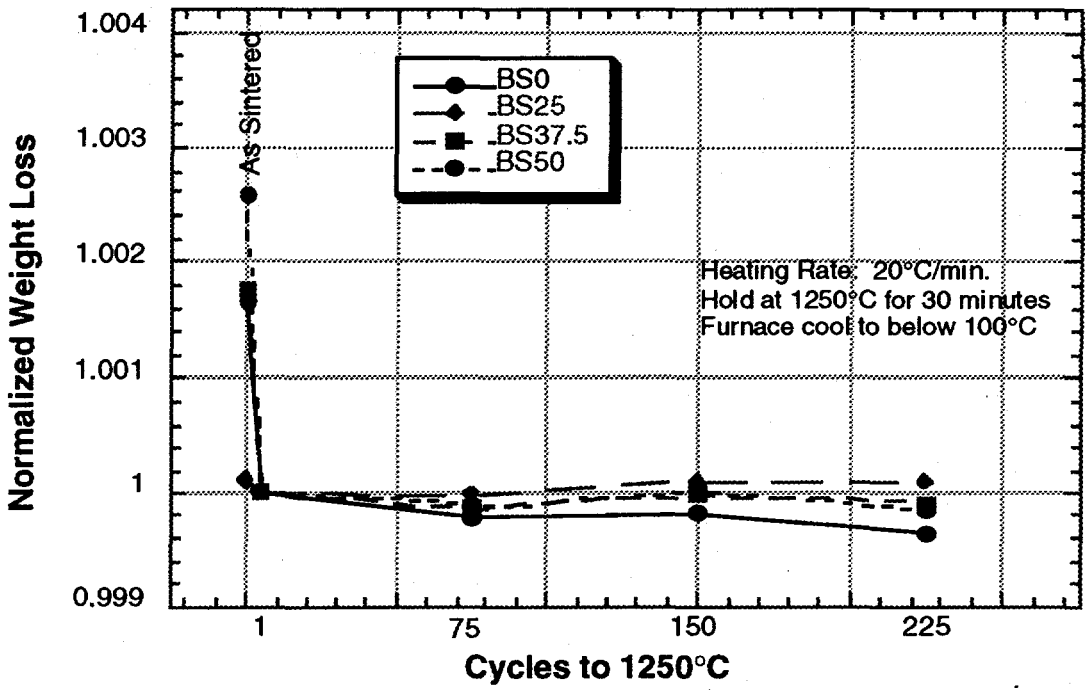

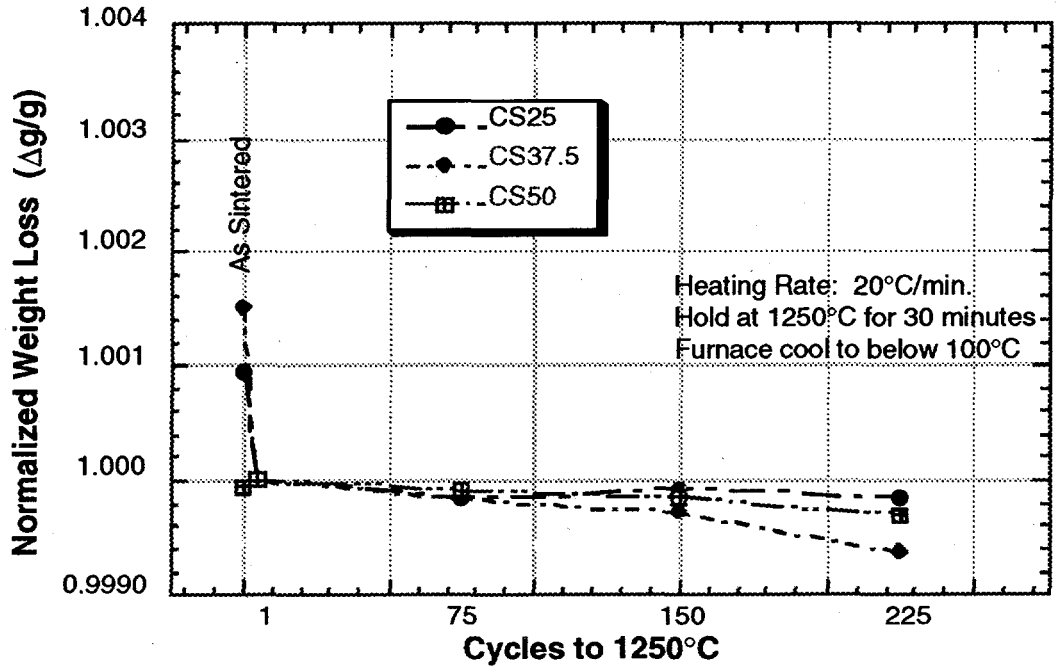

Figure 37 (a) & (b). Normalized weight loss as a function of cycles to 1250°C for the (a) BSX and (b) CSX compositions.

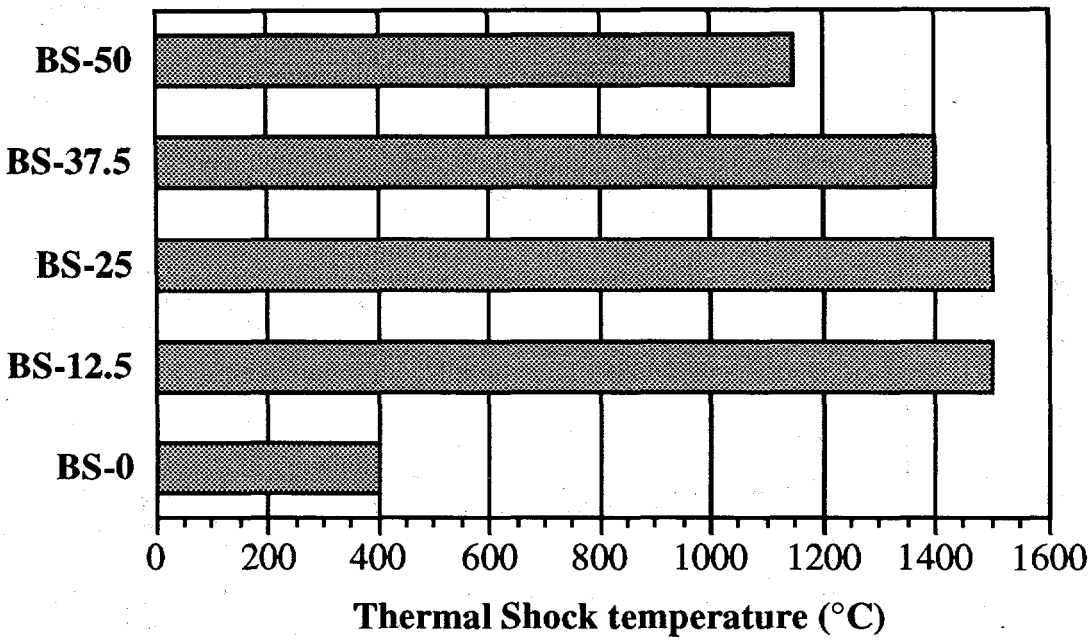

Figure 38. Maximum survivable thermal shock temperature for the BSX compositions.

isotropic compositions of the BSX series showed excellent thermal shock resistance as compared to the anisotropic ones, especially BS-37.5. Microcracking (which causes thermal expansion anisotropy) in the anisotropic compositions results in deterioration of these materials during thermal shock testing. However, of the anisotropic materials, the rather poor properties of BS-0 as compared to either BS-37.5 or BS-50 is likely related to its positive coefficient of thermal expansion as compared to the negative coefficients of the other two.

Figure 39 is a plot of the residual (four-point flexure) strengths of the cyclically thermal shocked samples for between 0 and 50 cycles. An interesting feature of the results is that the residual strengths of the samples quenched 10 cycles is about 2.5 times greater than the strengths of the as-sintered samples. This is thought to be due to the formation of a surface compressive layer of optimum thickness, which is in turn the result of freezing a lower thermal expansion high temperature NZP phase during quenching from 1250°C. Advantage could be taken of this phenomenon to strengthen NZP ceramics for various applications. Investigation of thermal shock resistance as a function of composition and any strengthening phenomenon in the CSX series materials is being currently carried out.

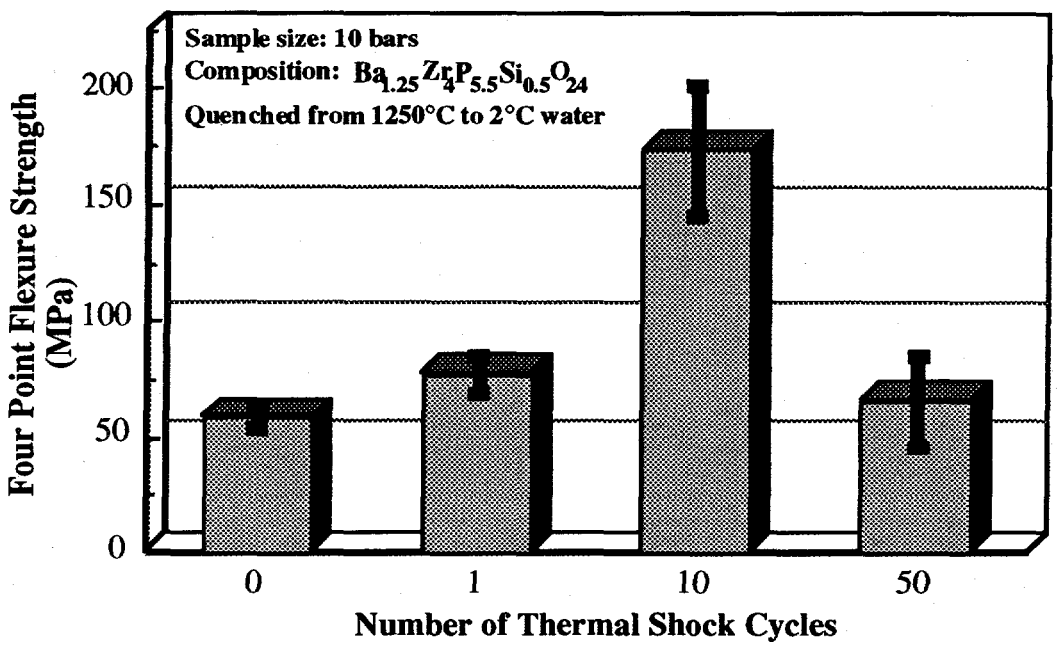

Figure 39. Residual flexure strengths of cyclically thermal shocked BSX specimens.

High Temperature Elastic Modulus

For this work, the BS-25 material alone was subjected to high temperature elastic modulus measurements during Phase I work. These measurements were performed using an ultrasonic measurement technique at Penn State University. In this procedure, a bar sample of the BS-25 ceramic was suspended in a furnace by two sapphire threads acting as ultrasonic waveguides, connected to two transducers, one acting as a source and the other as receiver. The temperature was raised slowly to 1325°C and the resonance frequency was noted at 100°C intervals. The Young's modulus was calculated from:

$$E = \frac{0.94645\ Cmf^2}{W} \quad \text{.....(3)}$$

In Equation (3), C is a constant that depends upon the Poisson's ratio, υ, specimen thickness, t, and length, l; and m is the mass; f is the flexural resonance frequency; and W is the width. Here the Poisson's ratio, υ, was assumed to be 0.23.

Figure 40 represents a plot of the elastic modulus of BS-25 as a function of temperature. It can be noted that the modulus is nearly the same at 1200°C as at room temperature. As seen in the figure, the Young's modulus increases with temperature due

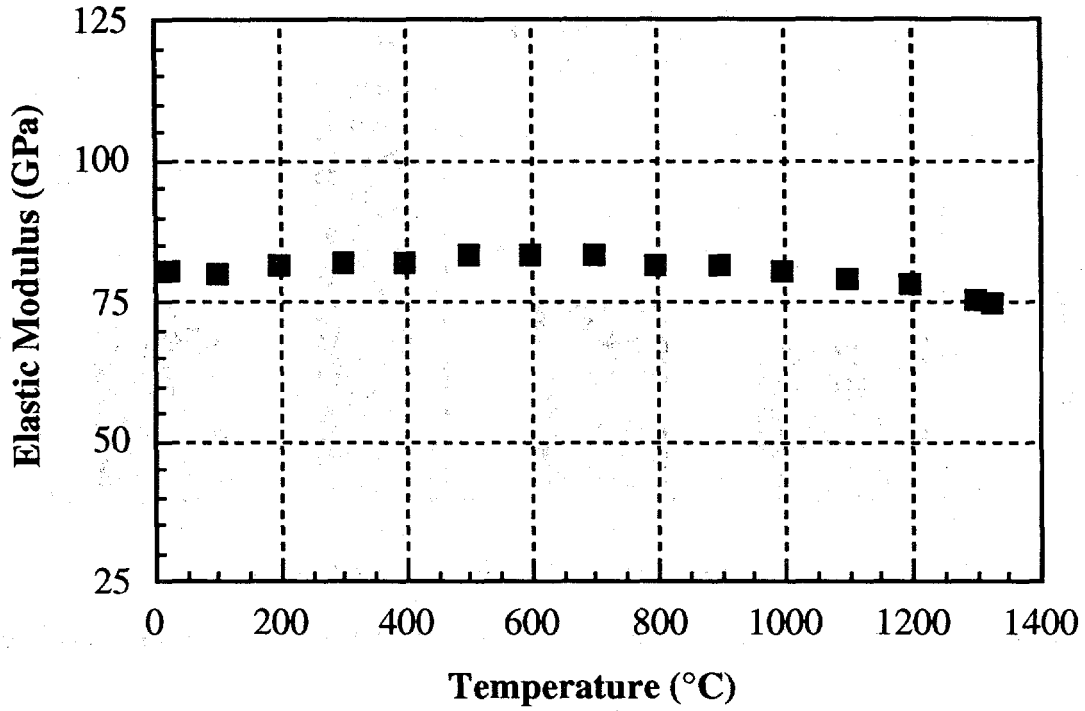

Figure 40. Elastic modulus of BS-25 as a function of temperature.

to the healing of microcracks, reaches a maximum between 500 and 700°C and then decreases as the temperature increases further. Measurements of high temperature elastic modulus of CS-50 and other materials have been planned for the Phase II part of this research.

MATERIALS AND PROCESSES' DEVELOPMENT

The materials and processes intended to be developed in this Phase I work included: (i) metal-NZP ceramic composites with the metal cast around the ceramic, (ii) alternative shape forming process such as pressure slip casting and gel casting, (iii) ultrasonics-based ND flaw detection technique, (iv) new low thermal expansion NZP compositions, and (iv) acoustic emission based microcrack detection process. The former three tasks were carried out on site and the latter two at Penn State University.

Molten Metal Casting Trials

One of the primary goals of this project is the demonstration of the ability to cast molten metal around a (NZP) type ceramic shape without causing damage to the ceramic or the solidified metal casting. Based on the results of characterization of the various NZP ceramic compositions, the mechanically and thermally superior BS-25 ($Ba_{1.25}Zr_4P_{5.5}Si_{0.5}O_{24}$) and CS-50 ($Ca_{0.5}Sr_{0.5}Zr_4P_6O_{24}$) materials were selected for the metal casting trials. These compositions have ultra-low and low coefficients of thermal expansion (the average CTE of BS-25 from room temperature to 1000°C is 0.7 x 10^{-6}/°C and for CS-50 over this range is 1.9 x 10^{-6}/°C.), respectively, and very low thermal expansion anisotropy. The ceramic test shapes were straight or 90°- elbow tubes with an outside diameter of approximately 50 mm, with a 5 mm wall thickness.

Initial metal casting trials with both the BS-25 and CS-50 ceramic tubes resulted in failure of the ceramic due to the large compressive stresses. These stresses were, in turn, created by the thermal expansion mismatch between the metal and the ceramic. As pointed out in an earlier section (Materials Requirement Analysis), finite element analysis of the metal casting process revealed large compressive stresses in the NZP ceramic-metal system. All these clearly demonstrated the need for reduced elastic modulus (increased strain to failure of the ceramic port liner) or providing a compliant layer to avoid large compressive stresses that would lead to the failure of the ceramic. To ensure that the ceramic survives the shrinkage stresses associated with the metal casting process, a test matrix approach was developed. Table 7 provides the details of this test matrix to improve the survivability of the ceramic during the metal casting.

Preliminary work on the lines of the summary in Table 7 involved the introduction of a compliant layer between the metal (cast iron or aluminum) and the ceramic (BS-25). The compliant layer was designed to absorb the thermal stresses (generated during cooling from a high temperature) associated with the thermal expansion mismatch between the ceramic and the metal. All of the casting trials involving the compliant layer were successful, demonstrating the ability to cast the ceramic in place. A crude test was performed to determine the impact resistance of the ceramic within the metal casting. The metal/ceramic composite tube was dropped repeatedly from approximately 2 meters height on to a concrete block. The ceramic tube was checked for cracks, chipping, and any loosening from the surrounding metal. There was no apparent damage to the ceramic, which is indicative of the beneficial effects of the compliant layer.

Table 7. Planned tests for improving NZP-ceramic survivability during the metal casting process.

Variables	Methods/Techniques	Comments
I. Elastic Modulus	a. Introduce porosity *Acicular* *Plate shaped* b. Reduce Sintering Temp. c. Microcracking $BaZr_4P_6O_{24}$ $Ca_{0.75}Sr_{0.25}Zr_4P_6O_{24}$ $Ba_{1.5}Zr_4P_5SiO_{24}$	Will reduce modulus however, will also reduce the strength
II. Compliant Layer	a. Porous coatings b. Thermal spray coatings c. Hollow spheres d. Misc. compliant coatings	Could increase cost, possible rattling during high operating temperature
III. Higher CTE	$BaZr_4P_6O_{24}$ $SrZr_4P_6O_{24}$ $Ca_{0.5}Sr_{0.5}Zr_4P_6O_{24}$	May not survive thermal shock associated with metal casting

Next, X-ray computer tomography was performed to examine the metal-compliant layer and ceramic-compliant layer interfaces. The interfaces were found to be intact in most cases as is evident from Figure 41 which is a X-ray computer tomography based picture of the interface. However, in a few cases where there was direct contact between the metal and the ceramic tube (a void in the compliant layer) a small crack had developed in the ceramic (see arrow in Figure 42). The cracks were approximately 0.05 to 0.1 mm wide and extended up to 5mm in length from the metal-ceramic contact point. This observation suggests that uniformity of the compliant layer is critical to maintain interface integrity and strength. It is also expected that the thickness of the compliant layer will influence the overall performance of the part in actual service. Work is continuing in the area of metal casting around the ceramic tube and subsequent evaluation of the composite tube in field testing. Refinements are being made and tested to improve the casting process and better understand the requirements of the compliant layer.

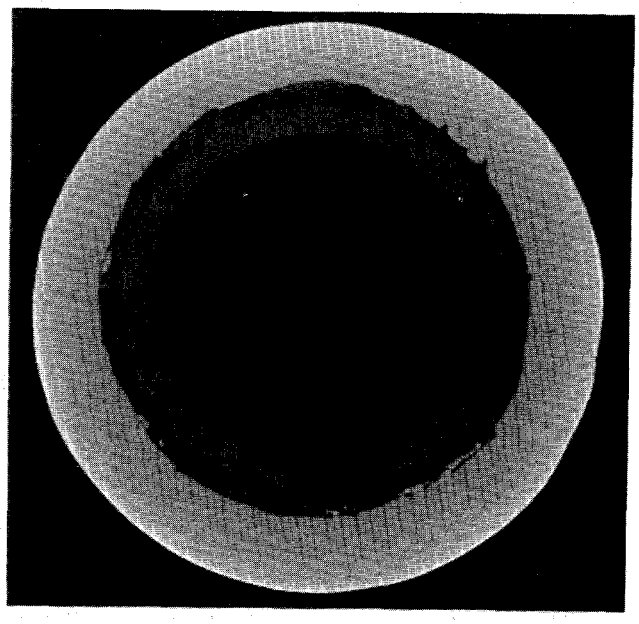

Figure 41. X-Ray computer tomography picture of the metal-ceramic composite tube with compliant layer in between.

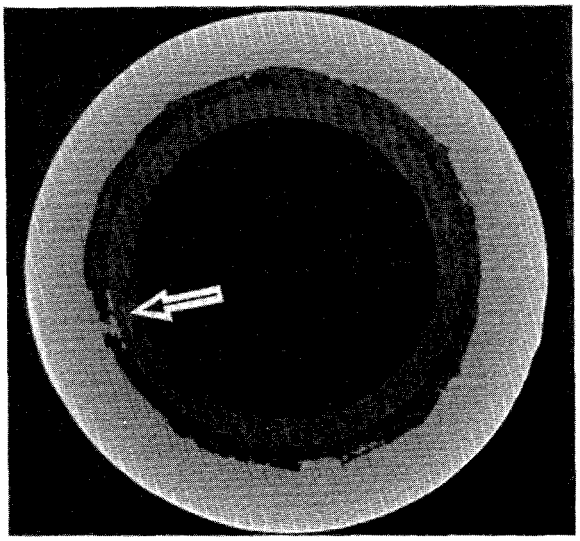

Figure 42. X-Ray computer tomography picture of the metal-ceramic composite tube showing crack (arrow) in the ceramic.

Pressure Slip Casting

An alternative shape forming process, pressure slip casting, was investigated. A large batch (20 kg) of BS-25 ($Ba_{1.25}Zr_4P_{5.50}Si_{0.50}O_{24}$) powders was synthesized and ball milled for eight hours with the appropriate binder and dispersant system, and the slip was prepared for pressure slip casting. The schematic diagram of the pressure slip casting set-up is shown in Figure 43. A series of plaster molds were fabricated for the purpose of pressure casting. Slip was poured into the molds and pressure exerted using compressed air. Wall thicknesses (dependent variable) of the cast bodies were measured as function of time and pressure (independent variables). Figures 44 and 45 show the effect of time and pressure on the wall thickness of the cast ceramic.

The results of pressure slip casting studies indicate that increased pressure leads to rapid build-up of the wall. For example, with an air pressure of 80 psi, the wall thickness builds up to 0.24" within two minutes as compared to a 0.25" wall thickness upon holding the slip for one hour without applying any pressure. This drastic improvement in the casting rates would provide the necessary rapid manufacturing capabilities and allow cost effective manufacturing of NZP ceramics. Further optimization of the pressure slip casting process parameters (as with the regular process) such as binders, dispersants and pH is likely to yield finished products with the best possible properties.

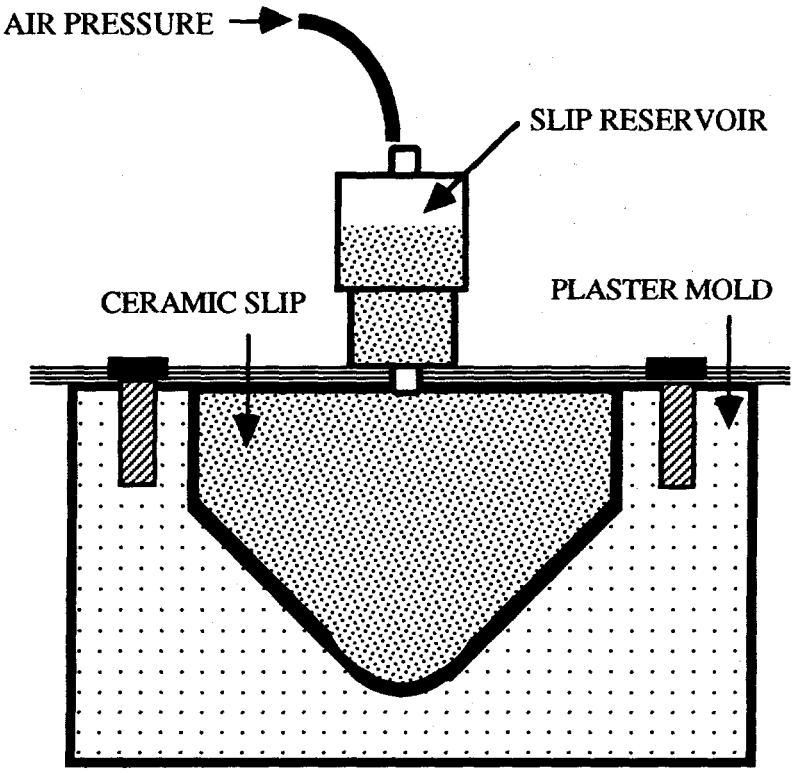

Figure 43. Schematic of set-up for Pressure Slip Casting (PSC) process.

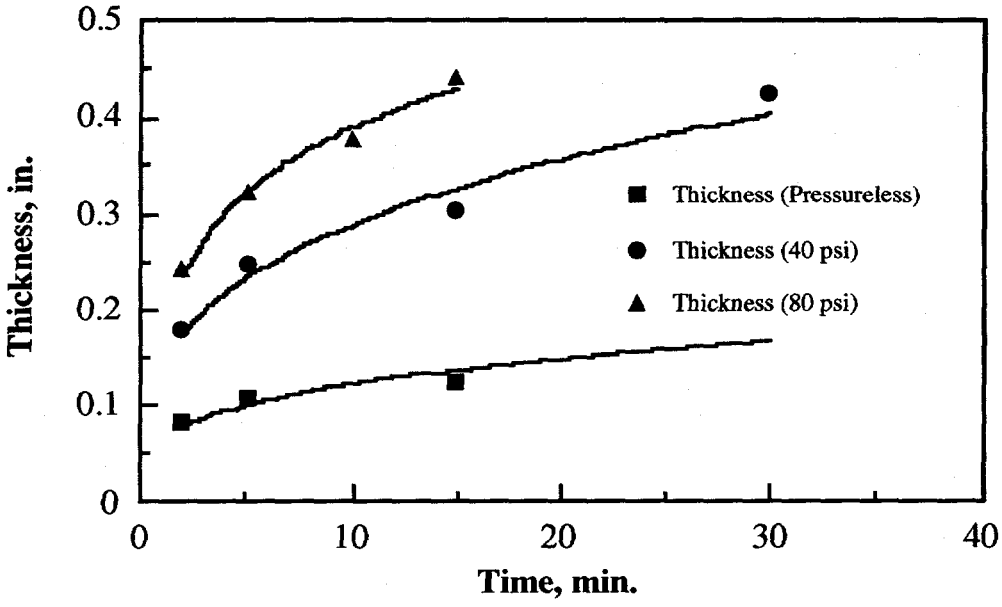

Figure 44. Effect of applied pressure on the wall thickness of cast body.

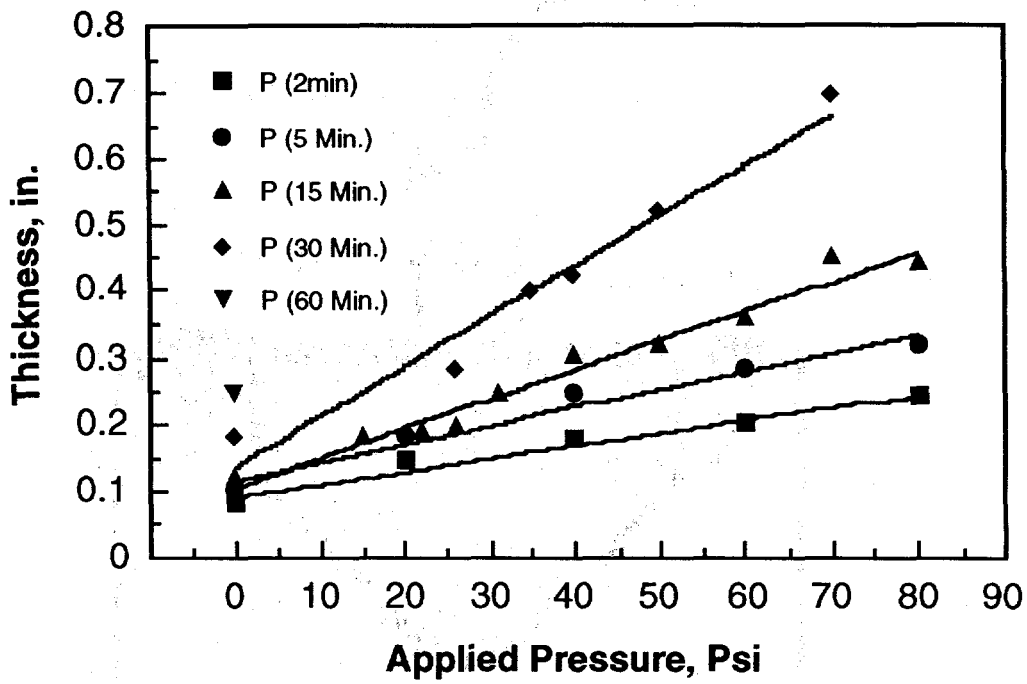

Figure 45. Effect of slip casting time on wall thickness of the cast body.

Gel Casting

This high potential near-net shape forming technique is being adapted to the fabrication of NZP ceramic based diesel engine port-liners and other components. Processing steps involved in the gel casting of NZP ceramics have been summarized in the flow chart of Fig. 46. Despite its advantages with respect to speed of forming and high green strength of the cast and dried part, several areas of this technique still need further examination; for instance, viscosity of the gel at the time of casting (which depends on the amount of solids loading), idle time between casting and gelation, flowing due to self weight of the semi-dry part after removal from the molds, and burn-out of the polymer. All of these areas will be adequately addressed during Phase II work.

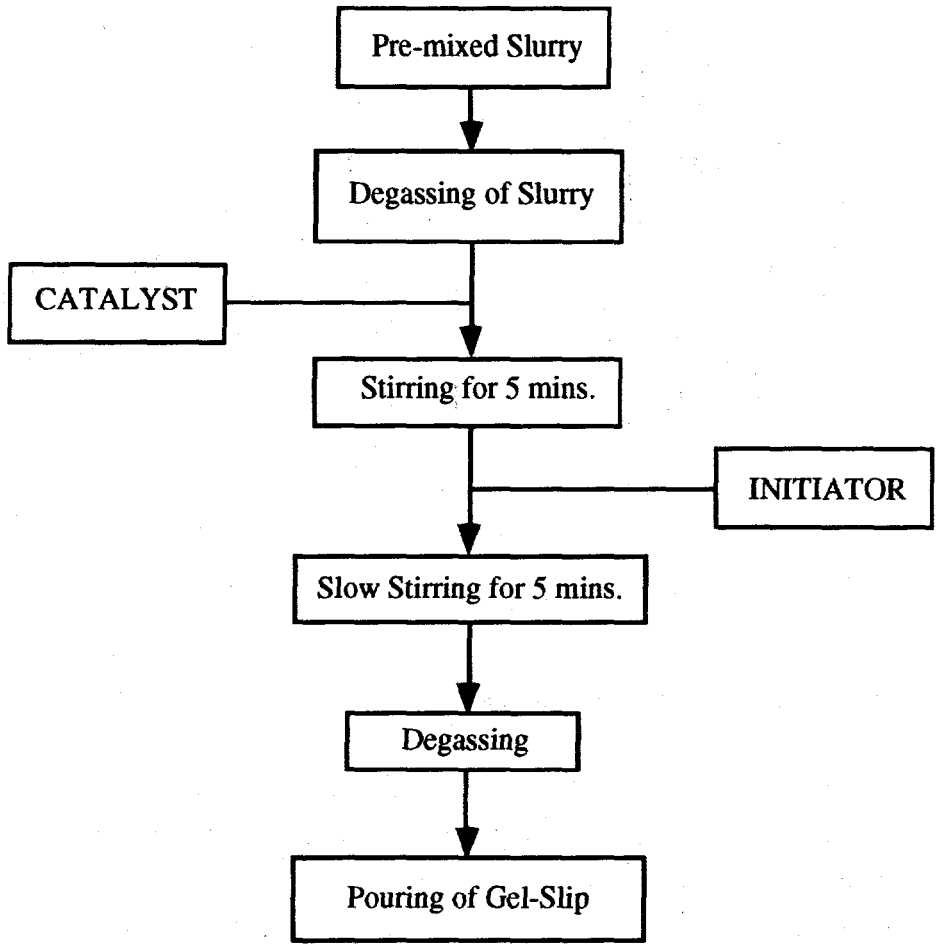

Figure 46. Schematic layout of the sequence involved in gel-casting procedure.

Ultrasonic NDE Technique

A "dry coupling", direct contact, transmission mode ultrasonic technique was tested and adapted for quality checks on finished NZP ceramic parts. As can be seen from Fig. 47, the technique employs dry coupling transmitting and receiving transducers[§] between which the test material (NZP ceramic) is inserted. The transducers used were W-series transducers capable of operating in the frequency range <50 kHz to >25 MHz and designed for velocity measurements and high resolution testing. A PR35 ultrasonic pulser/receiver[¶] acted as the source and transmitter of electric pulses which were recorded and analyzed using a Cathode Ray Oscilloscope (CRO).

§ Ultran Laboratories, Inc., Boalsburg, PA 16827-0719.

¶ JSR Ultrasonic Measurement Systems, Pittsford, NY 14534

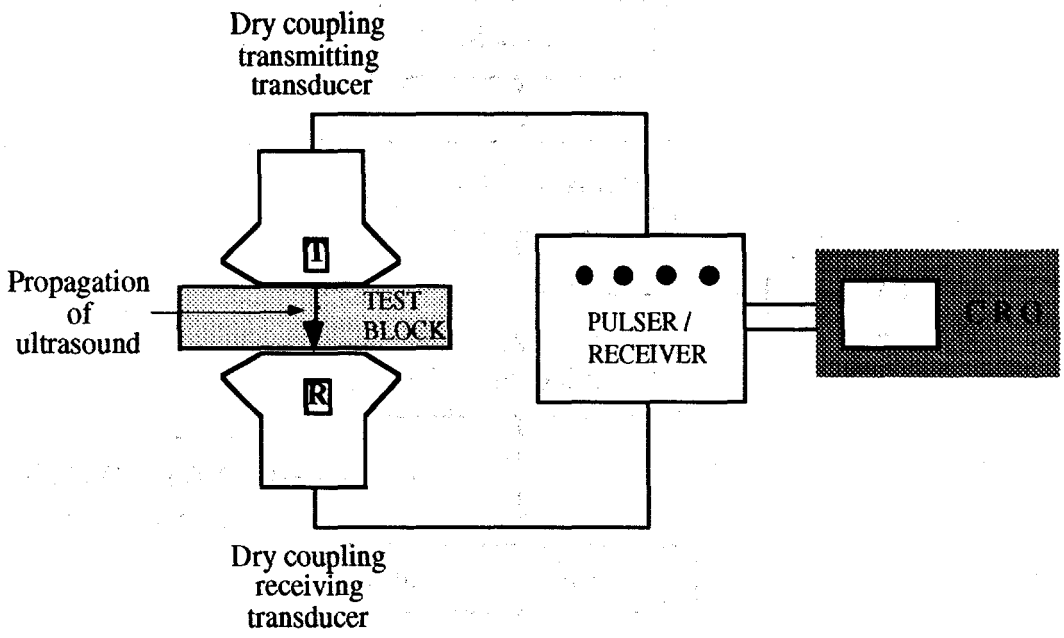

Figure 47. Schematic diagram of the ultrasonic NDE set-up used for flaw detection.

Parameters monitored were the time of flight, longitudinal wave velocity, and amplitude and number of pulses. This information was then processed for comparison with that of a standard. Deviations of the observed/measured parameters of the test sample from the standard were interpreted to be due to defects. In order to ascertain the technique's reliability, some of the seemingly defective samples were dissected to examine for defects. It was found that this technique gave a fairly accurate indication of the presence of flaws.

New NZP materials

As stated in the proposal, three more NZP systems where chosen for this study.

$Ca_{1+x}Zr_4P_{6-2x}Si_{2x}O_{24}$ (CSX) (x = 0.1, 0.25, 0.37)

$Sr_{1+x}Zr_4P_{6-2x}Si_{2x}O_{24}$ (S'SX) (x = 0.1, 0.25, 0.37)

$Ca_{(1+x)/2}Sr_{(1+x)/2}Zr_4P_{6-2x}Si_{2x}O_{24}$ (CS'SX) (x = 0.1, 0.25, 0.37)

Three compositions were synthesized by oxide mixing technique described earlier. Stoichiometric amounts of the precursors (after taking into account the LOI) for a specific composition were mixed, ball milled in alcohol for 20 hrs., dried in air and calcined for 6 hrs. at 1200°C. Calcined powders were then subjected to XRD analysis.

The XRD data indicated that the calcined material contained only the NZP phase in most compositions and, in a few, minor amounts of ZrP_2O_7 which typically disappeared after sintering. The corresponding XRD patterns are shown in Figures 48(a) to (c). Detailed characterization will be conducted during the Phase II effort.

Microcracking Investigation by Acoustic Emission

Using carefully selected wave guides, acoustic signal activity ("counts") emitted by test specimens were recorded. Initial tests consisted of recording acoustic emissions during heat-up of a specimen to and cool-down from 1000°C. A Locan 320 system which was capable of detecting signals in the range of 3 kHz to 1.2 MHz with amplitudes up to 80 dBel was used for detection of acoustic activities. The number of counts recorded was attempted to be correlated to the extent of microcracking in the specimen. It was observed that while no significant acoustic emission could be registered during heating, the opposite was true during cooling (specially below 350°C); which is in agreement with previous experimental observations. These experiments also indicated that the number of acoustic emission counts is a function of the maximum temperature to which the samples are heated. More work on acoustic emission based detection of microcracking has been planned for the Phase II program of this project.

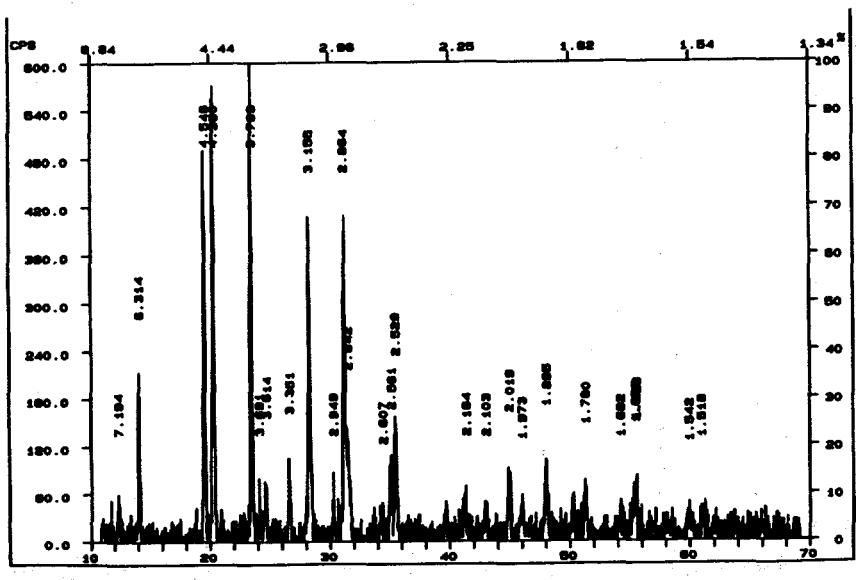

Figure 48 (a). XRD phase content data of C'SX material for x=0.25.

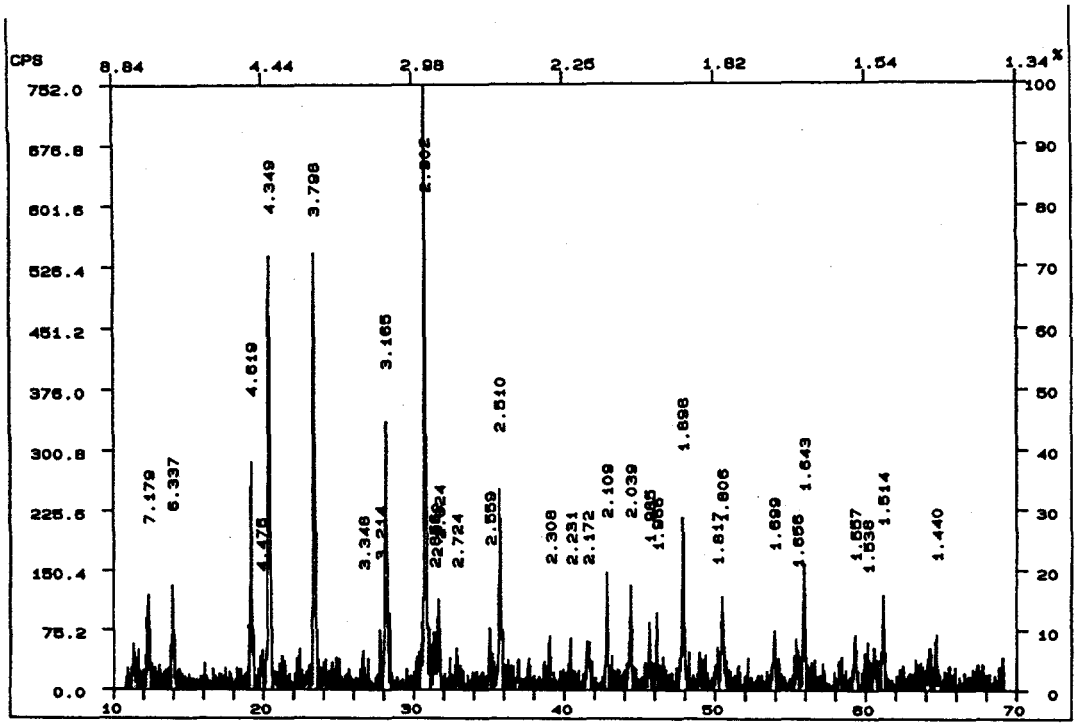

Figure 48(b). XRD phase content data of S'SX material for x=0.25.

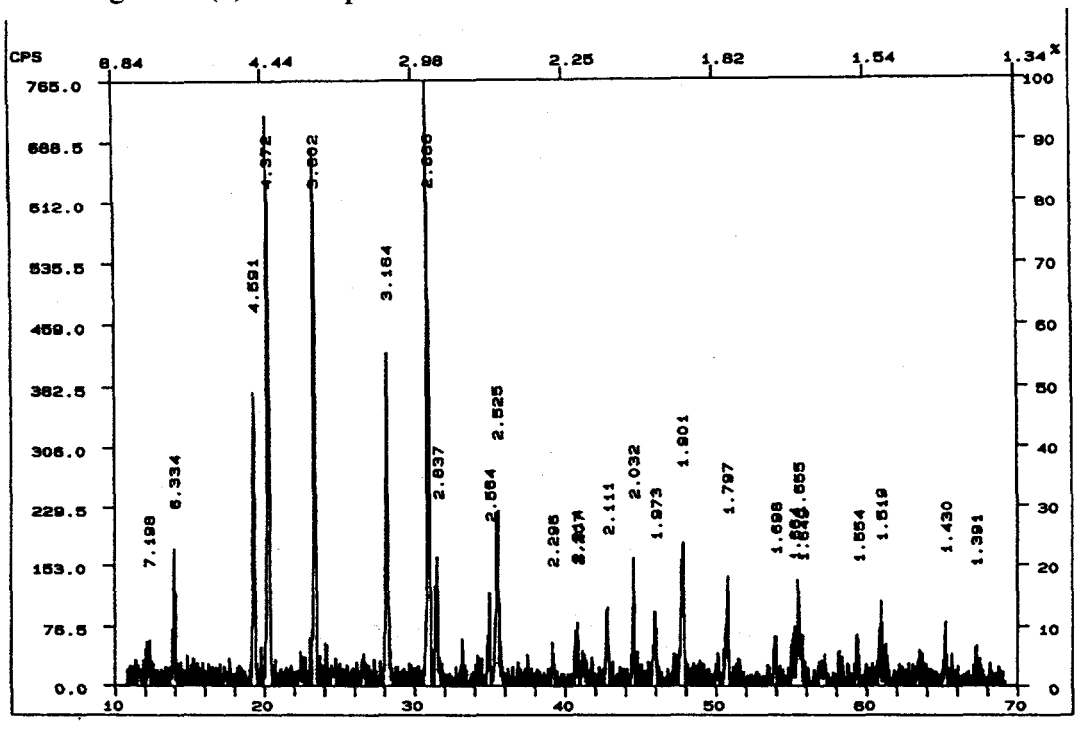

Figure 48(c). XRD phase content data of C'S'X material for x=0.25.

CONCLUSIONS

Work on this Phase I program has led to substantial progress towards the development of NZP ceramic based "cast-in-place" diesel engine port liners. Specific accomplishments and deductions have been summarized in the following:

1. Preliminary work on material property requirements using both finite element analysis (FEA) and metal casting trials converged on the following results: (i) large thermal gradients (and any associated stresses) in the NZP ceramic just at the start of metal casting and (ii) large compressive hoop (shrinkage) stresses that led to cracking of the NZP ceramic after the metal casting process.

2. Optimization of some of the process parameters involved in powder processing and slip casting of NZP ceramics was attempted. Specifically, studies of the effect of milling and calcination conditions; and moisture content of the mold on the final properties of the slip-cast and sintered body were completed.

3. Samples of BSX ($Ba_{1+x}Zr_4P_{6-2x}Si_{2x}O_{24}$) and CSX ($Ca_{1-x}Sr_xZr_4P_6O_{24}$) compositions for x = 0, 0.17, 0.25, 0.375, 0.5 and x = 0, 0.25, 0.5, respectively, were fabricated and subjected to detailed characterization. Characterization included evaluation of mechanical properties (flexure strength and elastic modulus), thermal properties (thermal diffusivity, thermal conductivity, thermal expansion, thermal stability and thermal shock) and microstructures.

4. Of the various BSX and CSX compositions, the BS-25 (x=0.25) and CS-50 (x=0.50) materials had the highest strengths. In addition, the BS-25 and CS-50 materials exhibited the least thermal expansion hysteresis during thermal expansion testing for up to 250 cycles to 1250°C. This result suggested that BS-25 and CS-50 were the most isotropic of all compositions tested.

5. The marked thermal expansion anisotropy of most of the other BSX and CSX materials was shown to be due to moisture-assisted microcracking during cooling (close to room temperature) through a carefully designed experiment. Direct evidence of the microcracking phenomenon was obtained through microstructural examinations.

6. Microcracking was not only responsible for the observed differences in thermal expansion during thermal cycling (hysteresis) of a given sample but also for the low strengths of the anisotropic compositions.

7. Metal casting trials with a compliant layer introduced in between the metal and ceramic tubes was successful in preventing cracking of either the ceramic or metal due to shrinkage stresses. The resulting composite tube was structurally sound as was evident from X-ray computer tomography studies. Requisite optimum properties of the compliant layer and the ceramic are being obtained through iterative refinement of the finite element model based on the results of metal casting trials.

8. Alternative forming processes such as pressure slip casting and gel casting are under assessment. This Phase I experience has shown that both processes hold significant promise for speedy manufacturing of near-net shape NZP ceramic parts without compromise of quality.

9. In the search for new NZP type materials three more systems were selected for investigation. Preliminary testing of thermal expansion behavior and flexure strengths to isolate ultra-low thermal expansion, isotropic and high strength compositions is being conducted. (Detailed characterization of these materials will be undertaken and a complete database will be created.)

10. NDE techniques based on acoustic emission, for the detection and analysis of microcracking behavior in NZP materials, and ultrasonic transmission, for the detection of flaws in finished parts have been developed. The latter technique is already in use for quality control purposes.

REFERENCES

1. J. J. Cleveland and R. C. Bradt, "Grain Size/Microcracking Relations for Psuedobrookite Oxides," *J. Am. Ceram. Soc.,* **61**[11-12], 478-81 (1978).

2. C. E. Holcombe, "Cyclic Plastic Deformation as a Possible Cause of Thermal Expansion Hysteresis of Fine-Grained Ceramic Materials," *High Temp. Sci.,* **12**, 63-66 (1980).

3. G. Harshe, D. Agrawal and S. Limaye, "High Temperature Mechanical Properties and Chemical Stability of $Ba_{1+x}Zr_4P_{6-2x}Si_{2x}O_{24}$ Low-Thermal-Expansion Ceramics," *J. Am. Ceram. Soc.,* **77**[7], 1965-68 (1994).

4. C. Y. Huang et al., "Synthesis, Thermal Expansion, and Microcracking in $Ba_{1+x}Zr_4P_{6-2x}Si_{2x}O_{24}$ and $Sr_{1-x}Zr_4P_{6-2x}Si_{2x}O_{24}$ Systems"; Presented at the 92nd Annual Meeting of the American Ceramic Society, Cincinnati, OH, April 29, 1991 (Basic Science Division, Paper No. 87-B-91).

5. S. Y. Limaye et al., "Synthesis, Sintering, and Thermal Expansion of $Ca_{1-x}Sr_x Zr_4P_6O_{24}$ - An Ultra Low Thermal Expansion Ceramic System," *J. Mater. Sci.,* **26**, 93-98 (1991).

6. MIL-STD-1941 (MR), " Flexure Strength of High Performance Ceramics at Ambient Temperature ", November 1983.

ACKNOWLEDGMENTS

LoTEC, Inc. gratefully acknowledges the funding provided the U.S. Department of Energy, Assistant Secretary for Energy Efficiency and Renewable Energy, Office of Transportation Technologies, as part of the Ceramic Technology Project of the Propulsion System Materials Program, under contract DE-AC05-96OR22464 with Lockheed Martin Energy Research Corporation.

Authors would like to thank T. Barrett Jackson for his work as an Industrial Fellow as the High Temperature Materials Laboratory of Oak Ridge National Laboratory. Authors would also like to acknowledge the help and guidance provided by various personnel (especially Dr. V. J. Tennery, Wally Porter, Ralph Dinwiddie) at HTML. The technical help and critique provided by David Stinton, S. Subramaniam was vital to the completion of Phase I research. The efforts by Michael Lehto of RAE Corp. in Salt Lake City, in completing the preliminary finite element analysis are gratefully acknowledged.

INTERNAL DISTRIBUTION

Central Research Library (2)
Document Reference Section
Laboratory Records Department (2)
Laboratory Records, ORNL RC
ORNL Patent Section
M&C Records Office (3)
L. F. Allard, Jr.
L. D. Armstrong
P. F. Becher
R. F. Bernal
T. M. Besmann
P. J. Blau
R. A. Bradley
K. Breder
C. R. Brinkman
V. R. Bullington
G. M. Caton
S. J. Chang
A. Choudhury
D. D. Conger
R. H. Cooper, Jr.
S. A. David
J. L. Ding
M. K. Ferber
R. L. Graves
D. L. Greene
H. W. Hayden, Jr.
E. E. Hoffman
C. R. Hubbard
M. A. Janney
D. R. Johnson (5)
D. Joslin
R. R. Judkins
M. A. Karnitz
B. L. Keyes
H. D. Kimrey, Jr.
W. Y. Lee
K. C. Liu
E. L. Long, Jr.
W. D. Manly
R. W. McClung
D. J. McGuire
T. A. Nolan
A. E. Pasto
K. P. Plucknett
M. H. Rawlins
M. L. Santella
A. C. Schaffhauser
E. J. Soderstrom
D. P. Stinton
R. W. Swindeman
T. N. Tiegs
B. H. West
S. G. Winslow
J. M. Wyrick

EXTERNAL DISTRIBUTION

Pioneering Research Info. Ctr.
E.I. Dupont de Nemours & Co.
Experimental Station
P.O. Box 80302
Wilmington DE 19880-0302

Jeffrey Abboud
U.S. Advanced Ceramics Assoc.
1600 Wilson Blvd., Suite 1008
Arlington VA 22209

James H. Adair
University of Florida
Materials Science & Engineering
317 MAE Bldg.
Gainesville FL 32611-2066

Donald F. Adams
University of Wyoming
Mechanical Engineering Dept.
P.O. Box 3295
Laramie WY 82071

Andrzej Aeamski
Materials Conversion Group
236-B Egidi Drive
Wheeling IL 60090

Jalees Ahmad
AdTech Systems Research Inc.
Solid Mechanics
1342 N. Fairfield Road
Dayton OH 45432-2698

Yoshio Akimune
NISSAN Motor Co., Ltd.
Materials Research Laboratory
1 Natsushima-Cho
Yokosuka 237
JAPAN

Mufit Akinc
Iowa State University
322 Spedding Hall
Ames IA 50011

Ilhan A. Aksay
Princeton University
A313 Engineering Quadrangle
Princeton NJ 08544-5263

Charles Aldridge
Heany Industries, Inc.
249 Briarwood Lane
Scottsville NY 14546

Joseph E. Amaral
Instron Corporation
Corporate Engineering Office
100 Royale Street
Canton MA 02021

Edward M. Anderson
Aluminum Company of America
N. American Industrial Chemical
P.O. Box 300
Bauxite AR 72011

Norman C. Anderson
Ceradyne, Inc.
Ceramic-to-Metal Division
3169 Redhill Avenue
Costa Mesa CA 92626

Don Anson
BCL
Thermal Power Systems
505 King Avenue
Columbus OH 43201-2693

Thomas Arbanas
G.B.C. Materials Corporation
580 Monastery Drive
Latrobe PA 15650-2698

Frank Armatis
3M Company
Building 60-1N-01
St. Paul MN 55144-1000

Everett B. Arnold
Detroit Diesel Corporation
Mechanical Systems Technology
13400 Outer Drive West
Detroit MI 48239-4001

Bertil Aronsson
Sandvik AB
S-12680
Stockholm Lerkrogsvagen 19
SWEDEN

Dennis Assanis
University of Michigan
Dept. of Mechanical Engineering
321 W.E. Lay, N.C.
Ann Arbor MI 48109

V. S. Avva
North Carolina A&T State Univ.
Dept. of Mechanical Engineering
Greensboro NC 27411

Patrick Badgley
Sky Technologies, Inc.
2815 Franklin Drive
Columbus IN 47201

Sunggi Baik
Pohang Institute Sci. & Tech.
P.O. Box 125
Pohang 790-600
KOREA

John M. Bailey
Consultant
Caterpillar, Inc.
P.O. Box 1875
Peoria IL 61656-1875

Bob Baker
Ceradyne, Inc.
3169 Redhill Avenue
Costa Mesa CA 92626

Frank Baker
Aluminum Company of America
Alcoa Technical Center
Alcoa Center PA 15069

Clifford P. Ballard
AlliedSignal Aerospace Company
Ceramics Program
P.O. Box 1021
Morristown NJ 07962-1021

B. P. Bandyopadhyay
ELID Team
Wako Campus
2-1 Hirosawa Wako-shi
Saitama 351-01
JAPAN

P. M. Barnard
Ruston Gas Turbines Limited
P.O. Box 1
Lincoln LN2 5DJ
ENGLAND

Harold N. Barr
Hittman Corporation
9190 Red Branch Road
Columbia MD 21045

Renald D. Bartoe
Vesuvius McDanel
510 Ninth Avenue
Box 560
Beaver Falls PA 15010-0560

David L. Baty
Babcock & Wilcox - LRC
P.O. Box 11165
Lynchburg VA 24506-1165

Donald F. Baxter, Jr.
ASM International
Advanced Materials & Processes
Materials Park OH 44073-0002

M. Brad Beardsley
Caterpillar Inc.
Technical Center Bldg. E
P.O. Box 1875
Peoria IL 61656-1875

John C. Bell
Shell Research Limited
Thornton Research Centre
P.O. Box 1
Chester CH1 3SH
ENGLAND

Larry D. Bentsen
BFGoodrich Company
R&D Center
9921 Brecksville Road
Brecksville OH 44141

Tom Bernecki
Northwestern University
1801 Maple Avenue
Evanston IL 60201-3135

Charles F. Bersch
Institute for Defense Analyses
1801 N. Beauregard Street
Alexandria VA 22311

Ram Bhatt
NASA Lewis Research Center
21000 Brookpark Road
Cleveland OH 44135

Deane I. Biehler
Caterpillar Inc.
Engineering Research Materials
P.O. Box 1875, Bldg. E
Peoria IL 61656-1875

William D. Bjorndahl
TRW, Inc.
One Space Park, MS:R6-2188
Building 01, Room 2040
Redondo Beach CA 90278

Keith A. Blakely
Advanced Refractory Technologies, Inc.
699 Hertel Avenue
Buffalo NY 14207

Edward G. Blanchard
Netzsch Inc.
119 Pickering Way
Exton PA 19341

Bruce Boardman
Deere & Company Technical Ctr.
3300 River Drive
Moline IL 61265

Lawrence P. Boesch
EER Systems Corp.
1593 Spring Hill Road
Vienna VA 22182-2239

Donald H. Boone
Boone & Associates
2412 Cascade Drive
Walnut Creek CA 94598-4313

Tom Booth
AlliedSignal, Inc.
AiResearch Los Angeles Division
2525 West 190th Street
Torrance CA 90509-2960

Raj Bordia
University of Washington
Roberts Hall
Box 35212
Seattle WA 98195-2120

Tibor Bornemisza
Energy Technologies Applications, Inc.
5064 Caminito Vista Lujo
San Diego CA 92130-2846

J.A.M. Boulet
University of Tennessee
Engineering Science & Mechanics
Knoxville TN 37996-2030

Leslie J. Bowen
Materials Systems
53 Hillcrest Road
Concord MA 01742

Steven C. Boyce
Air Force Office of Scientific Research
AFOSR/NA Bldg. 410
Bolling AFB DC 20332-6448

Steve Bradley
UOP Research Center
50 E. Algonquin Road
Des Plaines IL 60017-6187

Michael C. Brands
Cummins Engine Company, Inc.
P.O. Box 3005, Mail Code 50179
Columbus IN 47201

Raymond J. Bratton
Westinghouse Science & Technology
1310 Beulah Road
Pittsburgh PA 15235

John J. Brennan
United Technologies Corporation
Silver Lane, MS:24
East Hartford CT 06108

Terrence K. Brog
Golden Technologies Company
4545 McIntyre Street
Golden CO 80403

Gunnar Broman
317 Fairlane Drive
Spartanburg SC 29302

Alan Brown
P.O. Box 882
Dayton NJ 08810

Jesse J. Brown
VPI & SU
Ctr. for Adv. Ceram. Mater.
Blacksburg VA 24061-0256

Sherman D. Brown
University of Illinois
Materials Science & Engineering
105 South Goodwin Avenue
Urbana IL 61801

S. L. Bruner
Ceramatec, Inc.
2425 South 900 West
Salt Lake City UT 84119

Walter Bryzik
U.S. Army Tank Automotive Command
R&D Center, Propulsion Systems
Warren MI 48397-5000

Curt V. Burkland
AMERCOM, Inc.
8928 Fullbright Avenue
Chatsworth CA 91311

Bill Bustamante
AMERCOM, Inc.
8928 Fullbright Avenue
Chatsworth CA 91311

Oral Buyukozturk
Massachusetts Institute of Technology
77 Massachusetts Ave., Rm 1-280
Cambridge MA 02139

David A. Caillet
Ethyl Corporation
451 Florida Street
Baton Rouge La 70801

Roger Cannon
Rutgers University
P.O. Box 909
Piscataway NJ 08855-0909

Scott Cannon
P.O. Box 567254
Atlanta GA 30356

Harry W. Carpenter
1844 Fuerte Street
Fallbrook CA 92028

David Carruthers
Kyocera Industrial Ceramics
P.O. Box 2279
Vancouver WA 98668-2279

Calvin H. Carter, Jr.
Cree Research, Inc.
2810 Meridian Parkway
Durham NC 27713

J. David Casey
35 Atlantis Street
West Roxbury MA 02132

Jere G. Castor
J. C. Enterprise
5078 N. 83rd Street
Scottsdale AZ 85250

James D. Cawley
Case Western Reserve University
Materials Science & Engineering
Cleveland OH 44106

Thomas C. Chadwick
Den-Mat Corporation
P.O. Box 1729
Santa Maria CA 93456

Ronald H. Chand
Chand Kare Technical Ceramics
2 Coppage Drive
Worcester MA 01603-1252

William Chapman
Williams International Corp.
2280 W. Maple Road
Walled Lake MI 48390-0200

Ching-Fong Chen
LECO Corporation
3000 Lakeview Avenue
St. Joseph MI 49085

William J. Chmura
Torrington Company
59 Field Street
Torrington CT 06790-4942

Tsu-Wei Chou
University of Delaware
201 Spencer Laboratory
Newark DE 19716

R. J. Christopher
Ricardo Consulting Engineers
Bridge Works
Shoreham-By-Sea W. Sussex
BN435FG ENGLAND

Joel P. Clark
Massachusetts Institute of
Technology
Room 8-409
Cambridge MA 02139

Giorgio Clarotti
Commission of the European Comm
DGXII-C3, MO75, 1-53;
200 Rue de la Loi
B-1049 Brussels
BELGIUM

W. J. Clegg
ICI Advanced Materials
P.O. Box 11, The Heath
Runcorn Cheshire WA7 4QE
ENGLAND

William S. Coblenz
Adv. Research Projects Agency
3701 N. Fairfax Drive
Arlington VA 22203

Gloria M. Collins
ASTM
1916 Race Street
Philadelphia PA 19103

William C. Connors
Sundstrand Aviation Operations
Materials Science & Engineering
4747 Harrison Avenue
Rockford IL 61125-7002

John A. Coppola
Carborundum Company
Niagara Falls R&D Center
P.O. Box 832
Niagara Falls NY 14302

Normand D. Corbin
Norton Company
SGNICC/NRDC
Goddard Road
Northboro MA 01532-1545

Douglas Corey
AlliedSignal, Inc.
2525 West 190th Street, MS:T52
Torrance CA 90504-6099

Keith P. Costello
Chand/Kare Technical Ceramics
2 Coppage Drive
Worcester MA 01603-1252

Ed L. Courtright
Pacific Northwest Laboratory
MS:K3-59
Richland WA 99352

Anna Cox
Mitchell Market Reports
P.O. Box 23
Monmouth Gwent NP5 4YG
UNITED KINGDOM

J. Wesley Cox
BIRL
1801 Maple Avenue
Evanston IL 60201-3135

Art Cozens
Instron Corporation
3414 Snowden Avenue
Long Beach CA 90808

Mark Crawford
New Technology Week
4604 Monterey Drive
Annandale VA 22003

Richard A. Cree
Markets & Products, Inc.
P.O. Box 14328
Columbus OH 43214-0328

Les Crittenden
Vesuvius McDanel
Box 560
Beaver Falls PA 15010

M. J. Cronin
Mechanical Technology, Inc.
968 Albany-Shaker Road
Latham NY 12110

Gary M. Crosbie
Ford Motor Company
20000 Rotunda Drive
MD-2313, SRL Building
Dearborn MI 48121-2053

Floyd W. Crouse, Jr.
U.S. Department of Energy
Morgantown Energy Tech. Ctr.
P.O. Box 880
Morgantown WV 26505

John Cuccio
AlliedSignal Engines
P.O. Box 52180, MS:1302-2Q
Phoenix AZ 85072-2180

Raymond A. Cutler
Ceramatec, Inc.
2425 South 900 West
Salt Lake City UT 84119

Stephen C. Danforth
Rutgers University
P.O. Box 909
Piscataway NJ 08855-0909

Sankar Das Gupta
Electrofuel Manufacturing Co.
9 Hanna Avenue
Toronto Ontario MGK-1W8
CANADA

Frank Davis
AlliedSignal Aerospace Company
7550 Lucerne Drive, #203
Middleburg Heights OH 44130

Robert F. Davis
North Carolina State University
Materials Engineering Department
P.O. Box 7907
Raleigh NC 27695

George C. DeBell
Ford Motor Company
Scientific Research Lab
P.O. Box 2053, Room S2023
Dearborn MI 48121-2053

Michael DeLuca
RSA Research Group
1534 Claas Ave.
Holbrook NY 11741

Gerald L. DePoorter
Colorado School of Mines
Metallurgical & Materials Engr
Golden CO 80401

J. F. DeRidder
Omni Electro Motive, Inc.
12 Seely Hill Road
Newfield NY 14867

Nick C. Dellow
Materials Technology Publications
40 Sotheron Road
Watford Herts WD1 2QA
UNITED KINGDOM

L. R. Dharani
University of Missouri-Rolla
224 M.E.
Rolla MO 65401

Douglas A. Dickerson
Union Carbide Specialty Powders
1555 Main Street
Indianapolis IN 46224

John Dodsworth
Vesuvius Research & Development
Technical Ceramics Group
Box 560
Beaver Falls PA 15010

B. Dogan
Institut fur Werkstofforschung
GKSS-Forschungszentrum Geesthacht
Max-Planck-Strasse
D-2054 Geesthacht
GERMANY

Alan Dragoo
U.S. Department of Energy
ER-131, MS:F-240
Washington DC 20817

Jean-Marie Drapier
FN Moteurs S.A.
Material and Processing
B-4041 Milmort (Herstal)
BELGIUM

Kenneth C. Dreitlein
United Technologies Res. Ctr.
Silver Lane
East Hartford CT 06108

Robin A.L. Drew
McGill University
3450 University Street
Montreal Quebec H3A 2A7
CANADA

Winston H. Duckworth
BCL
Columbus Division
505 King Avenue
Columbus OH 43201-2693

Ernest J. Duwell
3M Abrasive Systems Division
3M Center
St. Paul MN 55144-1000

Chuck J. Dziedzic
GTC Process Forming Systems
4545 McIntyre Street
Golden CO 80403

Robert J. Eagan
Sandia National Laboratories
Engineered Mater. & Proc.
P.O. Box 5800
Albuquerque NM 87185-5800

Harry E. Eaton
United Technologies Corporation
Silver Lane
East Hartford CT 06108

Harvill C. Eaton
Louisiana State University
240 Thomas Boyd Hall
Baton Rouge LA 70803

J. J. Eberhardt
U.S. Department of Energy
Office of Transportation Mater.
CE-34, Forrestal Building
Washington DC 20585

Jim Edler
Eaton Corporation
26201 Northwestern Highway
P.O. Box 766
Southfield MI 48037

G. A. Eisman
Dow Chemical Company
Ceramics and Advanced Materials
52 Building
Midland MI 48667

William A. Ellingson
Argonne National Laboratory
Energy Technology Division
9700 S. Cass Avenue
Argonne IL 60439

Anita Kaye M. Ellis
Machined Ceramics
629 N. Graham Street
Bowling Green KY 42101

Glen B. Engle
Nuclear & Aerospace Materials
16716 Martincoit Road
Poway CA 92064

Kenneth A. Epstein
Dow Chemical Company
2030 Building
Midland MI 48674

Art Erdemir
Argonne National Laboratory
9700 S. Cass Avenue
Argonne IL 60439

E. M. Erwin
Lubrizol Corporation
17710 Riverside Drive
Lakewood OH 44107

John N. Eustis
U.S. Department of Energy
Industrial Energy Efficiency
CE-221, Forrestal Building
Washington DC 20585

W. L. Everitt
Kyocera International, Inc.
8611 Balboa Avenue
San Diego CA 92123

Gordon Q. Evison
332 S. Michigan Avenue
Suite 1730
Chicago IL 60604

John W. Fairbanks
U.S. Department of Energy
Office of Propulsion Systems
CE-322, Forrestal Building
Washington DC 20585

Tim Fawcett
Dow Chemical Company
Advanced Ceramics Laboratory
1776 Building
Midland MI 48674

Robert W. Fawley
Sundstrand Power Systems
Div. of Sundstrand Corporation
P.O. Box 85757
San Diego CA 92186-5757

Jeff T. Fenton
Vista Chemical Company
900 Threadneedle
Houston TX 77079

Larry Ferrell
Babcock & Wilcox
Old Forest Road
Lynchburg VA 24505

Raymond R. Fessler
BIRL
1801 Maple Avenue
Evanston IL 60201

Ross F. Firestone
Ross Firestone Company
188 Mary Street
Winnetka IL 60093-1520

Sharon L. Fletcher
Arthur D. Little, Inc.
15 Acorn Park
Cambridge MA 02140-2390

Michael Foley
Norton Company
Goddard Road
Northboro MA 01532-2527

Thomas F. Foltz
Textron Specialty Materials
2 Industrial Avenue
Lowell MA 01851

Renee G. Ford
Materials and Processing Report
P.O. Box 72
Harrison NY 10528

John Formica
Supermaterials
2020 Lakeside Avenue
Cleveland OH 44114

Edwin Frame
Southwest Research Institute
P.O. Drawer 28510
San Antonio TX 78284

Armanet Francois
French Scientific Mission
4101 Reservoir Road, N.W.
Washington DC 20007-2176

R. G. Frank
Technology Assessment Group
10793 Bentley Pass Lane
Loveland OH 45140

David J. Franus
Forecast International
22 Commerce Road
Newtown CT 06470

Marc R. Freedman
NASA Lewis Research Center
21000 Brookpark Road, MS:49-3
Cleveland OH 44135

Douglas Freitag
Bayside Materials Technology
17 Rocky Glen Court
Brookeville MD 20833

Brian R.T. Frost
Argonne National Laboratory
9700 S. Cass Avenue, Bldg. 900
Argonne IL 60439

Lawrence R. Frost
Instron Corporation
100 Royall Street
Canton MA 02021

Xiren Fu
Shanghai Institute of Ceramics
1295 Ding-xi Road
Shanghai 200050
CHINA

J. P. Gallagher
University of Dayton Research
Institute
300 College Park, JPC-250
Dayton OH 45469-0120

Garry Garvey
Golden Technologies Company
4545 McIntyre Street
Golden CO 80403

Richard Gates
NIST
Materials Bldg., A-256
Gaithersburg MD 20899

L. J. Gauckler
ETH-Zurich
Sonneggstrasse 5
CH-8092 Zurich 8092
SWITZERLAND

D. Gerster
CEA-DCOM
33 Rue De La Federation
Paris 75015
FRANCE

John Ghinazzi
Coors Technical Ceramics Co.
1100 Commerce Park Drive
Oak Ridge TN 37830

Robert Giddings
General Electric Company
P.O. Box 8
Schenectady NY 12301

A. M. Glaeser
University of California
Lawrence Berkeley Laboratory
Hearst Mining Building
Berkeley CA 94720

Joseph W. Glatz
510 Rocksville Road
Holland PA 18966

W. M. Goldberger
Superior Graphite Company
R&D
2175 E. Broad Street
Columbus OH 43209

Allan E. Goldman
U.S. Graphite, Inc.
907 W. Outer Drive
Oak Ridge TN 37830

Stephen T. Gonczy
Allied Signal Research
P.O. Box 5016
Des Plaines IL 60017

Robert J. Gottschall
U.S. Department of Energy
ER-131, MS:G-236
Washington DC 20585

Earl Graham
Cleveland State University
Dept. of Chemical Engineering
Euclid Avenue at East 24th St.
Cleveland OH 44115

John W. Graham
Astro Met, Inc.
9974 Springfield Pike
Cincinnati OH 45215

G. A. Graves
U. of Dayton Research Institute
300 College Park
Dayton OH 45469-0001

Robert E. Green, Jr.
Johns Hopkins University
Mater. Sci. and Engineering
Baltimore MD 21218

Alex A. Greiner
Plint & Partners
Oaklands Park
Wokingham Berkshire RG11 2FD
UNITED KINGDOM

Lance Groseclose
Allison Engine Company
P.O. Box 420, MS:W-5
Indianapolis IN 46206

Thomas J. Gross
U.S. Department of Energy
Transportation Technologies
CE-30, Forrestal Building
Washington DC 20585

Mark F. Gruninger
Union Carbide Corporation
Specialty Powder Business
1555 Main Street
Indianapolis IN 46224

Ernst Gugel
Cremer Forschungsinstitut
GmbH&Co.KG
Oeslauer Strasse 35
D-8633 Roedental 8633
GERMANY

John P. Gyekenyesi
NASA Lewis Research Center
21000 Brookpark Road, MS:6-1
Cleveland OH 44135

Nabil S. Hakim
Detroit Diesel Corporation
13400 Outer Drive West
Detroit MI 48239

Philip J. Haley
Allison Engine Company
P.O. Box 420, MS:T12A
Indianapolis IN 46206-0420

Judith Hall
Fiber Materials, Inc.
Biddeford Industrial Park
5 Morin Street
Biddeford ME 04005

Y. Hamano
Kyocera Industrial Ceramics
5713 E. Fourth Plain Blvd.
Vancouver WA 98661-6857

Y. Harada
IIT Research Institute
10 West 35th Street
Chicago IL 60616

Norman H. Harris
Hughes Aircraft Company
P.O. Box 800520
Saugus CA 91380-0520

Alan M. Hart
Dow Chemical Company
1776 Building
Midland MI 48674

Pat E. Hart
Battelle Pacific Northwest Labs
Ceramics and Polymers Development
P.O. Box 999
Richland WA 99352

Michael H. Haselkorn
Caterpillar Inc.
Technical Center, Building E
P.O. Box 1875
Peoria IL 61656-1875

Debbie Haught
U.S. Department of Energy
Off. of Transportation Mater.
EE-34, Forrestal Bldg.
Washington DC 20585

N. B. Havewala
Corning Inc.
SP-PR-11
Corning NY 14831

John Haygarth
Teledyne WAA Chang Albany
P.O. Box 460
Albany OR 97321

Norman L. Hecht
U. of Dayton Research Institute
300 College Park
Dayton OH 45469-0172

Peter W. Heitman
Allison Engine Company
P.O. Box 420, MS:W-5
Indianapolis IN 46206-0420

Robert W. Hendricks
VPI & SU
210 Holden Hall
Blacksburg VA 24061-0237

Thomas P. Herbell
NASA Lewis Research Center
21000 Brookpark Road, MS:49-3
Cleveland OH 44135

Robert L. Hershey
Science Management Corporation
1255 New Hampshire Ave., N.W.
Suite 1033
Washington DC 20036

Hendrik Heystek
Bureau of Mines
Tuscaloosa Research Center
P.O. Box L
University AL 35486

Robert V. Hillery
GE Aircraft Engines
One Neumann Way, M.D. H85
Cincinnati OH 45215

Arthur Hindman
Instron Corporation
100 Royall Street
Canton MA 02021

Shinichi Hirano
Mazda R&D of North America
1203 Woodridge Avenue
Ann Arbor MI 48105

Tommy Hiraoka
NGK Locke, Inc.
1000 Town Center
Southfield MI 48075

Fu H. Ho
5645 Soledad Mtn. Road
San Diego, CA 92037-7256

John M. Hobday
U.S. Department of Energy
Morgantown Energy Tech. Ctr.
P.O. Box 880
Morgantown WV 26507

Clarence Hoenig
Lawrence Livermore National Lab
P.O. Box 808, Mail Code L-369
Livermore CA 94550

Thomas Hollstein
Fraunhofer-Institut fur
Werkstoffmechanik
Wohlerstrasse 11
D-79108 Freiburg
GERMANY

Richard Holt
Natl. Research Council Canada
Structures and Materials Lab
Ottawa Ontario K1A OR6
CANADA

Woodie Howe
Coors Technical Ceramics
1100 Commerce Park Drive
Oak Ridge TN 37830

Stephen M. Hsu
NIST
Gaithersburg MD 20899

Hann S. Huang
Argonne National Laboratory
9700 S. Cass Avenue
Argonne IL 60439-4815

Gene Huber
Precision Ferrites & Ceramics
5576 Corporate Drive
Cypress CA 90630

Fred R. Huettic
Advanced Magnetics Inc.
45 Corey Lane
Mendham NJ 07945

Brian K. Humphrey
Lubrizol Petroleum Chemicals
3000 Town Center, Suite 1340
Southfield MI 48075-1201

Robert M. Humrick
Dylon Ceramic Technologies
3100 Edgehill Road
Cleveland Heights OH 44118

Michael S. Inoue
Kyocera International, Inc.
8611 Balboa Avenue
San Diego CA 92123-1580

Joseph C. Jackson
U.S. Advanced Ceramics Assoc.
1600 Wilson Blvd., Suite 1008
Arlington VA 22209

Osama Jadaan
U. of Wisconsin-Platteville
1 University Plaza
Platteville WI 53818

Said Jahanmir
NIST
Materials Bldg., Room A-237
Gaithersburg MD 20899

Curtis A. Johnson
General Electric Company
P.O. Box 8
Schenectady NY 12301

Sylvia Johnson
SRI International
333 Ravenswood Avenue
Menlo Park CA 94025

Thomas A. Johnson
Lanxide Corporation
P.O. Box 6077
Newark DE 19714-6077

Walter F. Jones
AFOSR/NA
110 Duncan Ave., Ste. B115
Washington DC 20332-0001

Jill E. Jonkouski
U.S. Department of Energy
9800 S. Cass Avenue
Argonne IL 60439-4899

L. A. Joo
Great Lakes Research Corporation
P.O. Box 1031
Elizabethton TN 37643

Adam Jostsons
Australian Nuclear Science &
Technology
New Illawarra Road
Lucas Heightss New South Wales
AUSTRALIA

Lyle R. Kallenbach
Phillips Petroleum
Mail Drop:123AL
Bartlesville OK 74004

Nick Kamiya
Kyocera Industrial Ceramics Corp. 25 NW
Point Blvd., #450
Elk Grove Village IL 60007

Roy Kamo
Adiabatics, Inc.
3385 Commerce Park Drive
Columbus IN 47201

Chih-Chun Kao
Industrial Technology Research
Institute
195 Chung-Hsing Road, Sec. 4
Chutung Hsinchu 31015 R.O.C.
TAIWAN

Keith R. Karasek
AlliedSignal Aerospace Company
50 E. Algonquin Road
Des Plaines IL 60017-5016

Robert E. Kassel
Ceradyne, Inc.
3169 Redhill Avenue
Costa Mesa CA 92626

Allan Katz
Wright Laboratory
Metals and Ceramics Division
Wright-Patterson AFB OH 45433

R. Nathan Katz
Worcester Polytechnic Institute
100 Institute Road
Worcester MA 01609

Ted Kawaguchi
Tokai Carbon America, Inc.
375 Park Avenue, Suite 3802
New York NY 10152

Noritsugu Kawashima
TOSHIBA Corporation
4-1 Ukishima-Cho
Kawasaki-Ku Kawasaki, 210
JAPAN

Lisa Kempfer
Penton Publishing
1100 Superior Avenue
Cleveland OH 44114-2543

Frederick L. Kennard, III
Delphi Energy & Engine Mgmt. Systems
Division of General Motors
1300 N. Dort Highway
Flint MI 48556

David O. Kennedy
Lester B. Knight Cast Metals
549 W. Randolph Street
Chicago IL 60661

George Keros
Photon Physics
3175 Penobscot Building
Detroit MI 48226

Thomas Ketcham
Corning, Inc.
SP-DV-1-9
Corning NY 14831

Pramod K. Khandelwal
Allison Engine Company
P.O. Box 420, MS:T10B
Indianapolis IN 46206

Jim R. Kidwell
AlliedSignal Engines
P.O. Box 52180
Phoenix AZ 85072-2180

Shin Kim
The E-Land Group
19-8 ChangJeon-dong
Mapo-gu, Seoul 121-190
KOREA

W. C. King
Mack Truck, Z-41
1999 Pennsylvania Avneue
Hagerstown MD 21740

Carol Kirkpatrick
MSE, Inc.
P.O. Box 3767
Butte MT 59702

Tony Kirn
Caterpillar Inc.
Defense Products Dept., JB7
Peoria IL 61629

James D. Kiser
NASA Lewis Research Center
21000 Brookpark Road, MS:49-3
Cleveland OH 44135

Max Klein
900 24th Street, N.W., Unit G
Washington DC 20037

Richard N. Kleiner
Golden Technologies Company
4545 McIntyre Street
Golden CO 80403

Stanley J. Klima
NASA Lewis Research Center
21000 Brookpark Road, MS:6-1
Cleveland OH 44135

Albert S. Kobayashi
University of Washington
Mechanical Engineering Dept.
Mail Stop:FU10
Seattle WA 98195

Shigeki Kobayashi
Toyota Central Research Labs
Nagakute Aichi, 480-11
JAPAN

Richard A. Kole
Z-Tech Corporation
8 Dow Road
Bow NH 03304

Joseph A. Kovach
Eaton Corporation
32500 Chardon Road
Willoughby Hills OH 44094

Kenneth A. Kovaly
Technical Insights Inc.
P.O. Box 1304
Fort Lee NJ 07024-9967

Edwin H. Kraft
Kyocera Industrial Ceramics
5713 E. Fourth Plain Boulevard
Vancouver WA 98661

Arthur Kranish
Trends Publishing Inc.
1079 National Press Building
Washington DC 20045

A. S. Krieger
Radiation Science, Inc.
P.O. Box 293
Belmont MA 02178

Pieter Krijgsman
Ceramic Design International Holding B.V.
P.O. Box 68
Hattem 8050-AB
THE NETHERLANDS

Waltraud M. Kriven
University of Illinois
105 S. Goodwin Avenue
Urbana IL 61801

Edward J. Kubel, Jr.
ASM International
Advanced Materials & Processes
Materials Park OH 44073

Dave Kupperman
Argonne National Laboratory
9700 S. Cass Avenue
Argonne IL 60439

Oh-Hun Kwon
North Company
SGNICC/NRDC
Goddard Road
Northboro MA 01532-1545

W. J. Lackey
GTRI
Materials Science and Tech. Lab
Atlanta GA 30332

Jai Lala
Tenmat Ltd.
40 Somers Road
Rugby Warwickshire CV22 7DH
ENGLAND

Hari S. Lamba
General Motors Corporation
9301 West 55th Street
LaGrange IL 60525

Richard L. Landingham
Lawrence Livermore National Lab
P.O. Box 808, L-369
Livermore CA 94550

James Lankford
Southwest Research Institute
6220 Culebra Road
San Antonio TX 78228-0510

Stanley B. Lasday
Business News Publishing Co.
1910 Cochran Road, Suite 630
Pittsburgh PA 15220

S. K. Lau
Carborundum Company
Technology Division
P.O. Box 832, B-100
Niagara Falls NY 14302

J. Lawrence Lauderdale
Babcock & Wilcox
1525 Wilson Blvd., #100
Arlington VA 22209-2411

Jean F. LeCostaouec
Textron Specialty Materials
2 Industrial Avenue
Lowell MA 01851

Benson P. Lee
Technology Management, Inc.
4440 Warrensville Rd., Suite A
Cleveland OH 44128

Burtrand I. Lee
Clemson University
Olin Hall
Clemson SC 29634-0907

June-Gunn Lee
KIST
P.O. Box 131, Cheong-Ryang
Seoul 130-650
KOREA

Stan Levine
NASA Lewis Research Center
21000 Brookpark Road, MS:49-3
Cleveland OH 44135

David Lewis, III
Naval Research Laboratory
Code 6370
Washington DC 20375-5343

Ai-Kang Li
Materials Research Labs., ITRI
195-5 Chung-Hsing Road, Sec. 4
Chutung Hsinchu 31015 R.O.C.
TAIWAN

Robert H. Licht
Norton Company
SGNICC/NRDC
Goddard Road
Northboro MA 01532-1545

E. Lilley
Norton Company
SGNICC/NRDC
Goddard Road
Northboro MA 01532-1545

Chih-Kuang Lin
National Central University
Dept. of Mechanical Engineering
Chung-Li 32054
TAIWAN

Laura J. Lindberg
AlliedSignal Aerospace Company
Garrett Fluid Systems Division
P.O. Box 22200
Tempe AZ 85284-2200

Hans A. Lindner
Cremer Forschungsinstitut
GmbH&Co.KG
Oeslauer Strasse 35
D-8633 Rodental 8866
GERMANY

Ronald E. Loehman
Sandia National Laboratories
Chemistry & Ceramics Dept. 1840
P.O. Box 5800
Albuquerque NM 87185

Bill Long
Babcock & Wilcox
P.O. Box 11165
Lynchburg VA 24506

L. A. Lott
EG&G Idaho, Inc.
Idaho National Engineering Lab
P.O. Box 1625
Idaho Falls ID 83415-2209

Raouf O. Loutfy
MER Corporation
7960 S. Kolb Road
Tucson AZ 85706

Lydia Luckevich
Ortech International
2395 Speakman Drive
Mississauga Ontario L5K 1B3
CANADA

James W. MacBeth
Carborundum Company
Structural Ceramics Division
P.O. Box 1054
Niagara Falls NY 14302

George Maczura
Aluminum Company of America
3450 Park Lane Drive
Pittsburgh PA 15275-1119

David Maginnis
Tinker AFB
OC-ALC/LIIRE
Tinker AFB OK 73145-5989

Frank Maginnis
Aspen Research, Inc.
220 Industrial Boulevard
Moore OK 73160

Tai-il Mah
Universal Energy Systems, Inc.
4401 Dayton-Xenia Road
Dayton OH 45432

Kenneth M. Maillar
Barbour Stockwell Company
83 Linskey Way
Cambridge MA 02142

S. G. Malghan
NIST
I-270 & Clopper Road
Gaithersburg MD 20899

Lars Malmrup
United Turbine AB
Box 13027
Malmo S-200 44
SWEDEN

John Mangels
Ceradyne, Inc.
3169 Redhill Avenue
Costa Mesa CA 92626

Murli Manghnani
University of Hawaii
2525 Correa Road
Honolulu HI 96822

Russell V. Mann
Matec Applied Sciences, Inc.
75 South Street
Hopkinton MA 01748

William R. Manning
Champion Aviation Products Div
P.O. Box 686
Liberty SC 29657

Ken Marnoch
Amercom, Inc.
8928 Fullbright Avenue
Chatsworth CA 91311

Robert A. Marra
Aluminum Company of America
Alcoa Technical Center
Alcoa Center PA 15069

Steve C. Martin
Advanced Refractory Technologies
699 Hertel Avenue
Buffalo NY 14207

Kelly J. Mather
William International Corp.
2280 W. Maple Road
Walled Lake MI 48088

James P. Mathers
3M Company
3M Center, Bldg. 201-3N-06
St. Paul MN 55144

Ron Mayville
Arthur D. Little, Inc.
15-163 Acorn Park
Cambridge MA 02140

F. N. Mazadarany
General Electric Company
Bldg. K-1, Room MB-159
P.O. Box 8
Schenectady NY 12301

James W. McCauley
Alfred University
Binns-Merrill Hall
Alfred NY 14802

Colin F. McDonald
McDonald Thermal Engineering
1730 Castellana Road
La Jolla CA 92037

B. J. McEntire
Norton Company
10 Airport Park Road
East Granby CT 06026

Chuck McFadden
Coors Ceramics Company
600 9th Street
Golden CO 80401

Thomas D. McGee
Iowa State University
110 Engineering Annex
Ames IA 50011

James McLaughlin
Sundstrand Power Systems
4400 Ruffin Road
P.O. Box 85757
San Diego CA 92186-5757

Matt McMonigle
U.S. Department of Energy
Improved Energy Productivity
CE-231, Forrestal Building
Washington DC 20585

J. C. McVickers
AlliedSignal Engines
P.O. Box 52180, MS:9317-2
Phoenix AZ 85072-2180

D. B. Meadowcroft
"Jura," The Ridgeway
Oxshott
Leatherhead Surrey KT22 OLG
UNITED KINGDOM

Joseph J. Meindl
Reynolds International, Inc.
6603 W. Broad Street
P.O. Box 27002
Richmond VA 23261-7003

Michael D. Meiser
AlliedSignal, Inc.
Ceramic Components
P.O. Box 2960, MS:T21
Torrance CA 90509-2960

George Messenger
National Research Council of Canada
Building M-7
Ottawa Ontario K1A OR6
CANADA

Arthur G. Metcalfe
Arthur G. Metcalfe & Assoc.
2108 East 24th Street
National City CA 91950

R. Metselaar
Eindhoven University
P.O. Box 513
Endhoven 5600 MB
THE NETHERLANDS

David J. Michael
Harbison-Walker Refractories
P.O. Box 98037
Pittsburgh PA 15227

Ken Michaels
Chrysler Motors Corporation
P.O. Box 1118, CIMS:418-17-09
Detroit MI 48288

Bernd Michel
Institute of Mechanics
P.O. Box 408
D-9010 Chemnitz
GERMANY

D. E. Miles
Commission of the European Community
rue de la Loi 200
B-1049 Brussels
BELGIUM

Carl E. Miller
AC Rochester
1300 N. Dort Highway, MS:32-31
Flint MI 48556

Charles W. Miller, Jr.
Centorr Furnaces/Vacuum Industries
542 Amherst Street
Nashua NH 03063

R. Minimmi
Enichem America
2000 Cornwall Road
Monmouth Junction NJ 08852

Michele V. Mitchell
AlliedSignal, Inc.
Ceramic Components
P.O. Box 2960, MS:T21
Torrance CA 90509-2960

Howard Mizuhara
WESGO
477 Harbor Boulevard
Belmont CA 94002

Helen Moeller
Babcock & Wilcox
P.O. Box 11165
Lynchburg VA 24506-1165

Francois R. Mollard
Concurrent Technologies Corp.
1450 Scalp Avenue
Johnstown PA 15904-3374

Phil Mooney
Panametrics
221 Crescent Street
Waltham MA 02254

Geoffrey P. Morris
3M Company
3M Traffic Control Materials
Bldg. 209-BW-10, 3M Center
St. Paul MN 55144-1000

Jay A. Morrison
Rolls-Royce, Inc.
2849 Paces Ferry Rd., Suite 450
Atlanta GA 30339-3769

Joel P. Moskowitz
Ceradyne, Inc.
3169 Redhill Avenue
Costa Mesa CA 92626

Brij Moudgil
University of Florida
Material Science & Engineering
Gainesville FL 32611

Christoph J. Mueller
Sprechsaal Publishing Group
P.O. Box 2962, Mauer 2
D-8630 Coburg
GERMANY

Thomas W. Mullan
Vapor Technologies Inc.
345 Route 17 South
Upper Saddle River NJ 07458

Theresa A. Mursick-Meyer
Norton Company
SGNICC/NRDC
Goddard Road
Northboro MA 01532-1545

M. K. Murthy
MkM Consultants International
10 Avoca Avenue, Unit 1906
Toronto Onntario M4T 2B7
CANADA

David L. Mustoe
Custom Technical Ceramics
8041 W I-70 Service Rd. Unit 6
Arvada CO 80002

Curtis V. Nakaishi
U.S. Department of Energy
Morgantown Energy Tech. Ctr.
P.O. Box 880
Morgantown WV 26507-0880

Yoshio Nakamura
Faicera Research Institute
3-11-12 Misono
Sagamihara, Tokyo
JAPAN

K. S. Narasimhan
Hoeganaes Corporation
River Road
Riverton NJ 08077

Robert Naum
Applied Resources, Inc.
P.O. Box 241
Pittsford NY 14534

Malcolm Naylor
Cummins Engine Company, Inc.
P.O. Box 3005, Mail Code 50183
Columbus IN 47202-3005

Fred A. Nichols
Argonne National Laboratory
9700 S. Cass Avenue
Argonne IL 60439

H. Nickel
Forschungszentrum Juelich (KFA)
Postfach 1913
D-52425 Juelich
GERMANY

Dale E. Niesz
Rutgers University
Center for Ceramic Research
P.O. Box 909
Piscataway NJ 08855-0909

Paul W. Niskanen
Lanxide Corporation
P.O. Box 6077
Newark DE 19714-6077

David M. Nissley
United Technologies Corporation
Pratt & Whitney Aircraft
400 Main Street, MS:163-10
East Hartford CT 06108

Daniel Oblas
50 Meadowbrook Drive
Bedford MA 01730

Don Ohanehi
Magnetic Bearings, Inc.
1908 Sussex Road
Blacksburg VA 24060

Hitoshi Ohmori
ELID Team
Itabashi Branch
1-7 13 Kaga Itabashi
Tokyo 173
JAPAN

Robert Orenstein
General Electric Company
55-112, River Road
Schenectady NY 12345

Richard Palicka
Cercom, Inc.
1960 Watson Way
Vista CA 92083

Joseph N. Panzarino
379 Howard Street
P. O. Box 652
Northboro MA 01532-1545

Pellegrino Papa
Corning Inc.
MP-WX-02-1
Corning NY 14831

Terry Paquet
Boride Products Inc.
2879 Aero Park Drive
Traverse City MI 49684

E. Beth Pardue
MPC
8297 Williams Ferry Road
Lenior City TN 37771

Soon C. Park
3M Company
Building 142-4N-02
P.O. Box 2963
St. Paul MN 55144

Vijay M. Parthasarathy
Caterpillar/Solar Turbines
2200 Pacific Highway
P.O. Box 85376
San Diego CA 92186-5376

Harmut Paschke
Schott Glaswerke
Christoph-Dorner-Strasse 29
D-8300 Landshut
GERMANY

James W. Patten
Cummins Engine Company, Inc.
P.O. Box 3005, Mail Code 50183
Columbus IN 47202-3005

Robert A. Penty
Penty & Associates
38 Oakdale Drive
Rocester NY 14618

Robert W. Pepper
Textron Specialty Materials
2 Industrial Avenue
Lowell MA 01851

Peter Perdue
Detroit Diesel Corporation
13400 Outer Drive West,
Speed Code L-04
Detroit MI 48239-4001

John J. Petrovic
Los Alamos National Laboratory
Group MST-4, MS:G771
Los Alamos NM 87545

Frederick S. Pettit
University of Pittsburgh
Pittsburgh PA 15261

Richard C. Phoenix
Ohmtek, Inc.
2160 Liberty Drive
Niagara Falls NY 14302

Bruce J. Pletka
Michigan Technological Univ.
Metallurgical & Materials Engr.
Houghton MI 49931

John P. Pollinger
AlliedSignal, Inc.
Ceramic Components
P.O. Box 2960, MS:T21
Torrance CA 90509-2960

P. Popper
High Tech Ceramics Int. Journal 22
Pembroke Drive - Westlands
Newcastle-under-Lyme
Staffs ST5 2JN
ENGLAND

F. Porz
Universitat Karlsruhe
Institut fur Keramik Im
Maschinendau
Postfach 6980
D-76128 Karlsruhe
GERMANY

Harry L. Potma
Royal Netherlands Embassy
Science and Technology
4200 Linnean Avenue, N.W.
Washington DC 20008

Bob R. Powell
General Motors Corporation
Metallurgy Department
Box 9055
Warren MI 48090-9055

Stephen C. Pred
Biesterfeld U.S., Inc.
500 Fifth Avenue
New York NY 10110

Karl M. Prewo
United Technologies Res. Ctr.
411 Silver Lane, MS:24
East Hartford CT 06108

Vimal K. Pujari
Norton Company
SGNICC/NRDC
Goddard Road
Northboro MA 01532-1545

Fred Quan
Corning Inc.
Sullivan Park, FR-02-08
Corning NY 14831

George Quinn
NIST
Ceramics Division, Bldg. 223
Gaithersburg MD 20899

Ramas V. Raman
Ceracon, Inc.
1101 N. Market Blvd., Suite 9
Sacramento CA 95834

Charles F. Rapp
Owens Corning Fiberglass
2790 Columbus Road
Granville OH 43023-1200

Dennis W. Readey
Colorado School of Mines
Metallurgy and Materials Engr.
Golden CO 80401

Wilfred J. Rebello
PAR Enterprises, Inc.
12601 Clifton Hunt Lane
Clifton VA 22024

Harold Rechter
Chicago Fire Brick Company
7531 S. Ashland Avenue
Chicago IL 60620

Robert R. Reeber
U.S. Army Research Office
P.O. Box 12211
Research Triangle Park NC
27709-2211

K. L. Reifsnider
VPI & SU
Engineering Science and Mechanics
Blacksburg VA 24061

Paul E. Rempes
McDonnell Douglass Aircraft Co.
P.O. Box 516, Mail Code:0642263
St. Louis MO 63166-0516

Gopal S. Revankar
John Deere Company
3300 River Drive
Moline IL 61265

K. Y. Rhee
Rutgers University
P.O. Box 909
Piscataway NJ 08854

James Rhodes
Advanced Composite Materials
1525 S. Buncombe Road
Greer SC 29651

Roy W. Rice
W. R. Grace and Company
7379 Route 32
Columbia MD 21044

David W. Richerson
2093 E. Delmont Drive
Salt Lake City UT 84117

Tomas Richter
J. H. France Refractories
1944 Clarence Road
Snow Shoe PA 16874

Michel Rigaud
Ecole Polytechnique
Campus Universite De Montreal
P.O. Box 6079, Station A
Montreal, P.Q. Quebec H3C 3A7
CANADA

John E. Ritter
University of Massachusetts
Mechanical Engineering Department
Amherst MA 01003

W. Eric Roberts
Advanced Ceramic Technology
990 "F" Enterprise Street
Orange CA 92667

Y. G. Roman
TNO TPD Keramick
P.O. Box 595
Einhoven 5600 AN
HOLLAND

Michael Rossetti
Arthur D. Little, Inc.
15 Acorn Park
Cambridge MA 01240

Barry Rossing
Lanxide Corporation
P.O. Box 6077
Newark DE 19714-6077

Steven L. Rotz
Lubrizol Corporation
29400 Lakeland Boulevard
Wickliffe OH 44092

Robert Ruh
Wright Laboratory
WL/MLLM
Wright-Patterson AFB OH 45433

Robert J. Russell
Riverdale Consulting, Inc.
24 Micah Hamlin Road
Centerville MA 02632-2107

Jon A. Salem
NASA Lewis Research Center
21000 Brookpark Road
Cleveland OH 44135

W. A. Sanders
NASA Lewis Research Center
21000 Brookpark Road, MS:49-3
Cleveland OH 44135

J. Sankar
North Carolina A&T State Univ.
Dept. of Mechanical Engineering
Greensboro NC 27406

Yasushi Sato
NGK Spark Plugs (U.S.A.), Inc.
1200 Business Center Dr., #300
Mt. Prospect IL 60056

Maxine L. Savitz
AlliedSignal, Inc.
Ceramic Components
P.O. Box 2960, MS:T21
Torrance CA 90509-2960

Ashok Saxena
GTRI
Materials Engineering
Atlanta GA 30332-0245

David W. Scanlon
Instron Corporation
100 Royall Street
Canton MA 02021

Charles A. Schacht
Schacht Consulting Services
12 Holland Road
Pittsburgh PA 15235

Robert E. Schafrik
Natl Materials Advisory Board
2101 Constitution Ave., N.W.
Washington DC 20418

James Schienle
AlliedSignal Engines
P.O. Box 52180, MS:1302-2P
Phoenix AZ 85072-2180

Gary Schnittgrund
PyroPacific Processes
16401 Knollwood Drive
Granada Hills, CA 91344

Mark Schomp
Lonza, Inc.
17-17 Route 208
Fair Lann NJ 07410

Joop Schoonman
Delft University of Technology
P.O. Box 5045
2600 GA Delft
THE NETHERLANDS

Robert B. Schulz
U.S. Department of Energy
Office of Transportation Mater.
CE-34, Forrestal Building
Washington DC 20585

Murray A. Schwartz
Materials Technology Consulting
30 Orchard Way, North
Potomac MD 20854

Peter Schwarzkopf
SRI International
333 Ravenswood Avenue
Menlo Park CA 94025

William T. Schwessinger
Multi-Arc Scientific Coatings
1064 Chicago Road
Troy MI 48083-4297

W. D. Scott
University of Washington
Materials Science Department
Mail Stop:FB10
Seattle WA 98195

Nancy Scoville
Thermo Electron Technologies
P.O. Box 9046
Waltham MA 02254-9046

Thomas M. Sebestyen
U.S. Department of Energy
Advanced Propulsion Division
CE-322, Forrestal Building
Washington DC 20585

Brian Seegmiller
Coors Ceramics Company
600 9th Street
Golden CO 80401

T. B. Selover
AICRE/DIPPR
3575 Traver Road
Shaker Heights OH 44122

Charles E. Semler
Semler Materials Services
4160 Mumford Court
Columbus OH 43220

Thomas Service
Service Engineering Laboratory
324 Wells Street
Greenfield MA 01301

Kish Seth
Ethyl Corporation
P.O. Box 341
Baton Rouge LA 70821

William J. Shack
Argonne National Laboratory
9700 S. Cass Avenue, Bldg. 212
Argonne IL 60439

Peter T.B. Shaffer
Shaffer Associates
3225 Chimney Cove Drive
Cumming GA 30131

Richard K. Shaltens
NASA Lewis Research Center
21000 Brookpark Road, MS:302-2
Cleveland OH 44135

Robert S. Shane
1904 NW 22nd Street
Stuart FL 34994-9270

Ravi Shankar
Chromalloy
Research and Technology
Blaisdell Road
Orangeburg NY 10962

Terence Sheehan
Alpex Wheel Company
727 Berkley Street
New Milford NJ 07646

Dinesh K. Shetty
University of Utah
Materials Science and Engineering
Salt Lake City UT 84112

Masahide Shimizu
New Ceramics Association
Shirasagi 2-13-1-208, Nakano-ku
Tokyo, 165
JAPAN

Thomas Shreves
American Ceramic Society, Inc.
735 Ceramic Place
Westerville OH 43081-8720

Jack D. Sibold
Coors Ceramics Company
4545 McIntyre Street
Golden CO 80403

Johann Siebels
Volkswagen AG
Werkstofftechnologie
Postfach 3180
Wolfsburg 1
GERMANY

George H. Siegel
Point North Associates, Inc.
P.O. Box 907
Madison NJ 07940

Richard Silberglitt
FM Technologies, Inc.
10529-B Braddock Road
Fairfax VA 22032

Mary Silverberg
Norton Company
SGNICC/NRDC
Goddard Road
Northboro MA 01532-1545

Gurpreet Singh
Department of the Navy
Code 56X31
Washington DC 20362-5101

Maurice J. Sinnott
University of Michigan
5106 IST Building
Ann Arbor MI 48109-2099

John Skildum
3M Company
3M Center
Building 224-2S-25
St. Paul MN 55144

Richard H. Smoak
Smoak & Associates
3554 Hollyslope Road
Altadena CA 91001-3923

Jay R. Smyth
AlliedSignal Engines
111 S. 34th Street, MS:503-412
Phoenix AZ 85034

Rafal A. Sobotowski
British Petroleum Company
Technical Center, Broadway
3092 Broadway Avenue
Cleveland OH 44115

S. Somiya
Nishi Tokyo University
3-7-19 Seijo, Setagaya
Tokyo, 157
JAPAN

Boyd W. Sorenson
DuPont Lanxide Composites
1300 Marrows Road
Newark DE 19711

Charles A. Sorrell
U.S. Department of Energy
Advanced Industrial Concepts
CE-232, Forrestal Building
Washington DC 20585

C. Spencer
EA Technology
Capenhurst Chester CH1 6ES
UNITED KINGDOM

Allen Spizzo
Hercules Inc.
Hercules Plaza
Wilmington DE 19894

Richard M. Spriggs
Alfred University
Ctr. for Advanced Ceramic Tech.
Alfred NY 14802

Charles Spuckler
NASA Lewis Research Center
21000 Brookpark Road, MS:5-11
Cleveland OH 44135-3191

Gordon L. Starr
Cummins Engine Company, Inc.
P.O. Box 3005, Mail Code:50182
Columbus IN 47202-3005

Tom Stillwagon
AlliedSignal, Inc.
Ceramic Components
P.O. Box 2960, MS:T21
Torrance CA 90509-2960

H. M. Stoller
TPL Inc.
3754 Hawkins, N.E.
Albuquerque NM 87109

Paul D. Stone
Dow Chemical USA
1776 "Eye" Street, N.W.,#575
Washington DC 20006

F. W. Stringer
Aero & Industrial Technology
P.O. Box 46, Wood Top
Burnley Lancashire BB11 4BX
UNITED KINGDOM

Thomas N. Strom
NASA Lewis Research Center
21000 Brookpark Road, MS:86-6
Cleveland OH 44135

M. F. Stroosnijder
Institute for Advanced Materials
Joint Research Centre
21020 Ispra (VA)
ITALY

Karsten Styhr
30604 Ganado Drive
Rancho Palos Verdes CA 90274

T. S. Sudarshan
Materials Modification, Inc.
2929-P1 Eskridge Center
Fairfax VA 22031

M. J. Sundaresan
University of Miami
P.O. Box 248294
Coral Gables FL 33124

Patrick L. Sutton
U.S. Department of Energy
Office of Propulsion Systems
CE-322, Forrestal Building
Washington DC 20585

Willard H. Sutton
United Technologies Corporation
Silver Lane, MS:24
East Hartford CT 06108

Robert E. Swanson
Metalworking Technology, Inc.
1450 Scalp Avenue
Johnstown PA 15904

Yo Tajima
NGK Spark Plug Company
2808 Iwasaki
Komaki-shi Aichi-ken, 485
JAPAN

Fred Teeter
5 Tralee Terrace
East Amherst NY 14051

Victor J. Tennery
113 Newell Lane
Oak Ridge TN 37830

Monika O. Ten Eyck
Carborundum Microelectronics
P.O. Box 2467
Niagara Falls NY 14302-2467

David F. Thompson
Corning Glass Works
SP-DV-02-1
Corning NY 14831

T. Y. Tien
University of Michigan
Materials Science & Engineering
Dow Building
Ann Arbor MI 48103

D. M. Tracey
Norton Company
SGNICC/NRDC
Goddard Road
Northboro MA 01532-1545

Marc Tricard
Norton Company, WGTC
1 New Bond Street, MS-413-201
Worcester MA 01615-0008

L. J. Trostel, Jr.
Box 199
Princeton MA 01541

W. T. Tucker
General Electric Company
P.O. Box 8, Bldg. K1-4C35
Schenectady NY 12301

Masanori Ueki
Nippon Steel Corporation
1618 Ida
Nakahara-Ku Kawasaki, 211
JAPAN

Filippo M. Ugolini
ATA Studio
Via Degli Scipioni, 268A
ROMA, 00192
ITALY

Donald L. Vaccari
Allison Gas Turbines
P.O. Box 420, Speed Code S49
Indianapolis IN 46206-0420

Carl F. Van Conant
Boride Products, Inc.
2879 Aero Park Drive
Traverse City MI 49684

John F. Vander Louw
3M Company
3M Center, Bldg. 60-1N-01
Saint Paul MN 55144

Marcel H. Van De Voorde
Commission of the European
Community
P.O. Box 2
1755 ZG Petten
THE NETHERLANDS

O. Van Der Biest
Katholieke Universiteit Leuven
Dept. Metaalkunde en Toegepaste
de Croylaan 2
B-3030 Leuven
BELGIUM

Michael Vannier
Washington University,
St. Louis
510 S. Kings Highway
St. Louis MO 63110

Stan Venkatesan
Southern Coke & Coal Corp.
P.O. Box 52383
Knoxville TN 37950

V. Venkateswaran
Carborundum Company
Niagara Falls R&D Center
P.O. Box 832
Niagara Falls NY 14302

Ted Vojnovich
U.S. Department of Energy
Office of Energy Research, 3F077P
Washington DC 20585

John D. Volt
E.I. Dupont de Nemours & Co.
P.O. Box 80262
Wilmington DE 19880

John B. Wachtman
Rutgers University
P.O. Box 909
Piscataway NJ 08855

Shigetaka Wada
Toyota Central Research Labs
Nagakute Aichi, 480-11
JAPAN

Janet Wade
AlliedSignal Engines
P.O. Box 52180, MS:1303-2
Phoenix AZ 85072-2180

Richard L. Wagner
Ceramic Technologies, Inc.
537 Turtle Creek South Dr.
Indianapolis IN 46227

J. Bruce Wagner, Jr.
Arizona State University
Center for Solid State Science
Tempe AZ 85287-1704

Daniel J. Wahlen
Kohler, Co.
444 Highland Drive
Kohler WI 53044

Ingrid Wahlgren
Royal Institute of Technology
Studsvik Library
S-611 82 Nykoping
SWEDEN

Ron H. Walecki
AlliedSignal, Inc.
Ceramic Components
P.O. Box 2960, MS:T21
Torrance CA 90509-2960

Michael S. Walsh
Vapor Technologies Inc.
6300 Gunpark Drive
Boulder CO 80301

Chien-Min Wang
Industrial Technology Research Institute
195 Chung-Hsing Road, Sec. 4
Chutung Hsinchu 31015 R.O.C.
TAIWAN

Robert M. Washburn
ASMT
11203 Colima Road
Whittier CA 90604

Kevin Webber
Toyota Technical Center, U.S.A.
1410 Woodridge, RR7
Ann Arbor MI 48105

Karen E. Weber
Detroit Diesel Corporation
13400 Outer Drive West
Detroit MI 48239-4001

James K. Weddell
Du Pont Lanxide Composites Inc.
P.O. Box 6100
Newark DE 19714-6100

R. W. Weeks
Argonne National Laboratory
MCT-212
9700 S. Cass Avenue
Argonne IL 60439

Ludwig Weiler
ASEA Brown Boveri AG
Eppelheimer Str. 82
D-6900 Heidelberg
GERMANY

James Wessel
127 Westview Lane
Oak Ridge TN 37830

Robert D. West
Therm Advanced Ceramics
P.O. Box 220
Ithaca NY 14851

Thomas J. Whalen
1845 Cypress Pointe Court
Ann Arbor MI 48108

Ian A. White
Hoeganaes Corporation
River Road
Riverton NJ 08077

Sheldon M. Wiederhorn
NIST
Building 223, Room A329
Gaithersburg MD 20899

John F. Wight
Alfred University
McMahon Building
Alfred NY 14802

D. S. Wilkinson
McMaster University
1280 Main Street, West
Hamilton Ontario L8S 4L7
CANADA

James C. Williams
General Electric Company
Engineering Materials Tech.
One Neumann Way, Mail Drop:H85
Cincinnati OH 45215-6301

Steve J. Williams
RCG Hagler Bailly, Inc.
1530 Wilson Blvd., Suite 900
Arlington VA 22209-2406

Thomas A. Williams
National Renewable Energy Lab
1617 Cole Boulevard
Golden CO 80401

Craig A. Willkens
Norton Company
SGNICC/NRDC
Goddard Road
Northboro MA 01532-1545

Roger R. Wills
Ohio Aerospace Institute (OAI)
22800 Cedar Point Road
Brook Park OH 44142

David Gordon Wilson
Massachusetts Institute of Technology
77 Massachusetts Ave., Rm 3-455
Cambridge MA 02139

J. M. Wimmer
AlliedSignal Ceramic Components
Department 27000, MS:T21
2525 W. 190th Street
Torrance CA 90509

Matthew F. Winkler
Seaworthy Systems, Inc.
P.O. Box 965
Essex CT 06426

Gerhard Winter
Hermann C. Starck Berlin GmbH
P.O. Box 25 40
D-3380 Goslar 3380
GERMANY

Thomas J. Wissing
Eaton Corporation
Engineering and Research Center
P.O. Box 766
Southfield MI 48037

James C. Withers
MER Corporation
7960 S. Kolb Road
Building F
Tucson AZ 85706

Dale E. Wittmer
Southern Illinois University
Mechanical Engineering Dept.
Carbondale IL 62901

Warren W. Wolf
Owens Corning Fiberglass
2790 Columbus Road, Route 16
Granville OH 43023

Egon E. Wolff
Caterpillar Inc.
Technical Center
P.O. Box 1875
Peoria IL 61656-1875

George W. Wolter
Howmet Turbine Components Corp.
Technical Center
699 Benston Road
Whitehall MI 49461

Wayne L. Worrell
University of Pennsylvania
3231 Walnut Street
Philadelphia PA 19104

John F. Wosinski
Corning Inc.
ME-2 E-5 H8
Corning NY 14830

Ruth Wroe
ERDC
Capenhurst Chester CH1 6ES
ENGLAND

Bernard J. Wrona
Advanced Composite Materials
1525 S. Buncombe Road
Greer SC 29651

Carl C. M. Wu
Naval Research Laboratory
Ceramic Branch, Code 6373
Washington DC 20375

David C. Wu
AlliedSignal Engines
P.O. Box 52181, MS:301-227
Phoenix AZ 85072-2181

John C. Wurst
U. of Dayton Research Institute
300 College Park
Dayton OH 45469-0101

Neil Wyant
ARCH Development Corp.
9700 S. Cass Avenue, Bldg. 202
Argonne IL 60439

Roy Yamamoto
Texaco Inc.
P.O. Box 509
Beacon NY 12508-0509

John Yamanis
AlliedSignal Aerospace Company
P.O. Box 1021
Morristown NJ 07962-1021

Harry C. Yeh
AlliedSignal, Inc.
Ceramic Components
P.O. Box 2960, MS:T21
Torrance CA 90509-2960

Hiroshi Yokoyama
Hitachi Research Lab
4026 Kuji-Cho
Hitachi-shi Ibaraki 319-12
JAPAN

Thomas M. Yonushonis
Cummins Engine Company, Inc.
P.O. Box 3005, Mail Code 50183
Columbus IN 47202-3005

Jong Yung
Sundstrand Aviation Operations
4747 Harrison Avenue
Rockford IL 61125

C. S. Yust
106 Newcrest Lane
Oak Ridge TN 37830

A. L. Zadoks
Caterpillar Inc.
Technical Center, Building L
P.O. Box 1875
Peoria IL 61656-1875

Avi Zangvil
University of Illinois
104 S. Goodwin Avenue
Urbana IL 61801

Charles H. Zenuk
Transtech
6662 E. Paseo San Andres
Tucson AZ 85710-2106

Carl Zweben
General Electric Company
P. O Box 8555, VFSC/V4019
Philadelphia PA 19101

Department of Energy
Oak Ridge Operations Office
Asst. Manager for Energy
Research and Development
P.O. Box 2001
Oak Ridge, TN 37871-8600

Department of Energy
Office of Scientific and
Technical Information
Office of Information Services
P.O. Box 62
Oak Ridge, TN 37831?